AN ABSTRACT OF THE DISSERTATION OF

Wiley Evans for the degree of Doctor of Philosophy in Oceanography presented on April 15, 2011.

Title: Sea-Air CO_2 Flux Variability on the Northeast Pacific Continental Margin.

Abstract approved:

_____

Peter G. Strutton Burke R. Hales

Carbon dioxide (CO_2) fluxes between the ocean and atmosphere on continental margins are difficult to diagnose because these regions experience large variability over spatial and temporal scales spanning meters to basins and hours to years, respectively. In a global sense, continental margins could represent a significant atmospheric CO_2 sink, equivalent to ~30% of the open ocean CO_2 uptake. However, many regions have inadequate data coverage to resolve the large inherent variability. The role of continental margins also becomes increasingly more complicated if nearshore waters, such as estuaries and salt marshes, are included in global or regional carbon budgets. This thesis addresses variability in surface seawater CO_2 partial pressure (pCO_2) and sea-air CO_2 flux across three sub-regions of the northeast Pacific continental margin: the Oregon shelf, the western Canadian coastal ocean, and the Columbia River Estuary and plume.

Chapter 1 describes the motivation for this work. Chapter 2 is an assessment of the seasonal cycle of pCO_2 on the Oregon shelf from both ship and mooring data. Results from this work demonstrate strong seasonality on the shelf, as well as interannual variability important for constraining regional flux estimates. The observations included the highest surface water pCO_2 reported for the region, and prolonged exposure of this water to the atmosphere had a large impact on the annual estimate of sea-air CO_2 flux.

Chapter 3 presents a new data set of ship-based pCO_2 observations made over a larger portion of the western Canadian coastal margin than had been previously sampled during winter, summer and autumn. Analyses of temporally well-resolved historical data collected on the southwest Vancouver Island shelf, combined with the spatially well-resolved new data showed that CO_2 outgassing during autumn is significantly greater than during winter over most of the margin, and both seasons play a key role in nearly balancing the influx of atmospheric CO_2 that occurs during the remainder of the year.

Chapter 4 reports water-air CO_2 fluxes from the Columbia River Estuary and plume across three seasons. The river plume is always a sink for atmospheric CO_2, likely from a combination of chemical and biological factors, while the estuary sink/source character is seasonally modified. During spring, the estuary acts as a sink for atmospheric CO_2, whereas it is a source during other seasons. Primary productivity and ecosystem respiration are important for determining the magnitude of fluxes in the estuary between seasons, and the spring freshet marks the transition between CO_2 sink and source functionality in the estuary.

Chapter 5 examines the weak phytoplankton response to strong and persistent upwelling on the Oregon shelf in July 2008 to understand the prolonged exposure of high-pCO_2 water. Using ship, mooring and satellite data, I argue the phytoplankton response time is long relative to the timescales of strong upwelling, cross shore transport, and subduction. The rapid physical processes are most likely responsible for maintaining low chlorophyll conditions when nutrients and pCO_2 are elevated. Chapter 6 is a discussion of the importance of the large flux events observed during these studies, and their relevance to regional and global CO_2 flux studies. In each region studied in this thesis there were occurrences of high-intensity pCO_2 conditions, which highlights the variable nature of the coastal ocean and the importance of resolving the temporal and spatial scales of variability in order to assess continental margin sea-air CO_2 fluxes.

Sea-Air CO_2 Flux Variability on the Northeast Pacific Continental Margin

by

Wiley Evans

A DISSERTATION

submitted to

Oregon State University

in partial fulfillment of
the requirements for the
degree of

Doctor of Philosophy

Presented April 15, 2011
Commencement June 2011

Doctor of Philosophy dissertation of Wiley Evans presented on April 15, 2011.

Approved:

_____

Co-Major Professor, representing Oceanography

_____

Co-Major Professor, representing Oceanography

_____

Dean of the College of Oceanic and Atmospheric Sciences

_____

Dean of the Graduate School

I understand that my dissertation will become part of the permanent collection of Oregon State University libraries. My signature below authorizes release of my dissertation to any reader upon request.

_____

Wiley Evans, Author

ACKNOWLEDGEMENTS

There are many people that have helped me along the way to completing this thesis. These people include, in no specific order, fellow students I had the pleasure of interacting with, researchers and technicians I had the privilege to learn from, close friends that gave me incredible support, PIs that let me come on their cruises or put gear on their moorings (most data collected for this thesis were from piggybacked platforms), fellow scientists who provided their data, the captains and crews of the ships I sailed to collect these measurements, and my family and loved ones that have given me amazing support through these incredible past many years of my life. Some to particularly note are:

(1) My longtime advisor, Peter G. Strutton, who got me incredibly excited about oceanography early on, and has been an extraordinary mentor through my entire graduate career. He has aided me in every aspect of becoming an oceanographer, and I owe him a large debt of gratitude. I probably also owe him a few beers.

(2) My co-advisor, Burke R. Hales, who also was an excellent mentor and gave me many of the tools I needed to complete this thesis. He provided the flow-through system used on nearly every cruise, he taught me how to use and debug this system, he instructed me on every aspect of pCO_2 data processing, and his knowledge and guidance helped me to analyze and interpret these data in their most appropriate context. Thank you very much Burke, I also owe you a significant debt of gratitude.

(3) My committee members Pat Wheeler, Dudley Chelton and George Boehlert, all provided valuable insight and guidance throughout my dissertation, and I'm incredibly grateful for all their support.

(4) Dale Hubbard, instructed me on every aspect to properly install/run/maintain the OSU pCO_2 system. He also gave me great insight on how to debug this system, and I greatly appreciate all his effort.

(5) My parents, whose love and support were influential in keeping me on track throughout this journey. Thank you both so much.

(6) Rachel Saraga, who has been instrumental in my life. The love and support she has given made me flourish throughout the final chapters of this thesis, and she deserves my sincere admiration for all her continued support.

CONTRIBUTION OF AUTHORS

Drs. Peter G. Strutton and Burke Hales provided valuable critiques that improved chapters 2, 3, 4 and 5. Both are coauthors on manuscripts from these chapters. Dr. Debby Ianson provided helpful feedback on chapter 3, and is a coauthor on the manuscript for that chapter. Drs. Pat Wheeler, Bill Peterson, Kipp Shearman and Jack Barth provided important input on chapter 5.

TABLE OF CONTENTS

LIST OF FIGURES

LIST OF FIGURES (Continued)

Figure Page

LIST OF FIGURES (Continued)

Figure Page

LIST OF FIGURES (Continued)

Figure Page

LIST OF TABLES

Table Page

SEA-AIR CO_2 FLUX VARIABILITY ON THE NORTHEAST PACIFIC CONTINENTAL MARGIN

CHAPTER 1: Introduction

The role of the open ocean in sequestering atmospheric CO_2 is well known [*Takahashi et al.*, 2002; 2009], but the role of continental margins is more uncertain because of the broad time and space variability in these regions relative to the open ocean [*Cai et al.*, 2006; *Laruelle et al.*, 2010]. On a global scale, coastal margins are thought to be sinks for atmospheric CO_2, whereas nearshore waters, such as estuaries and salt marshes, act as sources [*Cai*, 2011]. A recent budget suggests that the global coastal margin sink could be compensated for by the efflux from nearshore waters [*Cai*, 2011], but estimates for both regions are based on extremely sparse data sets [*Cai*, 2011; *Hales et al.*, 2008]. Sparse data coupled with the large variability in these regions make their role in net CO_2 exchange difficult to characterize. The shortcomings of existing data are highlighted in the near-neutral net annual sea-air CO_2 flux estimated for the North American coastal margin, which results from the near cancelation between large CO_2 influx in high-latitude under-sampled waters and large CO_2 efflux in low-latitude under-sampled waters [*Chavez and Takahashi*, 2007; *Hales et al.*, 2008]. Large regions of the coastal ocean on every continent have not been sampled, and a small number of sites globally have adequate data coverage to resolve the seasonal cycle (see Fig. 1 in *Laruelle et al*. [2010]).

The northeast Pacific continental margin is no exception to the problem of data scarcity. The Oregon shelf, the British Columbia coastal ocean and the Columbia River Estuary and plume are the specific sub-regions on the northeast Pacific continental margin that this thesis focused on, and published data in these areas are either exclusively from summer months made at variable spatial resolution [*Hales et al.,* 2005; *Ianson et al.,* 2003; *Nemcek et al.,* 2008; *van Geen et al.,* 2000], have very coarse spatial coverage of the seasonal cycle [*Wong et al.,* 2010], or are nonexistent. The central aim of this thesis was to aggressively utilize platforms-of-opportunity to better characterize the temporal and spatial variability of sea-air CO_2 exchange in these specific under-sampled regions. Chapter 2 describes the seasonal cycle of surface ocean pCO_2 on the Oregon shelf. Chapter 3 examines sea-air CO_2 fluxes on the western Canadian coastal margin. Chapter 4 reports air-water CO_2 fluxes in the Columbia River Estuary and plume. Chapter 5 describes a prolonged CO_2 outgassing event on the Oregon shelf during July 2008. Finally, Chapter 6 describes some extreme conditions observed during each study, and some aspects critical to characterizing sea-air CO_2 fluxes within the dynamic coastal ocean.

CHAPTER 2: The Seasonal Cycle of Surface Ocean pCO_2 on the Oregon Shelf

Wiley Evans

Published in *Journal of Geophysical Research – Oceans*

American Geophysical Union

ACKNOWLEDGEMENTS

We thank the crews of the OSU R/Vs *Wecoma* and *Elakha*, and of the NOAA Ships *McArthur II* and *Miller Freeman*. We thank the OrCOOS program for providing the buoy and Walt Waldorf for his help with buoy deployments. We thank Bill Peterson for allowing our participation in his NH Line surveys. We thank Mike DeGrandpre, Cory Beatty, and Katherine Harris for sharing SAMI pCO_2 data from the last buoy deployment presented in this manuscript. This work was supported by NSF Chemical Oceanography award OCE-0752576.

ABSTRACT

Previous work has shown the Oregon shelf is a sink for atmospheric carbon dioxide (CO_2) during the upwelling season, but until now summertime variability in CO_2 exchange and sign of the flux for the rest of the year were unknown. Observations of the partial pressure of CO_2 (pCO_2) in surface waters from August 2007 to May 2010 from ships and a buoy were used with historical data to produce a composite seasonal cycle for the central Oregon mid shelf. These data indicate the region is highly variable, at times either being a sink or strong source for atmospheric CO_2. Interannual wind variability was an important determining factor in shaping the sink/source nature of this system. Late summer/early autumn was most variable relative to the rest of the year. Winter pCO_2 was near or slightly below atmospheric levels. Strong shelf-wide undersaturated conditions were first observed in early spring and lasted until the upwelling season became developed. Peak upwelling season pCO_2 ranged from < 200 µatm to > 1000 µatm. In July 2008, ship and buoy data revealed previously unobserved high-pCO_2 waters (~1000 µatm) at the surface. These conditions persisted for nearly two months and drove this system to be only a weak net annual atmospheric CO_2 sink of -0.3 ± 6.8 mol m^{-2} yr^{-1}. These data showed, for the first time, the seasonal cycle of surface ocean pCO_2 on the central Oregon mid shelf and the impact of heretofore-undocumented pCO_2 levels on an estimate of sea-air CO_2 flux for this region.

INTRODUCTION

It is well known that the open ocean plays a key role in the exchange of CO_2 with the atmosphere, taking up nearly 2 Pg (1 Pg = 10^{15} g) C yr^{-1} [*Takahashi et al.*, 2009]. Recent syntheses have focused on the role of the coastal ocean in sea-air CO_2 flux because this is an important and poorly understood region of carbon exchange between the terrestrial environment, the open ocean and the atmosphere [e.g. *Chavez and Takahashi*, 2007; *Hales et al.*, 2008; *Liu et al.*, 2010]. The coastal ocean dominates in terms of per unit area rates of primary production [*Behrenfeld and Falkowski*, 1997] and export production [*Muller-Karger et al.*, 2005], and may be an important conduit of carbon into the deep sea by advection off the shelf (defined as inshore of 200 m) in bottom-boundary layer currents [*Hales et al.*, 2006]. Large uncertainty in coastal ocean carbon flux estimates persists, due to extreme variability observed on short temporal and small spatial scales relative to the open ocean. In addition to high localized variability, there is also large variability across regions. It has been stated that low latitude coastal areas are generally thought to be sources of atmospheric CO_2 while high latitude coastal margins act as sinks [*Cai et al.*, 2006; *Chavez and Takahashi*, 2007]. This broad generalization is poorly constrained because seasonal and interannual variability has only been characterized in a limited number of coastal regions. There is a general lack of observations to resolve even the seasonal cycle in most coastal locations, and the coastal margin of the US Pacific Northwest is no exception.

The Oregon coast is within the Cascadian margin, stretching from approximately Cape Mendocino, California, to the northern end of Vancouver Island, Canada. This represents the northern portion of the California Current System along the west coast of North America. In this region, equatorward winds that drive the Ekman transport of surface water offshore and subsequent

upwelling of cold nutrient- and CO_2-rich water from depth, nominally begin in April and last until October. These upwelling-favorable winds drive a southward mean current on the shelf during the summer months, that reverses direction with the change to northward and downwelling-favorable winds during winter [*Huyer and Smith*, 1978]. The large-scale seasonal change in physical forcing is accompanied by significant changes in water column structure and water property distributions. Winter months are characterized by large freshwater inputs [e.g. *Wetz et al.*, 2006; *Chase et al.*, 2007] and strong storms [*Strub et al.*, 1987]. In summer, freshwater fluxes from land are greatly reduced relative to winter [*Colbert and McManus*, 2003] and water property distributions are driven by upwelling [*Barth and Wheeler*, 2005].

Upwelling source waters along this coast have very high pCO_2 values, approaching or exceeding 1000 µatm [*Hales et al.*, 2005a; *Feely et al.*, 2008]. Outcrops of this water in nearshore settings off the Oregon coast have been observed with pCO_2 values near 700 µatm [*van Geen et al.*, 2000; *Hales et al.*, 2005a]. This water is then advected off- and along-shore and, because of its high preformed nutrient concentration [*Hales et al.*, 2005b], a lack of micronutrient limitation [*Chase et al.*, 2007], and fast-growing coastal phytoplankton assemblages [*Dugdale et al.*, 1990; *Dugdale et al.*, 2006; *Wetz and Wheeler*, 2003], the pCO_2 is rapidly drawn down to levels far below equilibrium with the atmosphere (~200 µatm or less). The net result is that on average the Oregon shelf appears to act as a sink for atmospheric CO_2 during the upwelling season [*Hales et al.*, 2005a]. Following the upwelling season, the winds reverse to become dominantly poleward and downwelling-favorable by about October and large storms impact the Oregon coast until about April.

To date programs studying pCO_2 variability on the Oregon shelf have focused on the upwelling season. No published data exist for fall, winter or spring conditions. Here we present the seasonal cycle of surface ocean pCO_2 on the Oregon shelf, and describe the physical and biological processes that influence the observed variability.

METHODS

To build a data set capable of resolving pCO_2 variability along the coast, we equipped a mooring (position shown in Fig. 2.1) and numerous vessels-of-opportunity with instruments to measure sea surface temperature (SST), salinity, pCO_2, dissolved oxygen, chlorophyll and colored dissolved organic matter (CDOM) fluorescence and turbidity. The following sections describe the ship and mooring measurement systems and the data processing for each.

Ship Measurements

We equipped vessels-of-opportunity with a new underway pCO_2 measurement system. This system, modified from that described in *Hales et al.* [2004], uses a LI-COR LI-840 infrared (IR) CO_2 sensor with a miniature membrane contactor (Liqui-Cel 1x5.5) as an equilibrator to achieve a faster analytical response than traditional systems using showerhead equilibrators. Prefiltration was achieved using a custom tangential flow filtration system with an 8-μm filter element, in which 1-10% of the main flow was directed tangentially to the primary flow and across the filter to the membrane contactor. Sample liquid flow through the contactor was typically ~300 ml min^{-1}, while the atmospheric air carrier flow rate was fixed at 30 ml min^{-1}. Data were collected at 1 Hz, and standard sequences using gases of known CO_2 mixing ratio (xCO_2, ppm) were run every two hours and used to correct for IR analyzer inaccuracy. Calibrated

xCO_2 data were adjusted to pCO_2 using the measured total pressure in the equilibrator. The calibrated atmospheric xCO_2 data were converted to pCO_2 using atmospheric pressure measured in the LI-COR cell. Measurement-temperature pCO_2 was then corrected to pCO_2 at SST using the difference between ship intake and equilibrator temperatures, after accounting for the flow-based lag time (usually ~ 50 s) between those two temperature sensor locations, and the relationship for the temperature effect on isochemical seawater described by *Takahashi et al.* [1993].

The pCO_2 system was integrated with a Seabird SBE45 for temperature and salinity, a Seabird SBE43 for dissolved oxygen, a chlorophyll fluorometer (WETLabs WetStar; excitation/emission wavelengths of 460/695 nm), CDOM fluorometer (WETLabs WetStar; excitation/emission wavelengths of 370/460 nm) and a beam transmissometer (WETLabs C-Star, wavelength 660 nm). Seawater flow rate was also monitored downstream of the pCO_2 equilibrator and used for data quality control; data from all measurements were removed during periods of low flow delivery to the equilibrator. All ancillary measurements are made at 1 Hz coincident with the pCO_2 measurement. The intake depth for the seawater flow-through system on most ships was typically 3 m. Optical instruments were kept clean during each cruise. Due to a computer theft we were unable to calibrate our fluorometer with bottle samples collected during all cruises. The chlorophyll calibration was done using surface Niskin bottle samples collected during the July 2008 cruise aboard the NOAA ship *McArthur II*. These data, although limited in time, cover a substantial portion of the dynamic range of chlorophyll concentrations encountered in this region (0-20 mg m^{-3}). Observations of CDOM will be presented elsewhere.

Moored Measurements

Moored pCO_2 measurements were made using a Submersible Autonomous Moored Instrument CO_2 sensor [SAMI-CO_2; *DeGrandpre et al.*, 1995] produced by Sunburst Sensors which was deployed immediately under the surface float on the OSU NH10 buoy (Fig. 2.1). The NH10 buoy is located at the 80m isobath, about 20 km from shore nearly due west of Newport, Oregon. This location was chosen by the Oregon Coastal Ocean Observing System (OrCOOS; http://agate.coas.oregonstate.edu/index.html) because it is almost exactly halfway between the shore and the shelf break. The SAMI was factory calibrated prior to each deployment. Buoy measurements agree well (typically within ± 5 µatm) with ship data collected during close ship-track passes to service and check the buoy throughout the deployments. In addition to the pCO_2 sensor, the mooring hosted a Seabird SBE16plus that measured and logged temperature and salinity and captured and logged the signals from a SBE43 sensor for dissolved oxygen and a WETLabs C-star transmissometer (660 nm) for optical beam transmission. Additional optics sensors deployed on the buoy include a WETLabs combination chlorophyll fluorometer and turbidity sensor (FLNTUSB which uses excitation/emission wavelengths of 470/695 nm for chlorophyll and backscatter at 700 nm for turbidity) and CDOM fluorometer (FLCDSB; excitation/emission of 370/460 nm). All sensors were positioned at approximately 1 m depth in the bridle of the buoy, and measurements were recorded hourly. Copper tape, faceplates and shutters were used to achieve a 4-month non-fouled record from our moored optical sensors. Optics data were first passed through a standard deviation filter to remove aberrant measurements caused by biofouling (by removing data outside of one standard deviation from the mean or the raw counts). All measurements were subsequently smoothed with a Loess filter with a six-hour filter span. The chlorophyll fluorometer was calibrated using data collected during the NOAA ship *McArthur II* July 2008 cruise.

Sea-air CO_2 Flux Estimate

The mooring data were used to calculate the first annual estimate of sea-air CO_2 flux for this region. The sea-air CO_2 flux (F) was calculated using the following equation:

$$F = k_{CO2}K_{CO2}\Delta pCO_2,$$

where k_{CO2} is the gas transfer velocity (m d^{-1}), K_{CO2} is the solubility of CO_2 (mol m^{-3} atm^{-1}) and ΔpCO_2 is the seawater pCO_2 minus the atmospheric pCO_2 (atm). The atmospheric pCO_2 was taken here to be an average measured during fall, spring and summer cruises (392 µatm). All input parameters were hourly values (wind magnitude, SST, salinity, and surface water pCO_2). k_{CO2} was calculated with the parameterization by *Ho et al.* [2006] using wind speeds from the NOAA C-Man station in Newport, OR. k_{CO2} were corrected to SST using the relationship for the Schmidt number dependence of gas transfer velocity described by *Wanninkhof* [1992]. A salinity correction of k_{CO2} was not conducted here because the difference between k_{CO2} at SST in freshwater versus saltwater (S=35) is on the order of a few percent. Note that we used shore-based winds because the NOAA and NH10 buoy wind records had large gaps during the wintertime. C-Man winds have a strong diurnal signal, and are typically weaker than offshore winds (nearshore wind magnitude ~75 % of offshore magnitude over this study period; data not shown), therefore, for a given delta pCO_2, our flux estimate using these winds is lower than a calculation based on offshore winds.

RESULTS

This data set has captured pCO_2 variability across all seasons on the Oregon shelf for the first time. Between August 2007 and May 2010, 21 cruises

(104 days of total ship time; Table 2.1) and 4 mooring deployments (572 days of total data) were completed. Ship-based measurements were collected between August 2007 and September 2008, and coverage over the shelf varied by month, with cruises during 6 out of 10 months surveying much of the coast between Grays Harbor, Washington (WA) and Newport, Oregon (OR). During October 2007 and February, March and August 2008, ship coverage was limited to the NH Line (our most intensely sampled transect; shown in Fig. 2.1). No ship data were available for December and January. The first mooring time-series took place from August 13, 2007 to November 8, 2007. A mooring time-series was attempted in winter 2007/2008 but a storm broke the buoy from its anchor shortly after deployment. Subsequent mooring time-series were from April 10, 2008 to September 15, 2008; March 20, 2009 to May 25, 2009; and August 25, 2009 to May 11, 2010, respectively. To compare our buoy data to ship measurements we have defined an area around the buoy position for selecting ship-based observations (Fig. 2.1), with dimensions ~10 nm east-west and ~20 nm north-south (44.45°N to 44.81°N and 124.3925°W to 124.2155°W). This area was chosen to capture ship data in the vicinity of the buoy and it should be noted that the dimensions are large compared to the scales of variability we observe, which can result in an imperfect agreement between buoy and ship data. Historical Carbon Dioxide Information and Analysis Center (CDIAC) pCO_2 data and ship-based observations made during this study were selected from this region and used for the construction of a composite year of pCO_2 for the central Oregon mid shelf.

CDIAC pCO_2 data for the central Oregon shelf from within our defined region near the NH10 buoy are non-existent for the winter season [Dec-Feb*; Hales et al.* 2005a]. However, CDIAC pCO_2 data do exist for the remainder of the year. Using both historical data and data collected during this project for a region

representing the central Oregon mid shelf (Fig. 2.1), we have constructed a seasonal cycle of pCO_2 (Fig. 2.2). Currently our winter ship observations are very limited (5 cruises), but the existing data suggest that pCO_2 conditions are at most near equilibrium with the atmosphere during this season. Data from our 2009/2010 buoy deployment demonstrate that pCO_2 levels may be slightly undersaturated with respect to the atmosphere over a majority of the winter. pCO_2 on the shelf trends toward strongly undersaturated conditions in the spring (Mar-May), punctuated by brief periods of elevated values during early upwelling season southward wind events (Fig. 2.3). Summer (Jun-Aug) values show the highest pCO_2 variability on the shelf, with values ranging from < 200 to > 1000 µatm. pCO_2 variability is decreased in the autumn (Sep-Nov) relative to summer, with the range of values trending towards equilibrium with the atmosphere as wind conditions seasonally reverse from upwelling to downwelling-favorable and net photosynthetic productivity decreases over the Oregon shelf.

Winter

Although ship-based winter sampling was temporally and spatially limited, pCO_2 on the shelf was near equilibrium with the atmosphere during all cruises in 2008. Surface water with SSTs ~8ºC and salinity ~28 was adjacent to the coast. Chlorophyll concentrations were observed to be low during this time of year, and winds were persistently downwelling-favorable (Fig. 2.3). Data from our winter 2009/2010 buoy deployment show that during at least some years the shelf can maintain a state of undersaturated pCO_2 (~340 µatm) with respect to the atmosphere for the entire season. By March, pCO_2 had fallen well below atmospheric equilibrium and chlorophyll increased to 3 mg m^{-3}, consistent with the general timing of the spring bloom on the Oregon shelf [*Huyer et al.*, 2007].

Spring

The month of April is nominally when the spring transition from downwelling to upwelling conditions occurs on the Oregon shelf (e.g. http://www.cbr.washington.edu/data/trans.html), and during this month in 2008 the shelf had transitioned from winter pCO_2 values near equilibrium with respect to the atmosphere to a strong sink for atmospheric CO_2. Buoy data showed pCO_2 values undersaturated with respect to the atmosphere by over 150 µatm, and pCO_2 observed from the ship showed similarly undersaturated conditions over the entire Oregon shelf off Newport (Fig. 2.4).

Spring SSTs were between 9ºC and 10ºC and freshwater originating from the Columbia River mouth was observed over the shelf both north and south of Astoria, OR (46.2ºN; Fig. 2.1). Chlorophyll was generally ~5 mg m^{-3} throughout the survey region, with the highest concentrations observed within and near the Columbia River (> 10 mg m^{-3}). MODIS chlorophyll shows the bulk of phytoplankton biomass along the Oregon coast in the vicinity of the Columbia River at this time (Fig. 2.5).

In late spring (May), SSTs were warmer by 2-3°C from the values observed in early spring 2008 and low salinity water was only observed south of the Columbia River mouth. The occurrence of plume water south of the Columbia River is indicative of the change in circulation along the Washington and Oregon coasts from winter-downwelling conditions to summer-upwelling conditions [*Hickey*, 1989], although this pattern is sensitive to the intensity and duration of upwelling-favorable winds [*Hickey and Banas*, 2008]. The change to upwelling conditions is reflected in the change to a positive upwelling index for the OR coast (45ºN) beginning in April

(http://www.pfeg.noaa.gov/products/PFEL/modeled/indices/upwelling/NA/upwell_menu_NA.html), and is also evident in the pattern of SST and salinity on the southern portion of our ship survey during this time. In the region near Newport, OR, SST was 10ºC and salinity was 32, substantially cooler and saltier compared with the surface water properties over the shelf on the northern portion of our ship survey. Widespread undersaturation with respect to atmospheric CO_2 was evident on the shelf and extending out into the North Pacific. Buoy and ship pCO_2 observations were the lowest in our record during this time (Fig. 2.4). Chlorophyll was between 3 and 5 mg m^{-3} on the shelf north of Newport, OR, but exceeded 10 mg m^{-3} in the region of active upwelling near and south of Newport, OR. Satellite chlorophyll (Fig. 2.5) and moored chlorophyll measurements (Fig. 2.6) show that this was the first period within the 2008 upwelling season where substantial primary production (indicated by increased chlorophyll) was observed in the vicinity of Newport, OR.

Summer

The greatest inter-annual and intra-seasonal variability in surface water pCO_2 occurs in summer over the central Oregon shelf (Fig. 2.2). June and July 2008 marked a sharp transition in the functioning of the coast from being a sink for atmospheric CO_2 to a source. We lack ship-based measurements for June, but it is clear from our mooring observations that the Oregon shelf transitioned radically from pCO_2 near ~200 µatm, increasing to ~1000 µatm over the course of a < 10-day period with the onset of continuous and strong (> 10 m s^{-1}) upwelling-favorable winds around June 10th (Fig. 2.6). The mooring data reveal a significant drop in oxygen percent saturation, a 4°C decrease in SST, and a low standing stock of phytoplankton biomass that persisted for the entire ~15-day upwelling event in June 2008. A brief increase in chlorophyll and oxygen saturation, and a decrease in pCO_2 were observed at NH10 during two periods of

reduced upwelling-favorable winds before an intense, prolonged upwelling event began, spanning most of July 2008.

The ship data for July show distributions of SST and salinity typical of coastal upwelling, but variability in surface pCO_2 not observed before for this region (Fig. 2.7). Ship surveys show that cold SST (~8ºC), high salinity (≥ 33) water spanned the coast from Cape Meares, OR (45.5ºN) south to Cape Blanco, OR (42.8ºN). pCO_2 in the upwelled water reached values broadly in excess of 800 µatm, and > 1000 µatm at the NH10 mooring site (Fig. 2.4). This high-pCO_2 water extended out past the shelf break (25 nm off Newport; Fig. 2.7) within the upwelling plume. Previous observations show that surface expressions of recently upwelled water off Oregon approach 700 µatm [*van Geen et al.*, 2000]. Subsurface upwelling source waters over the shelf can have a pCO_2 approaching 1000 µatm early in the upwelling season, and significantly exceeding those levels by the end of the summer growing season [*Hales et al.*, 2006]. These observations of > 1000 µatm pCO_2 at the surface are the highest values yet observed, and represent close coupling between the nearshore-midshelf surface waters and deep upwelling source waters. The frequency and persistence of these events would have a significant impact on the net annual sea-air CO_2 flux for this region.

August 2007 was the warmest month sampled by ships in our record, and SSTs over the shelf mostly exceeded 14ºC, except off Newport, OR where cold, recently upwelled waters were evident. Low salinity water (< 30) originating from the Columbia River was present on the shelf from Grays Harbor, WA (47ºN) to Cape Meares, OR (45.5ºN), but only resulted in an elevated pCO_2 signal near the Columbia River mouth. The entire shelf was undersaturated with respect to

atmospheric CO_2, and therefore functioned as an atmospheric CO_2 sink. The pCO_2 levels observed at the NH10 buoy just following deployment in August 2007 were < 200 µatm, and track well the levels across the mid shelf (Fig. 2.4). The standing stock of chlorophyll was high over the entire shelf (> 7 mg m^{-3}), presumably the result of net photosynthetic uptake of inorganic carbon that drove the large-scale CO_2 undersaturation observed during this time.

Autumn

September and October 2007 both experienced periods of upwelling-favorable winds (Fig. 2.3) and coincident elevated pCO_2 conditions at NH10 (Fig. 2.4), but limited ship data for October indicate that this high-pCO_2 water was confined to inshore of NH10 and pCO_2 over the mid-outer shelf was below equilibrium with respect to the atmosphere. Autumn on the Oregon shelf marks the transition from summer-upwelling to winter-downwelling conditions. During the first portion of our November survey, SSTs had decreased by more than 3°C from those observed in October. Surface water pCO_2 had risen to approach atmospheric equilibrium, but with a significant degree of spatial variability. pCO_2 was still undersaturated in the region between the Columbia River and Newport, OR, but was oversaturated with respect to atmospheric CO_2 on the southern end of the survey; a pattern that resulted from late-season upwelling that caused cooler SSTs (10°C) and higher salinity (33) in the southern portion of our survey, and chlorophyll concentrations near 5 mg m^{-3} in the region of active upwelling. During the second portion of this cruise the wind conditions changed from upwelling-favorable to strongly downwelling over the course of two days as the first winter storm impacted the coast. This drove a rapid change in seawater pCO_2. The variability observed during the first portion of the cruise was eliminated and the shelf pCO_2 transitioned to being homogenously distributed just slightly above equilibrium with the atmosphere. Chlorophyll also showed a

similar response to the arrival of winter storm conditions, with variable concentrations prior to the change in the weather and then driven to < 1 mg m^{-3} as the standing stocks of phytoplankton were diluted by storm generated mixing.

DISCUSSION

Composite Seasonal Cycle and Interannual pCO_2 Variability

It is important to note that our composite year includes a continuous record of summer surface pCO_2 values that reached previously unobserved levels in excess of 1000 μatm. During our sample period the Oregon shelf transitioned from being a sink for atmospheric CO_2 in the 2008 spring/early summer, to a strong source for nearly a two-month period in the late summer (June/July). There is likely large interannual variability driving the sink/source function of the coast, and this variability is demonstrated by our buoy time-series spanning multiple years. The buoy records captured autumn conditions during three years in September 2007, 2008 and 2009. The differences in pCO_2 observed between these three autumns (Fig. 2.2) are likely due to interannual variability in the wind forcing (Fig. 2.3).

Winds were more persistent and strongly upwelling-favorable in September 2008 compared to September 2007 and 2009 (Fig. 2.3), and that resulted in large differences in pCO_2 between these time periods (Fig. 2.2). At the start of August 2008 there was a near month-long relaxation in N/S winds (Fig. 2.3) and the shelf experienced a general warming. The pCO_2 dropped to below atmospheric equilibrium by the start of September 2008 (Fig. 2.4). During September 2008 the shelf experienced a period of strong and prolonged equatorward wind with few wind reversals (Fig. 2.3). pCO_2 at NH10 during this

event reached ~700 µatm, but was rapidly drawn down to below equilibrium with the atmosphere by a phytoplankton bloom which followed the wind event (Fig. 2.5). The winds in September 2007 were more weakly upwelling-favorable and pCO_2 increased to only ~500 µatm. Winds in September 2009 were very weak and variable (Fig. 2.3), and pCO_2 was ~90 µatm undersaturated with respect to the atmosphere for nearly the entire month.

The winds are driven by large-scale atmospheric pressure cells that are themselves heavily influenced by interannual variability [*Chavez et al.*, 2003; *Schwing et al.*, 2002], therefore year-to-year differences in pCO_2 conditions should be anticipated. Given the intensity of interannual pCO_2 variability observed in the much longer record from Monterey Bay, California [*Chavez et al.*, 2007; *Friederich et al.*, 2002], it is no surprise that interannual variability is important on the Oregon shelf and this is a significant motivation for producing longer data records. In our record, the largest variability in pCO_2 is during the late summer and early autumn (Fig. 2.2) when strong and persistent winds occur with undersaturated surface water and bottom waters that are highly oversaturated caused in part by the buildup of respired CO_2 from organic matter remineralization over the shelf during the growing season [*Hales et al.,* 2005a; *Hales et al.,* 2006]. Wind conditions during the late summer and early autumn have the potential to expose strongly supersaturated bottom water to the atmosphere, resulting in the massive variability in surface pCO_2 observed during this study; simultaneously, rapid photosynthetic response to abundant upwelled nutrients has the potential to draw surface pCO_2 to levels far below atmospheric saturation. Winter and early spring surface water pCO_2 does not show this degree of variability (Fig. 2.2) because winds during this time are predominantly downwelling-favorable (Fig. 2.3), driving offshore waters towards the coast and not exposing deep high-pCO_2 water to the atmosphere. Upwelling conditions

show a transition, with low pCO_2 persisting through the early part of the upwelling season, and high and highly variable values seen later in the summer. Measurements of bottom water pCO_2 show that they are near 1000 µatm in May, but significantly exceed that level by August [*Hales et al.,* 2005a]. If these waters are exposed during early upwelling season southward wind events, the elevated CO_2 levels will be lower than seen later in the summer. Ventilation of this high-pCO_2 water in late summer/early autumn has the potential then to drive the largest fluxes. The period of prolonged outgassing of CO_2 to the atmosphere in the summer of 2008 may not occur every year, but is in part be driven by the co-occurrence of persistent and strong upwelling conditions and typically high late summer upwelling source water pCO_2 concentrations.

The Spring Atmospheric CO_2 Sink

The surface oxygen content was oversaturated with respect to equilibration with the atmosphere over the majority of the April to June 2008 period at NH10 (Fig. 2.6). Oxygen oversaturation has been consistently observed over the OR shelf during the growing season [*Hales et al.,* 2006] and maintenance of these conditions in the face of gas exchange suggests high rates of net primary production. This is also indicated by the persistent undersaturated pCO_2 conditions relative to the atmosphere over this period (Fig. 2.6). Note that these spring CO_2 sink conditions seem to be more consistent between years than are the late-summer/early autumn conditions discussed above (Fig. 2.2). Satellite chlorophyll data (Fig. 2.5) and buoy data (Fig. 2.6) show, however, that phytoplankton biomass was highest in spring near the Columbia River and generally low along the entire coast relative to the summer. The chemical signals of primary productivity occurring without the optical signals of phytoplankton standing stocks suggests one of two things; that the water mass at the mooring site in spring experienced high productivity elsewhere along the coast, not at our

mooring site, or that the system was experiencing high net productivity without a concurrent accumulation of biomass.

Given the low salinities observed in tandem with these geochemical signals (Fig. 2.6), the large signals of primary production occurring in the vicinity the Columbia River, and the mean southward flow this time of year, one possibility that must be explored is that this is the result of high net productivity occurring on the shelf near the Columbia River. An estimate of the transit time for a water mass from the Columbia River mouth to Newport is 10 to 27 days, given southward current speeds between 10 and 30 cm s^{-1} [*Huyer*, 1977; *Kosro*, 2005] over the shortest possible transit pathway. As a water mass ages, there is often a lag time between measures of biomass and the chemical signals of primary production [e.g. *Martz et al.*, 2009]. In this setting, primary productivity is often supported by large coastal diatoms [*Wilkerson et al.*, 2000], which are known to have very rapid bloom dynamics [*Dugdale et al.*, 2006]. Rapid growth and nutrient uptake initiates the bloom, and rapid termination of the bloom follows nutrient depletion [*Wetz and Wheeler*, 2003]. The large individual cells and chains sink rapidly, leaving behind the signals of CO_2 depletion and O_2 enrichment, which will be reset towards atmospheric saturation only slowly by gas exchange. The response time for gas exchange is uncertain but can be estimated. Assuming an average wind speed of 10 m s^{-1} (consistent with the high estimated water velocities), the wind-speed dependences of *Wanninkhof* [1992] or *Ho et al.* [2006] and a 10 m surface mixed layer (consistent with the plume-associated low salinity waters), the gas exchange response time will be about 2-3 days for a simple gas like O_2 and approximately 10 times longer for CO_2 [*Sarmiento and Gruber*, 2006]. Therefore, it is possible that the spring/early summer undersaturated pCO_2 conditions on the shelf result from non-local productivity associated with the Columbia River system.

Potential problems with this explanation include (1) the shortest-distance transport pathway is simplistic, and does not account for the fact that strong upwelling circulation typically pushes the plume offshore of the shelfbreak, (2) southward velocities vary across the shelf from ~50 cm s^{-1} in the upwelling jet [*Barth et al.*, 2005] to 0 or even northward nearshore [*Huyer and Smith*, 1978], and (3) the observed close coupling between O_2 oversaturation and pCO_2 undersaturation is not consistent with the transport arguments given above. Oxygen appears oversaturated in our record, when over the time period of our transport argument above it should have reached equilibrium with the atmosphere if the supporting productivity were confined to the mouth of the Columbia River. It is possible that the phytoplankton community was efficiently exported, so we were not able to observe 'bloom-like' concentrations of chlorophyll in tandem with the low pCO_2 and high O_2 at the mooring. The winter and spring freshening from Oregon coastal rivers is also likely important and hard to distinguish from Columbia River inputs early in the season from salinity alone. These rivers deliver most of their annual discharge in the winter/early spring [e.g. *Chase et al.*, 2007], and the early season freshening must come at least in part from those sources.

Summer pCO_2 Variability

Given the magnitude of the effect of the summer upwelling events on the mooring and ship-based pCO_2 observations, one would expect the increase in pCO_2 to be accompanied by the upwelling of nutrients that could fuel photosynthetic CO_2 drawdown [e.g. *Hales et al.*, 2005b]. The ship-based chlorophyll observations reveal only moderately high values north and south of the upwelling plume and off the shelf during July (Fig. 2.7). MODIS satellite

chlorophyll data and our mooring observations (Figs. 2.5 and 2.6) suggest a ~20-day lag between the physical signals of upwelling and the chlorophyll response from the July upwelling event on the shelf, which is long compared to coastal diatom responses [*Dugdale et al.*, 2006]. The MODIS chlorophyll data show that a weak bloom (3 mg m^{-3}) translated offshore during this event, but chlorophyll concentrations did not increase above 5 mg m^{-3} until the bloom moved back onshore when upwelling conditions abated toward the end of July (Fig. 2.6). That is, there was only a minor biological response from this intense upwelling period until the winds decreased and reversed at the end of July 2008, allowing high-pCO_2 surface water to persist on the shelf for nearly a two-month period. We are currently uncertain why the photosynthetic community did not respond as quickly as expected, but believe there may have been a shift in the community composition compared to those seen early in the season. This issue will be addressed in a future publication.

Sea-air CO_2 fluxes

The fluxes calculated from all buoy data collected at NH10 between August 2007 and May 2010 were averaged for each Julian day to produce a composite year of sea-air CO_2 flux for the central Oregon shelf (Fig. 2.8). From this record the central Oregon mid shelf is a small net annual CO_2 sink of -0.3 ± 6.8 mol m^{-2} yr^{-1} (-0.7 ± 18.7 mmol m^{-2} d^{-1}). Our upwelling season estimate is 4.4 ± 24.4 mmol m^{-2} d^{-1} (April to October), which contrasts the previous average estimate of -20 mmol m^{-2} d^{-1} [*Hales et al.*, 2005a]. The composite year of sea-air CO_2 flux shows that the late upwelling season (June to September) is a period when the central Oregon mid shelf can be a substantial CO_2 source of 14.3 ± 30.6 mmol m^{-2} d^{-1}. This source period in 2008 was compensated by the mild and strong sink conditions during the winter and spring, respectively. This caused the system to function as only a weak sink on an annual basis. The dynamic nature

of sea-air CO_2 fluxes on the central Oregon mid shelf is clearly shown in Figure 2.8, which adds uncertainty to our estimates of average sea-air CO_2 fluxes (reported here as standard deviations). Different years may experience different conditions based on the variable nature of this upwelling system.

It is at this time not clear why the high-pCO_2 water observed in June and July 2008 persisted as long as it did, or how representative these conditions are of other years. Until this study, there were no pCO_2 observations during these types of events, although wind records suggest they have probably occurred before. For example, there were periods of persistent, strong, upwelling winds that coincided with the most extreme hypoxic events of 2002 and 2006 [*Grantham et al.*, 2004; *Chan et al.*, 2008]. In 2008 winds were upwelling-favorable for the majority of time between May and August, but in June and July there were multiple 10-day or greater periods of 10-day running-averaged southward wind magnitude in excess of 4 m s^{-1} (Fig. 2.3) that coincided with the observed high-pCO_2 water at the surface. Wind events like this might represent a threshold that drives periods of high pCO_2. It is clear that these wind conditions have occurred repeatedly in the past (e.g. 2002, 2005 and 2006; Fig. 9), but why high-pCO_2 water persisted on the shelf in 2008 as long as it did is unclear. The co-occurrence of upwelled-source waters that are strongly enriched in CO_2 and nutrient levels with fast-growing coastal diatom phytoplankton communities makes this system inherently tend toward extreme variations. If the productivity response is fast in comparison to supply of upwelled waters, very low surface pCO_2 conditions will be experienced; if the balance is tipped such that upwelled waters are supplied faster than the biology can respond, very high levels of surface pCO_2 will dominate.

Previous work from observations in May and August 2001 has shown that the Oregon coast is a strong sink for atmospheric CO_2 during the upwelling season [*Hales et al.*, 2005a]. There are three important points that help explain the differences in the results between this prior study and ours. First, in 2001 there were no extended periods of uninterrupted, strong upwelling favorable winds comparable to that seen in mid-late summer of 2008 (Fig. 2.9), suggesting a fundamentally different forcing regime during that time. Second, only two two-week periods bracketing the upwelling season were sampled during this prior study and we now have continuous measurements through the entire season. Although the wind records of 2001 do not suggest a major event was missed, it is easy to imagine a sparse sampling of the time-series record we present here that could yield different net flux estimates. Third, the results of *Hales et al.* [2005a] were strongly influenced by observations over the broad shelf region to the south of the NH line, where the surface pCO_2 levels were more uniformly undersaturated. The sea-air CO_2 flux estimates presented here are from the central Oregon mid shelf, and there is likely to be important along- and cross-shelf variability not captured here in our flux estimates. It is clear from the contrasting results between the 2001 work and the present study that spatially and temporally comprehensive and well-resolved pCO_2 observations are needed to diagnose the dynamic nature of sea-air CO_2 fluxes on the Oregon shelf.

CONCLUSIONS

These data indicate four important features about the Oregon shelf: (1) The net fluxes of the upwelling season are not canceled out by fluxes in the downwelling season, but rather the latter appears to be near-neutral or undersaturated with respect to sea-air exchange; (2) There are strong interannual variations in the system's functioning, particularly during the upwelling-season, that can change it from a strong sink in some years to a strong

source in others, casting uncertainty on the system's long-term role as source or sink; (3) the balance between the strength/persistence of upwelling-favorable wind forcing and photosynthetic response to that forcing is critically important in determining the overall function of the Oregon shelf, (4) this region is highly dynamic over a variety of time and space scales, and requires near continuous interannual observation to characterize the variability in pCO_2.

REFERENCES

Barth, J. A., and P. A. Wheeler (2005), Introduction to special section: Coastal Advances in Shelf Transport, *Journal of Geophysical Research*, *110*, C10S01, doi: 10.1029/2005JC003124.

Barth, J. A., S. D. Pierce, and T. Cowles (2005), Mesoscale structure and its seasonal evolution in the northern California Current System, *Deep-Sea Research II*, *52*, 5-28.

Behrenfeld, M. J., and P. G. Falkowski (1997), Photosynthetic rates derived from satellite-based chlorophyll concentration, *Limnology and Oceanography*, *42*(1), 1-20.

Cai, W.-J., M. Dai, and Y. Wang (2006), Air-sea exchange of carbon dioxide in ocean margins: A province-based synthesis, *Geophysical Research Letters*, *33*, L12603, doi:12610.11029/12006GL026219.

Chan, F., J. A. Barth, J. Lubchenco, A. Kirincich, H. Weeks, W. T. Peterson, and B. A. Menge (2008), Emergence of Anoxia in the California Current Large Marine Ecosystem, *Science*, *319*(5865), doi:10.1126/science.1149016.

Chase, Z., P. G. Strutton, and B. Hales (2007), Iron links river runoff and shelf width to phytoplankton biomass along the U.S. West Coast, *Geophysical Research Letters*, *34*, L04607, doi: 04610.01029/02006GL028069.

Chavez, F. P., J. Ryan, L.-C. E. Salvador, and Ñ. C. Miguel (2003), From Anchovies to Sardines and Back: Multidecadal Change in the Pacific Ocean, *Science*, *299*(217), doi:10.1126/science.1075880.

Chavez, F. P., and T. Takahashi (2007), Coastal Oceans*Rep.*, 157-166 pp, U.S. Climate Change Science Program, Washington, DC.

Colbert, D., and J. McManus (2003), Nutrient Biogeochemistry in an Upwelling-Influenced Estuary of the Pacific Northwest (Tillamook Bay, Oregon, USA), *Estuaries*, *26*(5), 1205-1219.

DeGrandpre, M. D., T. R. Hammar, S. P. Smith, and F. L. Sayles (1995), In situ measurements of seawater pCO2, *Limnology and Oceanography*, *40*(5), 969-975.

Dugdale, R. C., F. P. Wilkerson, and A. Morel (1990), Realization of new production in coastal upwelling areas: A means to compare relative performance, *Limnology and Oceanography*, *35*(4), 822-829.

Dugdale, R. C., F. P. Wilkerson, V. E. Hogue, and A. Marchi (2006), Nutrient controls on new production in the Bodega Bay, California, coastal upwelling plume, *Deep-Sea Research II*, *53*(25-26), 3049-3062.

Feely, R. A., C. L. Sabine, M. Hernandez-Ayon, D. Ianson, and B. Hales (2008), Evidence for Upwelling of Corrosive "Acidified" Water onto the Continental Shelf, *Science*, *320*(5882), 1490-1492.

Friederich, G. E., P. M. Walz, M. G. Burczynski, and F. P. Chavez (2002), Inorganic carbon in the central California upwelling system during the 1997-1999 El Nino-La Nina event, *Progress In Oceanography*, *54*(1-4), 185-203.

Grantham, B. A., F. Chan, K. Nielsen, D. S. Fox, J. A. Barth, A. Huyer, J. Lubchenco, and B. A. Menge (2004), Upwelling-driven nearshore hypoxia signals ecosystem and oceanographic changes in the northeast Pacific, *Nature*, *429*, 749-754.

Hales, B., D. Chipman, and T. Takahashi (2004), High-frequency measurements of partial pressure and total concentration of carbon dioxide in seawater using microporous hydrophobic membrane contactors, *Limnology and Oceanography: Methods*, *2*, 356-364.

Hales, B., T. Takahashi, and L. Bandstra (2005a), Atmospheric CO2 uptake by a coastal upwelling system, *Global Biogeochemical Cycles*, *19*, GB1009, doi: 1010.1029/2004GB002295.

Hales, B., J. N. Moum, P. Covert, and A. Perlin (2005b), Irreversible nitrate fluxes due to turbulent mixing in a coastal upwelling system, *Journal of Geophysical Research*, *110*, C10S11, doi:10.1029/2004JC002685.

Hales, B., L. Karp-Boss, A. Perlin, and P. A. Wheeler (2006), Oxygen production and carbon sequestration in an upwelling coastal margin, *Global Biogeochemical Cycles*, *20*, GB3001, doi: 3010.1029/2005GB002517.

Hales, B., W.-J. Cai, B. G. Mitchell, C. L. Sabine, and O. Schofield (2008), *North American Continental Margins: A Synthesis and Planning Workshop*, 110 pp., U.S. Carbon Cycle Science Program, Washington DC.

Hickey, B. (1989), Patterns and processes of circulation over the Washington continental shelf and slope, in *Coastal Oceanography of Washington and Oregon*, edited, Elsevier Science Publishers B.V., New York

Hickey, B., and N. S. Banas (2008), Why is the Northern End of the California Current System so Productive?, *Oceanography*, *21*(4), 91-107.

Ho, D. T., C. S. Law, M. J. Smith, P. Schlosser, M. Harvey, and P. Hill (2006), Measurements of air-sea gas exchange at high wind speeds in the Southern Ocean: Implications for global parameterizations, *Geophysical Research Letters*, *33*, L16611, doi: 16610.11029/12006GL026817.

Huyer, A. (1977), Seasonal variation in temperature, salinity, and density over the continental shelf off Oregon, *Limnology and Oceanography*, *22*(3), 442-453.

Huyer, A., and R. L. Smith (1978), Physical characteristics of Pacific northwestern coastal waters. , in *The Marine Plant Biomass of the Pacific Northwest Coast*, edited by R. Knauss, pp. 37-55, Oregon State University Press.

Huyer, A., P. A. Wheeler, P. T. Strub, R. L. Smith, R. Letelier, and P. M. Kosro (2007), The Newport line off Oregon - Studies in the North East Pacific, *Progress in Oceanography*, *75*, 126-160.

Kosro, P. M. (2005), On the spatial structure of coastal circulation off Newport, Oregon, during spring and summer 2001 in a region of varying shelf width, *Journal of Geophysical Research*, *110*, C10S06, doi: 10.1029/2004JC002769.

Liu, K.-K., L. Atkinson, R. A. Quiñones, and L. Talaue-McManus (2010), Biogeochemistry of Continental Margins in a Global Context, in *Carbon and Nutrient Fluxes in Continental Margins*, edited by K.-K. Liu, L. Atkinson, R. A. Quiñones and L. Talaue-McManus, pp. 3-24, Springer, Stockholm.

Martz, T. R., M. D. DeGrandpre, P. G. Strutton, W. R. McGillis, and W. M. Drennan (2009), Sea surface pCO_2 and carbon export during the Labrador Sea spring-summer bloom: An in situ mass balance approach, *Journal of Geophysical Research*, *114*(C09008), doi:10.1029/2008JC005060.

Muller-Karger, F., R. Varela, R. Thunell, R. Luerssen, C. Hu, and J. J. Walsh (2005), The importance of continental margins in the global carbon cycle, *Geophysical Research Letters*, *32*, L01602, doi: 01610.01029/02004GL021346.

Sarmiento, J. L., and N. Gruber (2006), *Ocean Biogeochemical Dynamics*, Princeton University Press, Princeton.

Schwing, F. B., T. Murphree, L. deWitt, and P. M. Green (2002), The evolution of oceanic and atmospheric anomalies in the Pacific during the El Niño and La Niña events of 1995-2001, *Progress in Oceanography*, *54*, 459-491.

Strub, P. T., J. S. Allen, A. Huyer, and R. L. Smith (1987), Seasonal Cycles of Currents, Temperatures, Winds, and Sea Level over the Northeast Pacific Continental Shelf: 35ºN to 48ºN, *Journal of Geophyiscal Research*, *92*(C2), 1507-1526.

Takahashi, T., J. Olafsson, J. G. Goddard, D. W. Chipman, and S. C. Sutherland (1993), Seasonal Variation of CO2 and Nutrients in the High-Latitude Surface Oceans: a Comparative Study, *Global Biogeochemical Cycles*, *7*(4), 843-878; doi:810.1029/1093GB02263.

Takahashi, T., et al. (2009), Climatological mean and decadal change in surface ocean pCO2 and net sea-air CO2 flux over the global oceans, *Deep-Sea Research II*, *56*, 554-577.

van Geen, A., R. K. Takesue, J. Goddard, T. Takahashi, J. A. Barth, and R. L. Smith (2000), Carbon and nutrient dynamics during coastal upwelling off Cape Blanco, Oregon, *Deep-Sea Research II*, *47*, 975-1002.

Wanninkhof, R. (1992), Relationship Between Wind Speed and Gas Exchange Over the Ocean, *Journal of Geophysical Research*, *97*(C5), 7373-7382.

Wetz, M. S., and P. A. Wheeler (2003), Production and partitioning of organic matter during simulated phytoplankton blooms, *Limnology and Oceanography*, *48*(5), 1808-1817.

Wetz, M. S., B. Hales, Z. Chase, P. A. Wheeler, and M. M. Whitney (2006), Riverine input of macronutrients, iron, and organic matter to the coastal ocean off Oregon, U.S.A., during the winter, *Limnology and Oceanography*, *51*(5), 2221-2231.

Wilkerson, F. P., R. C. Dugdale, R. M. Kudela, and F. P. Chavez (2000), Biomass and productivity in Monterey Bay, California: contribution of the large phytoplankton, *Deep-Sea Research II*, *47*, 1003-1022.

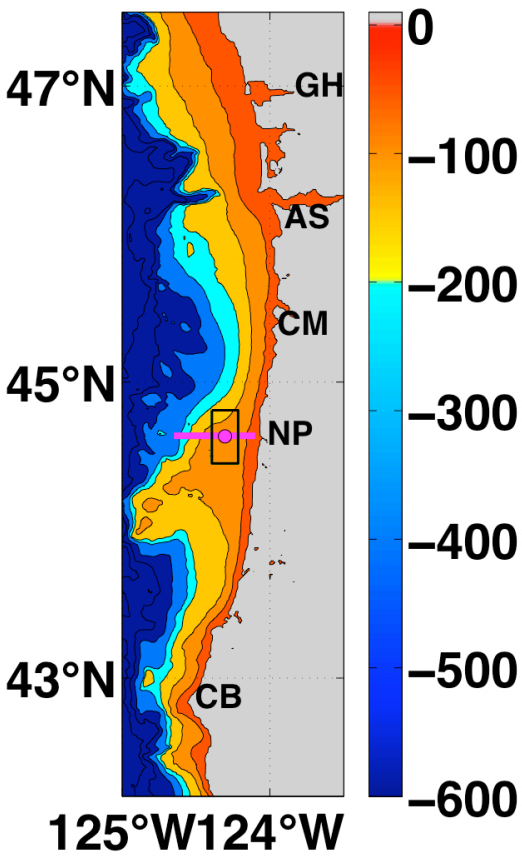

Figure 2.1: ETOPO1 1-Arc Minute Global Relief Model bathymetry for the Oregon highlighting the shelf (0 – 200 m). Coastal locations mentioned in the text are shown (GH = Grays Harbor, WA; AS = Astoria, OR; CM = Cape Meares, OR; NP = Newport, OR; CB = Cape Blanco, OR). Circle near Newport, OR is the position of the NH10 buoy, the platform for our moored system. The east-west bar is the Newport Hydrographic line (NH line) extending from shore out past the shelf break (25 nm). The region where data are selected for construction of a composite year of pCO_2 (box; dimensions are 44.45°N to 44.81°N and 124.3925°W to 124.2155°W) is inshore of the 200 m isobath, centered on the NH10 buoy position (44.633ºN, 124.304ºW), extends ~20 nm in the north/south direction and ~10 nm in the east/west direction, and represents the central Oregon mid shelf. Bathymetry data provided by the National Geophysical Data Center (http://www.ngdc.noaa.gov/mgg/global/global.html).

Table 2.1: Dates of cruise observations spanning August 2007 to September 2008.

OSU R/V *Wecoma*	Aug. 14-31, 2007
OSU R/V *Elakha*	Oct. 12, 2007
OSU R/V *Wecoma*	Nov. 1-19, 2007
OSU R/V *Elakha*	Nov. 20, 2007
OSU R/V *Elakha*	Feb. 11, 2008
OSU R/V *Elakha*	Feb. 14, 2008
OSU R/V *Elakha*	Feb. 17, 2008
OSU R/V *Wecoma*	Feb. 20-21, 2008
OSU R/V *Elakha*	Mar. 4, 2008
OSU R/V *Wecoma*	Mar. 18-21, 2008
OSU R/V *Elakha*	Mar. 24-25, 2008
OSU R/V *Wecoma*	Apr. 10-17, 2008
NOAA Ship *McArthur II*	Apr. 20-27, 2008
OSU R/V *Elakha*	May 5-6, 2008
NOAA Ship *Miller Freeman*	May 21-23, 2008
OSU R/V *Wecoma*	May 28-June 7, 2008
OSU R/V *Elakha*	Jul. 1, 2008
OSU R/V *Elakha*	Jul. 2-3, 2008
NOAA Ship *McArthur II*	Jul. 12-21, 2008
OSU R/V *Elakha*	Aug. 22, 2008
OSU R/V *Wecoma*	Sep. 13-24, 2008

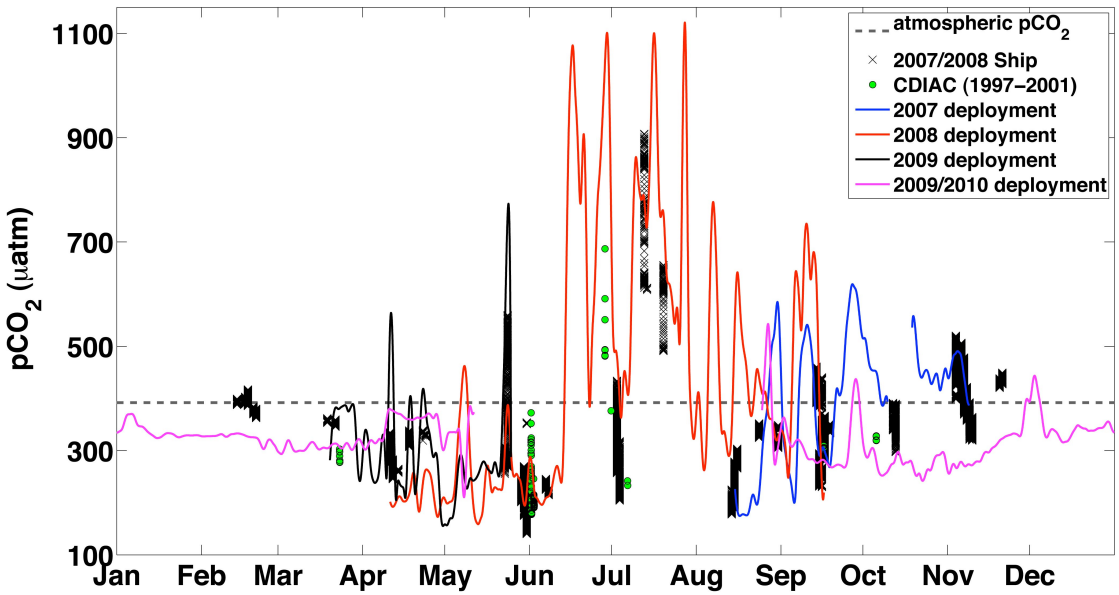

Figure 2.2: Composite seasonal cycle of pCO_2 (µatm) collected from ships (within the box region defined in Fig. 2.1) and moorings near the NH10 station position off Newport, Oregon.

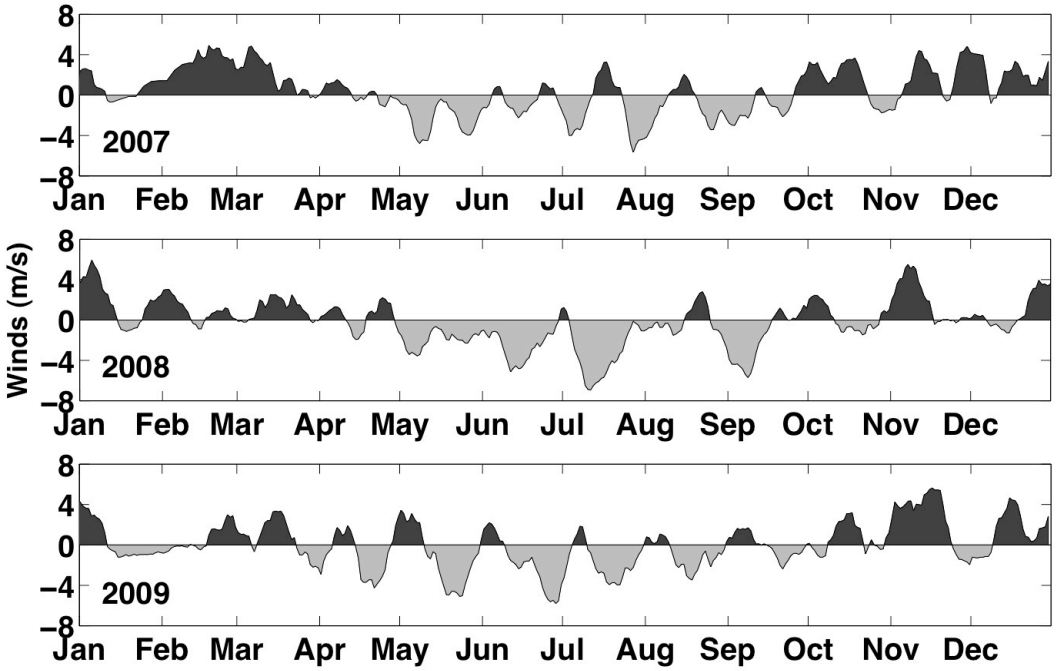

Figure 2.3: 10-day running averaged daily median N/S wind magnitude for 2007 (upper panel), 2008 (middle panel) and 2009 (lower panel) observed at the NOAA C-Man station in Newport, OR. Dark is northward (downwelling-favorable) and light is southward (upwelling-favorable).

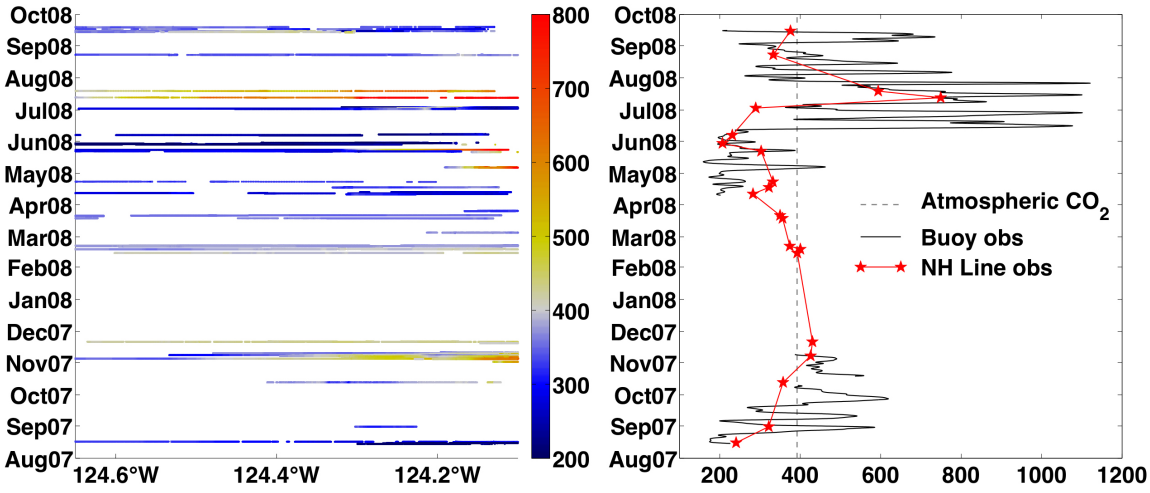

Figure 2.4: Left panel is pCO_2 (µatm) from all cruise data collected over the shelf along the NH Line (shown in Fig. 2.1). Right panel is buoy and ship (averaged for the central Oregon mid shelf region defined in Fig. 2.1) pCO_2 (µatm) data plotted with the average atmospheric pCO_2 measured during this study (392 µatm).

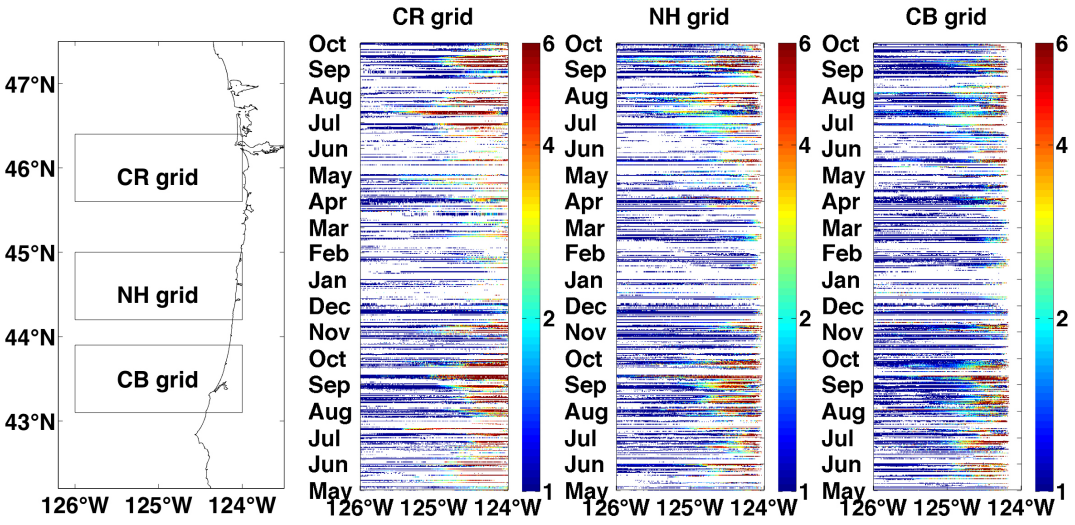

Figure 2.5: MODIS Level 2 chlorophyll (mg m^{-3}) from individual satellite passes (usually two per day) from May 2007 to October 2008 for select regions off the Columbia River (CR grid), Newport, OR (NH grid) and Coos Bay, OR (CB grid). Data are plotted in log scale.

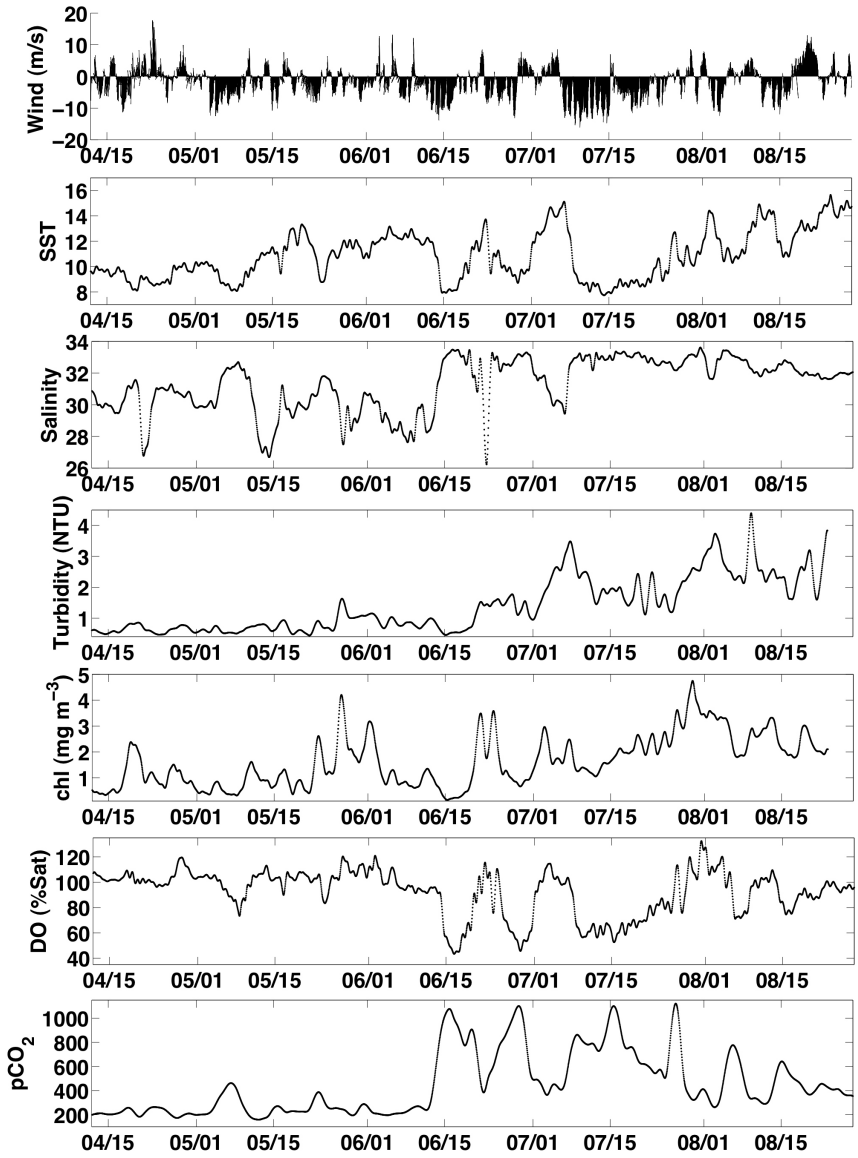

Figure 2.6: Hourly vector winds (m/s) from the NOAA C-Man station in Newport, OR and SST (°C), salinity, turbidity (NTU), chlorophyll (mg m^{-3}), dissolved oxygen (% saturation) and pCO_2 (µatm) from the NH10 buoy for the time period April 12th to August 28th, 2008.

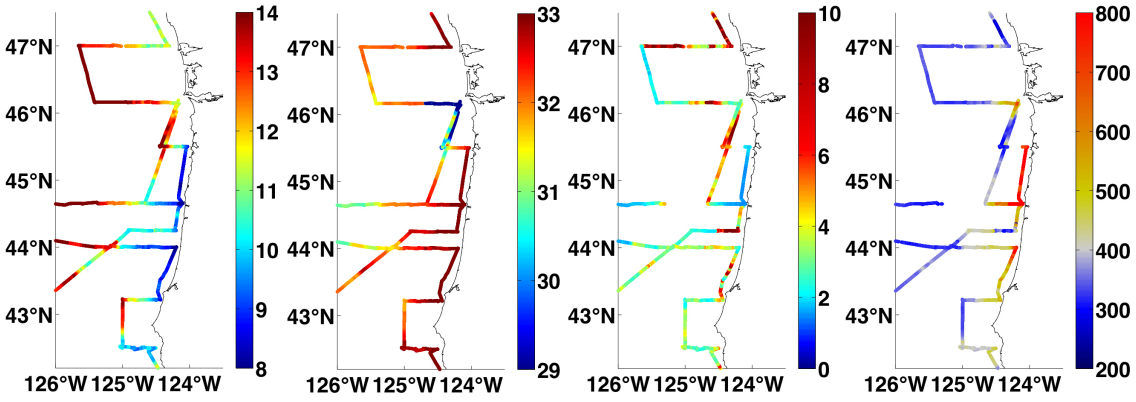

Figure 2.7: Underway SST (° C), salinity, chlorophyll (mg m^{-3}) and pCO_2 (µatm) from cruises during July 2008.

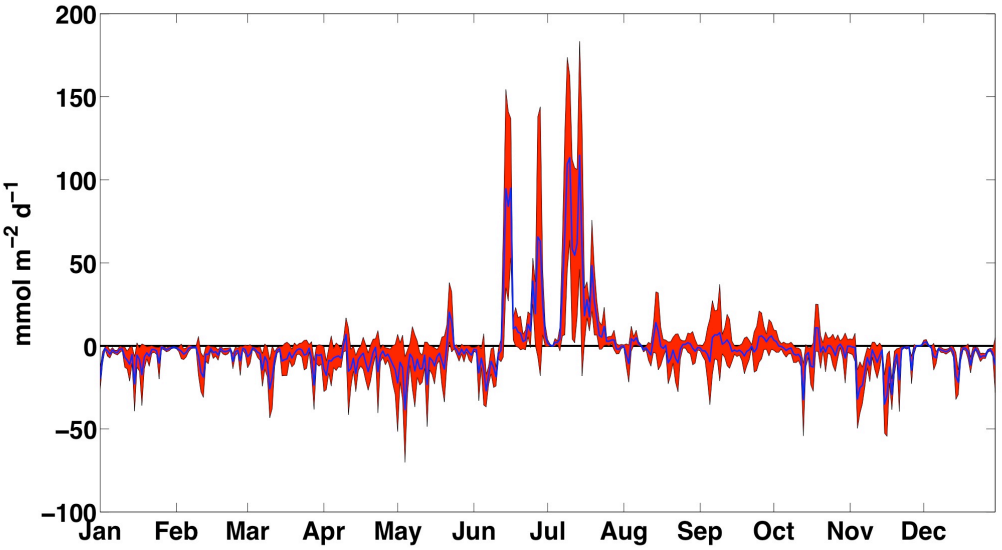

Figure 2.8: A composite year of sea-air CO_2 flux (mmol m^{-2} d^{-1}) on the central Oregon mid shelf calculated from NH10 buoy data. The blue line is the daily mean flux, and the red area represents the standard deviation about the daily means.

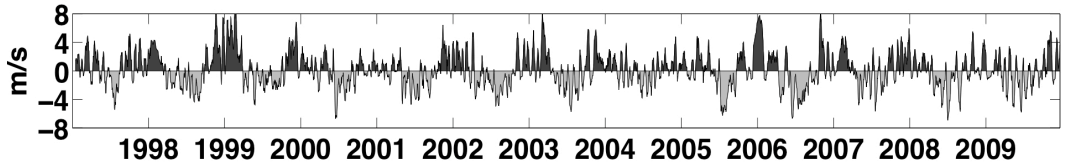

Figure 2.9: Record of 10-day running averaged daily median N/S wind component (m/s) from Newport, OR from January 1997 through December 2009. Dark is northward (downwelling-favorable) and light is southward (upwelling-favorable).

CHAPTER 3: Sea-Air CO_2 Fluxes in the Western Canadian Coastal Ocean

Wiley Evans

For submission to *Progress in Oceanography*

Elsevier

ACKNOWLEDGEMENTS

We would like to express our deep gratitude to Marc Trudel for allowing our participation in his High Seas Salmon cruises aboard the CCGS *W.E. Ricker*. We thank Marc also for the valued discussions of this work through its development. We also thank the captains and crews of the CCGS *W.E. Ricker* and *J.P. Tully*. We thank the Earth Systems Research Laboratory for providing the annual mean atmospheric CO_2 used in the reanalysis of CDIAC pCO_2 data. This work was supported by NSF Chemical Oceanography award OCE-0752576.

ABSTRACT

There is large uncertainty in carbon dioxide (CO_2) exchange between the ocean and atmosphere on coastal margins due to the broad range of spatial and temporal variability inherent to these regions. The western Canadian coastal margin is a data-limited region thought to be a moderate atmospheric CO_2 sink because outgassing in winter almost counterbalances strong CO_2 drawdown in summer. Here we present both an analysis of historical CO_2 partial pressure (pCO_2) measurements from the southwest Vancouver Island shelf and a new data set of winter, summer and autumn surface ocean pCO_2 collected over a larger portion of the margin than has been previously sampled. Climatologies of sea-air CO_2 flux were calculated from the historical measurements using two approaches: one based on fluxes calculated from climatological sea-air pCO_2 differences and gas transfer velocity, and the other from instantaneous flux estimates. Area-specific and area-weighted sea-air CO_2 fluxes were also calculated from the new data for subregions of the margin. These independent analyses show dominant outgassing of CO_2 in autumn relative to winter. Fluxes from the climatologies indicate spring is the strongest atmospheric CO_2 sink period, and both data sets show drawdown in summer. Our climatologies indicate autumn and winter outgassing nearly balance spring and summer drawdown on the southwest Vancouver Island shelf. Fluxes from the new data also show the straits around Vancouver Island have a significant impact on area-weighted estimates of sea-air CO_2 flux for this coastal region of complex bathymetry.

INTRODUCTION

The role of coastal margins in the exchange of CO_2 with the atmosphere is poorly constrained because of the significant spatial and temporal heterogeneity in these regions [*Hales et al.,* 2008]. Existing data suggest that most open shelves in the mid to high latitudes are sinks for atmospheric CO_2 [*Borges et al.,* 2005; *Cai et al.,* 2006], while inner waterways and estuaries act as sources [*Borges et al.*, 2005; *Cai et al.*, 2006; *Chen and Borges*, 2009]. However, few coastal regions have sufficient spatial and temporal coverage of pCO_2 data to make precise estimates of net annual CO_2 exchange. The few coastal sites where sufficient temporal coverage of data exists show the importance of resolving the seasonal cycles, and that interannual sources of variability could be the dominant cause of fluctuations in sea-air CO_2 fluxes [*Evans et al.*, 2011; *Fransson et al.*, 2006; *Friederich et al.*, 2002; *McNeil*, 2010]. Inadequacies in existing data highlight the need to increase the temporal and spatial coverage of observations to better characterize coastal regions.

The western Canadian coastal margin (British Columbia; BC) is an important region of high primary productivity along the North American west coast [*Ware and Thomson*, 2005]. Thus far it has been characterized as a weak to moderate annual sink for atmospheric CO_2 based on spatially limited data [*Chavez and Takahashi*, 2007] and a biogeochemical model [*Ianson and Allen*, 2002]. Until recently, data with the greatest spatial coverage existed for summer [*Ianson et al.*, 2003; *Nemcek et al.*, 2008], and the best temporally-resolved data are available for the southwest Vancouver Island shelf and within the Strait of Juan de Fuca [*Chavez and Takahashi*, 2007; *Hales et al.*, 2008; *Wong et al.*, 2010]. There are also very limited measurements of CO_2 in the other straits and fjords that make up the complex BC coastline [*Nemcek et al.*, 2008]. The annual flux of CO_2 for this region has been estimated to be near -6 g C m^{-2} yr^{-1} [negative

fluxes are directed into the ocean; *Ianson and Allen*, 2002; *Chavez and Takahashi*, 2007]. The estimate from *Chavez and Takahashi* [2007] is based on an analysis of the Carbon Dioxide Information and Analysis Center (CDIAC) pCO_2 measurements collected around North America from the coast to 1000 km from shore. These data were combined into a monthly-resolved composite year and binned into 1° latitude by 1° longitude pixels. These pixels were then averaged into 5°-wide latitude zones around the North American continent, and averaged into nearshore and offshore bands within each zone. The nearshore bands extended from the coastline to 80 km from shore, and the annual mean flux for the BC margin was weakly negative (approximately -5 g C m^{-2} yr^{-1}). The seasonal variability was the largest of any zone on the North American Pacific coast (see their Fig. 15.4). *Hales et al.* [2008] subsequently showed that most of the pixels on the western Canadian coastal margin had observations of pCO_2 in fewer than two months of the composite year. The majority of BC margin observations in the CDIAC data set are on the southwest Vancouver Island shelf because of the tracks of ships-of-opportunity exiting the Strait of Juan de Fuca enroute to the open North Pacific.

At seasonal time scales, observations from CDIAC, *Ianson et al.* [2003], and *Nemcek et al.* [2008] show strong drawdown of surface ocean pCO_2 occurs on the shelf in the summer. This region is the most northern portion of the California Current [*Pennington et al.,* 2010], so summer values on the shelf at times can exceed atmospheric levels as a result of wind-driven upwelling that brings high-CO_2 water to the surface [*Nemcek et. al.*, 2008]. Other areas where high-pCO_2 surface waters have been observed are in the straits around Vancouver Island [*Ianson et al.*, 2003; *Nemcek et al.*, 2008], and in the nearshore region of the southwest Vancouver Island shelf where low salinity water from the Strait of Juan de Fuca flows northward in the Vancouver Island Coastal Current

[*Ianson et al.,* 2003]. Data for the remainder of the year only existed for the southwestern coast of Vancouver Island until now.

Here we present new data from a large portion of the margin during winter, summer and autumn. These new data are placed in context with an analysis of the historical CDIAC measurements from the southwestern Vancouver Island shelf. We first calculate climatologies using the CDIAC data from this well-resolved region of the BC margin, and then estimate the seasonal and net annual sea-air CO_2 fluxes. We then use the new observations to make estimates of the sea-air CO_2 fluxes for winter, summer and autumn for six distinct subregions of the BC margin. These subregions were chosen to delineate the large semi-enclosed body of water north of Vancouver Island, some of the major straits around Vancouver Island, and two areas of the Vancouver Island shelf that are separated by a large promontory known as Brooks Peninsula. Area-specific flux estimates for each subregion are then combined to create area-weighted fluxes for each season. Both analyses of the historical and new data show the dominance of outgassing in autumn. Comparing the area-specific and area-weighted fluxes reveals the importance of including other regions beyond just the shelf (*i.e.* the straits) in estimates of sea-air CO_2 exchange on the BC margin. These analyses have shown that the greatest exchange of CO_2 with the atmosphere occurs in spring (uptake) and autumn (outgassing), and that the autumn and winter conditions nearly balance spring and summer CO_2 drawdown in this dynamic coastal region.

METHODS

To examine sea-air CO_2 fluxes on the western Canadian coastal margin, we analyzed historical measurements of pCO_2 from the CDIAC repository and

collected new pCO_2 data over a large portion of the margin using two different ships during three seasons. The Canadian Coast Guard ship (CCGS) *W.E. Ricker* was equipped with a new underway pCO_2 measurement system [referred to as the OSU underway pCO_2 system; *Hales et al.*, 2004, as modified by *Evans et al.,* 2011] for cruises in autumn (October 8 to November 14, 2008) and winter (February 25 to March 14, 2009). Summer data were collected using the Fisheries and Oceans Canada, Institute of Ocean Sciences' (IOS) pCO_2 system during the West Coast Ocean Acidification cruise aboard the CCGS *J.P. Tully* from July 20 to August 15, 2010. The intake depth for the seawater flow-through system was 3 m on both ships.

The sea-air CO_2 flux estimates were made from data collected within specific subregions of the BC coastal margin (Fig. 3.1). These subregions comprised two areas of the Vancouver Island shelf (subregions 1 and 2) separated by Brooks Peninsula, the large semi-enclosed body of water north of Vancouver Island (collectively referred to as Queen Charlotte Sound, but is a combination of Queen Charlotte Sound and Hecate Strait; subregion 3), the straits on the northern side of Vancouver Island (collectively referred to as Johnstone Strait, but is a combination of Queen Charlotte Strait, Broughton Strait, Johnstone Strait and Discovery Passage; subregion 4), the Strait of Georgia (subregion 5), and the Strait of Juan de Fuca (subregion 6). The sections below describe the CDIAC data, the OSU underway pCO_2 system, the IOS underway pCO_2 system, the calculation of sea-air CO_2 fluxes from the new underway data, the calculations of flux climatologies from the CDIAC data, and the procedure for making area-weighted flux estimates from our new measurements on the BC margin.

CDIAC Data

We conducted an analysis of the CDIAC underway pCO_2 measurements (http://cdiac3.ornl.gov/waves/underway/) collected within subregion 1 shown in Fig. 3.1. This region is temporally well-resolved in the CDIAC data set, with the majority of measurements collected between January 1995 and August 2001, so our analysis focused on this period. To estimate sea-air CO_2 flux from these seawater measurements, annual mean atmospheric CO_2 was acquired from the Earth System Research Laboratory (ESRL; http://www.esrl.noaa.gov/gmd/ccgg/trends/global.html#global). The atmospheric values provided by ESRL were annual global averages of all marine surface sites in their network. Wind data were not present in the CDIAC underway pCO_2 data repository, so measurements from the Environment Canada buoy 46206 (position shown in Fig. 3.1) were used here to estimate the gas transfer velocity using the parameterization by *Ho et al.* [2006]. Gas transfer velocity (k_{600}, the gas transfer velocity for CO_2 at a Schmidt number of 600) was calculated from each hourly wind speed measurement made over the January 1995 to August 2001 period. A weekly running average of k_{600} was then calculated to reduce some of the high-frequency variability in the winds, but maintain variability relevant to surface seawater pCO_2, such as on the time scale of phytoplankton bloom formation (~days) and water mass residence time (~weeks).

OSU Underway pCO_2 System

The OSU underway pCO_2 measurement system used a LI-COR LI-840 infrared (IR) CO_2 analyzer to detect the CO_2 content of a gas stream equilibrated with flowing seawater using a miniature membrane contactor (Liqui-Cel 1x5.5). Prefiltration was achieved using a custom 8-μm tangential flow filter, in which 1-10% of the main flow was directed tangentially to the membrane contactor.

Sample liquid flow through the contactor was typically ~300 ml min^{-1}, while the atmospheric air carrier flow rate was fixed at 30 ml min^{-1}. Data were collected at 1 Hz, and standard sequences using gases of known CO_2 mixing ratio (xCO_2, ppm) were run every two hours and used to correct for IR analyzer inaccuracy. Atmospheric samples were also run with every standard sequence. Calibrated seawater xCO_2 data were adjusted to pCO_2 using the measured total pressure in the equilibrator. The calibrated atmospheric xCO_2 data were converted to pCO_2 using atmospheric pressure measured in the LI-COR cell. Measurement-temperature pCO_2 was then corrected to pCO_2 at sea surface temperature (SST) using the difference between ship intake and equilibrator temperatures following *Takahashi et al.* [1993] as recommended in *Dickson et al.* [2007], after accounting for the flow-based lag time (~ 50 s) between those two temperature sensor locations. Seawater flow rate was also monitored downstream of the pCO_2 equilibrator and used for data quality control; data from all measurements were removed during periods of low flow delivery to the equilibrator.

A computer and hard drive theft following the winter cruise resulted in the partial loss of pCO_2 data as well as GPS information. Therefore we were forced to present only the measurements that were collected near CTD casts, where we could interpolate the GPS and time information between adjacent cast locations. We were also required to correct the pCO_2 at the equilibrator temperature to pCO_2 at SST using a constant temperature offset of 0.5°C, which was the average temperature offset observed during the autumn cruise.

IOS Underway pCO_2 System

Summer cruise pCO_2 data collected aboard the CCGS *J.P. Tully* were measured using the IOS underway pCO_2 system described by *Wong et al.*

[2010]. This system used a traditional showerhead equilibrator that has a pressure compensator to maintain the equilibrator at atmospheric pressure. Inflow and equilibrator temperatures were measured continuously. xCO_2 was measured every 2.5 minutes in the equilibrated air with a LI-COR LI-6262 IR CO_2 sensor. A series of 20 consecutive measurements were made, and at the end of the seawater sample series gases of known xCO_2 were sampled to correct for IR analyzer inaccuracy. An atmospheric sample was run following the sampling of the gas standards, and the entire sequence of seawater, standard gas and atmospheric sampling took approximately 70 minutes. Calibrated seawater and atmospheric xCO_2 measurements were adjusted to pCO_2 using atmospheric pressure measured in line between the equilibrator and the LI-COR cell. Measurement-temperature pCO_2 was then corrected to pCO_2 at SST using the difference between inflow and equilibrator temperatures, after accounting for the flow-based lag time between those two temperature sensor locations (<2.5 min), and the relationship for the temperature effect on isochemical seawater described by *Takahashi et al.* [1993]. Seawater temperature and salinity were monitored continuously throughout the cruise using a Seabird SBE45.

Sea-air CO_2 Fluxes From New Data

The sea-air CO_2 flux (F_{CO2}) was calculated using the following equation:

$$F_{CO2} = k_{SST} K_{CO2} \Delta pCO_2,$$

where k_{SST} is the gas transfer velocity for CO_2 at the *in situ* SST (m d^{-1}), K_{CO2} is the solubility of CO_2 (mol m^{-3} atm^{-1}) and ΔpCO_2 is the seawater pCO_2 minus the atmospheric pCO_2 (atm). k_{SST} was converted from k_{600}, the gas transfer velocity for CO_2 at a Schmidt number of 600 (Schmidt number for CO_2 in freshwater at 20ºC), using the temperature relationship for the Schmidt number dependence of gas transfer velocity described by *Wanninkhof* [1992]. A salinity correction of k_{SST}

data was not conducted here because the difference between k_{SST} in freshwater versus saltwater (S=35) is on the order of 4%. The ΔpCO_2 for each cruise was calculated as the difference between the seawater pCO_2 measurements collected within each subregion and an average of the atmospheric pCO_2 measured during each cruise.

We lack ship-based measurement of winds, therefore we used wind speeds from the Port Hardy Airport on Vancouver Island, Environment Canada buoys 46206, 46204, and 46131, and the NOAA NDBC buoy 46088 (positions shown in Fig. 3.1) to calculate k_{600} for each subregion using the parameterization by *Ho et al.* [2006]. These wind data were hourly (with the exception of NOAA NDBC buoy 46088 record that was 10 minute winds) and were interpolated to the temporal resolution of the pCO_2 data. This treatment inherently makes the assumption of spatio-temporal coherence in the wind fields across each subregion, which introduces a source of uncertainty. While the winds are probably not coherent over such large distances, any lack of wind coherence is not likely to have short-term correlation to pCO_2. That is, surface seawater pCO_2 does not correlate with the wind speed.

Note that subregion 2 contained no reliable wind record (Fig. 3.1). A cross-correlation analysis was conducted on the wind records from buoys 46206 and 46204 over a 6-month period (August 1, 2009 to March 1, 2010) to determine the coherence of the records between these buoys. These winds were most coherent at a 1-hour lag ($r = 0.66$), and there was no large offset between these two wind speed records after accounting for the lag. Because of the proximity of subregion 2 to buoy 46204 and the fact that the winds were not

largely different between the two buoy locations, winds from 46204 were used to compute fluxes in subregion 2.

CDIAC Sea-Air CO_2 Flux Climatologies

We calculated sea-air CO_2 flux climatologies from the CDIAC data using two approaches. For the first approach we calculated climatologies of ΔpCO_2, solubility, and k_{600} from the 81-month records of CDIAC data and buoy winds using 30-Julian day running averages made at weekly intervals (Fig. 3.2). The k_{600} climatology was converted to k_{SST} using a climatology of SST computed in the same manner as for ΔpCO_2 and the *Wanninkhof* [1992] relationship for the Schmidt number dependence of gas transfer velocity. We then calculated the sea-air CO_2 flux as the product of these climatologies using the equation described in the previous section. For this approach (subsequently referred to as the climatology approach), we also estimated the variability in the flux as ± the product of the standard deviations from the 30-Julian day running averages of ΔpCO_2 and k_{SST} multiplied by the solubility climatology. For the second approach we calculated a climatology of sea-air CO_2 flux from individual fluxes computed by time-syncing the ΔpCO_2 and solubility with the weekly running average k_{600} record (Fig. 3.2). Prior to calculating individual fluxes, k_{600} was converted to k_{SST}. The second approach is subsequently referred to as the instantaneous approach. The fluxes from both of approaches were then averaged to produce seasonal and annual sea-air CO_2 flux estimates for the southwest Vancouver Island shelf. The seasons are delineated in Fig. 3.2, and follow those used by (*Zeng et al.,* 2002) with winter as January 1 to March 31, spring as April 1 to June 30, summer as July 1 to September 30, and autumn as October 1 to December 31.

Seasonal Area-Weighted Fluxes From New Data

The sea-air CO_2 fluxes from the new data collected within each subregion in Fig. 3.1 were used to calculate the seasonal area-weighted fluxes. Means and standard deviations were computed from the flux estimates for each subregion. Area-weighted seasonal fluxes were calculated using these means with the following equation:

$$F_{aw} = \sum(F_i * A_i)/\sum A_i$$

where F_{aw} is the area-weighted flux, F_i is the mean flux in each subregion and A_i is the area of the subregion.

RESULTS

Southwest Vancouver Island Shelf Seasonality

ΔpCO_2 was strongly seasonally modified on the southwest Vancouver Island shelf (Fig. 3.2). During winter, values ranged from -50 to +200 μatm. Minimum ΔpCO_2 values dropped from late February to May, and the lowest ΔpCO_2 was observed in mid-spring (May). Multiple years showed consistently negative mid-spring values of ΔpCO_2 with no evidence of oversaturation until late spring (June). The positive late-spring values are presumably caused by the initiation of the upwelling season. Undersaturated conditions persisted in summer, but variability in ΔpCO_2 increased. Values ranged between -200 and +300 μatm, which was the largest dynamic range observed during any season. This large summer range of ΔpCO_2 was likely the result of upwelling that drove elevated surface water pCO_2 during a period of otherwise low pCO_2 conditions caused by strong biological drawdown. Autumn ΔpCO_2 was generally well above equilibrium with the atmosphere. Some of the largest positive ΔpCO_2 values were observed during this season, and multiple years of observations during mid-autumn (November) showed the dominance of oversaturated conditions. Overall,

these data indicated the potential for CO_2 uptake from the atmosphere on the southwest Vancouver Island shelf was highest in spring. Conversely, the potential for CO_2 outgassing appeared greatest in autumn.

The sea-air CO_2 fluxes calculated using the CDIAC data with the two approaches showed outgassing in winter and autumn, and uptake of atmospheric CO_2 in spring and summer (Fig. 3.2C and D). Both flux estimates showed that winter efflux of CO_2 was lower than the autumn efflux, but there were subtle differences between the two approaches. The climatology approach (Fig. 3.2C) showed that the average fluxes become negative in late March, earlier in the season than the early-April transition to negative fluxes seen in the instantaneous approach. The largest CO_2 influx was in spring in both approaches, with the most negative fluxes observed between late-April and mid-May. Fluxes were reduced in summer because the gas transfer velocities were lowest during this season (Fig. 3.2B) and the large variability in summer ΔpCO_2 described above caused positive and negative fluxes that resulted in lower mean fluxes. The strongest outgassing of CO_2 occurred in autumn in both climatologies, which resulted from the larger positive ΔpCO_2 and higher gas transfer velocities during that season.

Winter Margin Survey

This cruise started at the Pacific Biological Station in Nanaimo on Vancouver Island on February 25, 2009 and sampled the Strait of Georgia before entering the Strait of Juan de Fuca and traveling out onto the southwest Vancouver Island shelf. The cruise track covered a large portion of the shelf, and included observations in some of the sounds on the southwest Vancouver Island coast (those data not included in our analysis) before circling the northern tip of the island and entering Queen Charlotte Sound. The cruise proceeded north into

Alaska waters before data collection was interrupted by a computer hard drive crash. The pCO_2 system was revived using a different computer for the remainder of the cruise through Alaska waters, into several mainland fjords, down through the waterways north of Vancouver Island and back to Nanaimo on March 14, 2009. Unfortunately, the working computer used to run the pCO_2 system after data collection was interrupted and the backup hard drive were both stolen following the cruise. However the computer that initially ran the pCO_2 system and had crashed part way through the cruise was not stolen, and what we present here are the data we were able to recover from that computer's hard drive.

The SST, salinity and pCO_2 measurements from the winter cruise ranged from 4.5°C to 8.9°C, 10.0 to 32.3 and 259 µatm to 864 µatm, respectively (Fig. 3.3). Owing to the data loss described above, we are only able to present measurements that were collected in the vicinity of CTD casts where we were able to interpolate between closely neighboring CTD stations. This, unfortunately, meant that the entire Johnstone Strait region was not included in this season's analysis. pCO_2 was most variable within the Strait of Georgia, where most of the data showed it was potentially functioning as a source of CO_2 to the atmosphere. However, there were a number of observations of pCO_2 below atmospheric levels that demonstrate large variability can exist within this strait even during the stormiest time of year (*i.e.* winter). The measurements made on the Vancouver Island shelf were more homogenous with values between 350 and 400 µatm. The waters within Queen Charlotte Sound were above saturation with respect to the atmosphere with values ranging from 400 to 450 µatm. The mean atmospheric pCO_2 measured during this cruise was 394 µatm.

Summer Margin Survey

This cruise started at IOS in Sidney on Vancouver Island on July 20, 2010 and proceeded north in the Strait of Georgia, through Johnstone Strait up out into Queen Charlotte Sound. The track then turned southeast out into the Pacific, then north past the western coast of the Haida Gwaii archipelago and into Alaskan waters. The cruise sampled offshore waters near Sitka, Alaska before turning south, then east back into Queen Charlotte Sound. Our cruise track zigzagged much of the sound before again entering Pacific waters, and then traveling south to sample the west coast of Vancouver Island. The Vancouver Island shelf was sampled intensively, including a search and rescue box pattern in the vicinity of Brooks Peninsula, before traveling into the US waters off Washington State, and then into the Strait of Juan de Fuca and back to Sidney on August 15, 2010. The data collected west of the Haida Gwaii archipelago, and within the US waters of Alaska and Washington are not discussed here or included in our analysis.

The SST, salinity and pCO_2 data from the summer 2010 cruise ranged from 9.6°C to 20.7°C, 19.3 to 33.0 and 145 µatm to 794 µatm, respectively (Fig. 3.3). Most of the observations during this cruise were strongly undersaturated with respect to atmospheric pCO_2. Regions where pCO_2 was above atmospheric levels were on the shelf off the northwestern portion of Vancouver Island during a period of upwelling, and within Johnstone Strait and the Strait of Juan de Fuca. Excluding these regions, the margin was potentially acting as a strong sink for atmospheric CO_2, with the lowest pCO_2 values observed within Queen Charlotte Sound and on the southwest Vancouver Island shelf. The mean atmospheric pCO_2 measured during this cruise was 388 µatm.

3.4 Autumn Margin Survey

This cruise occurred in two legs and started at the Pacific Biological Station in Nanaimo on Vancouver Island on October 8, 2008. We first proceeded north through Johnstone Strait, briefly into the BC Inside Passage, and then up into Queen Charlotte Sound. The cruise tracked through the sound into Alaska waters, sampled several straits and fjords in southeast Alaska before turning south and traveling down the BC Inside Passage, back through Johnstone Strait, into the Strait of Georgia and back to Nanaimo on October 25, 2008. The second leg started in Nanaimo on November 4, 2008 and traveled south through the Strait of Georgia, into the Strait of Juan de Fuca, up the west coast of Vancouver Island, around the northern tip of the island and then back south through Johnstone Strait, into the Strait of Georgia and ending in Nanaimo on November 14, 2008. The data collected within the straits and fjords of Alaska, along the BC Inside Passage and within the Vancouver Island sounds are not included in our analysis, and will not be discussed further here.

In waters within the identified subregions, sea surface temperature (SST), salinity, and pCO_2 ranged from 7.9°C to 13.5°C, 10 to 31.9, and 365 µatm to 867 µatm, respectively (Fig. 3.3). The majority of observations were above saturation with respect to the atmosphere, except waters within Queen Charlotte Sound. All the subregions around Vancouver Island including Johnstone Strait, the Strait of Georgia, the Strait of Juan de Fuca and the west coast of Vancouver Island were significantly oversaturated with respect to atmospheric CO_2. The mean atmospheric pCO_2 measured during this cruise was 388 µatm.

Sea-air CO_2 fluxes

We calculated sea-air CO_2 fluxes from winter, summer and autumn cruise data collected in each subregion shown in Fig. 3.1 (Fig. 3.4). In any season, almost all regions experienced some level of both influx and efflux conditions (Table 3.1). In winter, the Strait of Georgia experienced one instance of CO_2 offgassing of 49 mmol m^{-2} d^{-1}, while the southwest Vancouver Island shelf experienced a maximum influx of -12 mmol m^{-2} d^{-1}. In summer, the Strait of Georgia experienced maximum efflux of 37 mmol m^{-2} d^{-1} and maximum influx of -32 mmol m^{-2} d^{-1}. In autumn, the efflux of CO_2 peaked at 141 mmol m^{-2} d^{-1} in the Strait of Juan de Fuca, while the influx was greatest in Queen Charlotte Sound at -7 mmol m^{-2} d^{-1}. These instantaneous fluxes demonstrate that the BC margin experiences a large dynamic range in sea-air CO_2 fluxes both within and across seasons. In general, the largest CO_2 fluxes into the ocean from each subregion were during summer, and the largest fluxes out of the ocean were during autumn. CO_2 influx was not observed to occur within the Strait of Juan de Fuca or Johnstone Strait.

Means and standard deviations of the sea-air CO_2 fluxes for each subregion (Table 3.1) represent seasonal estimates for winter, summer and autumn over a broad spatial range. The variance in the fluxes is caused by variability in surface water pCO_2, wind speed and solubility in each subregion, and reflects system variability as opposed to measurement inaccuracy. It is important to realize that these broad spatial averages are snapshots in time, and can include extreme flux events. For instance, most of the subregions on the margin during winter acted on average as sources of atmospheric CO_2, however there was strong variability factored into these means. The Strait of Georgia had the largest area-specific winter efflux (6 ± 10 mmol m^{-2} d^{-1}), but Fig. 4 shows that this was dominated by the occurrence of large positive fluxes on the northern portion of the strait and that a majority of the strait was near zero, with even a

few instances of influx. In summer, Johnstone Strait had the largest area-specific efflux (16 ± 6 mmol m^{-2} d^{-1}), while the Strait of Georgia was a region of strong uptake (-18 ± 10 mmol m^{-2} d^{-1}). However, the Strait of Georgia had the largest instantaneous summer efflux of any subregion. Finally, the largest area-specific fluxes were during autumn, and directed out of the ocean. Yet this season also contained the largest variability (indicated by the standard deviation; Table 3.1), and the means for most subregions were impacted by large flux events (Fig. 3.4). This extreme spatial variability is averaged into these seasonal estimates, and is important to consider when examining seasonal fluxes based on snapshots of spatial data.

The area-weighted seasonal sea-air CO_2 fluxes calculated using the means from the subregions were 2.5, -6.6 and 4.2 mmol m^{-2} d^{-1} for winter, summer and autumn, respectively. Note that the area-weighted flux for winter does not include Johnstone Strait because of a lack of data. The seasonal average sea-air CO_2 fluxes computed from the climatologies (Fig. 3.2) of CDIAC data are shown in Table 3.2. Both the area-weighted seasonal averages and the climatologies show largest CO_2 efflux in autumn. The area-weighted seasonal fluxes are slightly different from the climatological means, however they are within the variance computed from approach 1 (Fig. 3.2c). The variance in the climatology approach reflects interannual variability in this system. Since more than one year is considered, these climatologies provide a good method for ensuring extremes are appropriately represented in the means. Interestingly, both climatologies show the strongest influx of CO_2 during spring, but on an annual basis the strong autumn and moderate winter outgassing nearly offsets the strong spring and moderate summer drawdown. The annual mean sea-air CO_2 fluxes for the southwest Vancouver Island shelf from the analysis of CDIAC

data were -0.06 and 0.54 g C m^{-2} yr^{-1} from the climatology and instantaneous approaches, respectively (Table 3.2).

DISCUSSION

This new data set has shown pCO_2 and sea-air CO_2 flux distributions over a large portion of the western Canadian margin during winter, summer and autumn. The computation of sea-air CO_2 fluxes from CDIAC data complemented these new measurements by providing a clearer representation of the time-variability of the flux for one specific part of the margin. These two independent analyses have revealed important seasonal trends of sea-air CO_2 flux in this region. Autumn is the largest atmospheric CO_2 source period (Figs. 3.2 and 3.4) with efflux occurring to a lesser degree during winter, while spring is the largest influx period, with smaller oceanic CO_2 uptake in summer. The new data have also shown that undersaturated pCO_2 conditions with respect to the atmosphere are prevalent during summer and cause a large area-weighted influx of CO_2, but the fluxes from CDIAC data showed largest CO_2 influx during spring as a result of both the higher winds then relative to summer and less variable ΔpCO_2. This strong spring and moderate summer drawdown is nearly balanced on an annual basis because of strong autumn and moderate winter outgassing (Table 3.2). Taken together, these results imply the periods of greatest exchange with the atmosphere, and with the largest impact on net annual fluxes, are the transition seasons, spring (ocean sink) and autumn (ocean source).

The seasonal cycle of sea-air CO_2 flux had previously been estimated using a biogeochemical model [*Ianson and Allen,* 2002] that was tuned for the southwest Vancouver Island shelf. The results from this model showed the region was a moderate annual CO_2 sink because outgassing mostly occurred in winter,

with influx the rest of the year. It has been theorized that outgassing in winter almost counterbalances the summer pCO_2 drawdown [*Ianson and Allen,* 2002; *Ianson et al.*, 2009] that has been observed on the west coast of Vancouver Island [*Ianson et al.,* 2003; *Nemcek et al.,* 2008]. The analyses we present here suggest that outgassing is important during both autumn and winter, and that autumn is a stronger atmospheric CO_2 source period relative to winter (Fig. 3.2) over more of the margin than just the southwest Vancouver Island shelf (Figs. 3.3 and 3.4). Our results show the climatological ΔpCO_2 is higher during autumn relative to winter, and that high gas transfer velocities drive higher fluxes during this time of year. The high fluxes in autumn, in conjunction with winter outgassing, resulted in near balanced net annual CO_2 exchange for the southwest Vancouver Island shelf. The strong autumn efflux is an important result from the computation of sea-air CO_2 fluxes from CDIAC data that is verified by our new data set. It is clear that strong drawdown is a nearly margin-wide summer characteristic in this region (Fig. 3.3), but these large positive fluxes during the less favorable period of the year for oceanographic sampling have a significant impact on net exchanges and need to be further examined.

We have produced seasonal sea-air CO_2 flux estimates from both fluxes calculated using CDIAC data and a new data set of underway pCO_2 measurements spanning a much broader area of the margin than has been surveyed in the past. Area-specific estimates from the new data set were combined into area-weighted seasonal fluxes, both of which can be compared with the seasonal flux estimates from the CDIAC data. That is, in one case we have seasonal estimates from data well resolved in time, but not in space. In the other case we have seasonal estimates well resolved in space, but not in time. The comparison of these estimates reveals the biases from different observational strategies that are important to consider in any field program

focused on diagnosing net ocean-atmosphere CO_2 exchange, and in a global context for better constraining coastal fluxes. For instance, the autumn fluxes from the climatologies suggest the southwest Vancouver Island shelf emits between 6.8 and 7.9 mmol CO_2 m^{-2} d^{-1} to the atmosphere (Table 3.2), while the area-specific flux for this subregion is 17.4 mmol CO_2 m^{-2} d^{-1} (Table 3.1) and the area-weighted autumn flux for the margin is 4.2 mmol CO_2 m^{-2} d^{-1}. The difference here (neglecting the difference between the climatology and instantaneous approaches) is temporal versus spatial averaging. The area estimates are based on snapshots in time, and don't capture important time variability in this system. The differences between sampling strategies can lead to substantial differences in even estimating the sign of the flux (Table 3.2). Conversely, the estimates from the climatologies capture time variability within one portion of the margin, but miss entirely the spatial variability seen across the different subregions. Area-specific seasonal flux does not match the area-weighted seasonal flux because of the differences between the subregions. CO_2 influx was never observed in subregions 4 and 6, and these functional differences between subregions are important to consider when estimating margin-wide fluxes. It is understandable that the flux estimates from the two different frames of reference would produce different answers because the record of instantaneous fluxes from the CDIAC data showed that positive and negative fluxes are experienced in every season, and a snapshot in time can capture either of these conditions. The power in our new data set is that it spans more of the margin, and it is important to realize that the most precise estimate of net CO_2 exchange within such a dynamic coastal setting requires the simultaneous use data well resolved in space and time.

A unique aspect of this new data set is that it captures sea-air CO_2 flux variability within some of the straits on the BC margin. It is important to note that the Johnstone and Juan de Fuca Straits both were persistent atmospheric CO_2

sources, while the Strait of Georgia was an atmospheric CO_2 sink during the summer. CDIAC data from the Strait of Juan de Fuca (Fig. 3.5) confirm the overall dominance of high-pCO_2 conditions in this subregion. The processes leading to these site-specific differences are difficult to diagnose with the present data set, but possible causes include the degree and source of fresh water, mixing rates and tidal energy dissipation, all of which can drive elevated pCO_2 and higher effluxes. Tidal mixing has been suggested to drive enhanced nutrients [*Masson*, 2006] and pCO_2 [*Ianson et al.,* 2003; *Nemcek et al.,* 2008] in the straits around Vancouver Island, and is likely responsible for the large CO_2 source regions that persist between seasons (*i.e.* Johnstone Strait and the Strait of Juan de Fuca). The combined area of Johnstone Strait and the Strait of Juan de Fuca in this study was only 10% of the total margin area considered and yet these two subregions were a strong influence on the area-weighted fluxes for the margin. Excluding these subregions from the area-weighted flux calculation resulted in a 30% increase in the summer influx and a 31% decrease in the autumn efflux. It is therefore expected that the fluxes from these straits have an important effect on the net exchange of CO_2 on the margin. In addition to the autumn and winter outgassing we observed in the other subregions, the signal from these straits is important for counterbalancing spring and summer CO_2 drawdown in open-shelf and sound waters.

Numerous studies have documented the importance of interannual variability in net annual sea-air CO_2 fluxes [*Evans et al.*, 2011; *Fransson et al.*, 2006; *Friederich et al.*, 2002; *McNeil*, 2010]. The CDIAC analysis presented here spans almost 7 years of observation across both strong El Niño and La Niña events (*i.e.* 1998 and 1999, respectively), and therefore likely has little bias towards El Niño or La Niña. This is perhaps not the case for lower frequency climate variability such as the Pacific Decadal Oscillation [PDO; *Mantua et al.*,

1997]. *Feely et al.* [2006] describe in detail how the 1997-1998 shift in PDO had increased outgassing flux in the equatorial Pacific by 27%. Because the climate variability associated with PDO is centered in the North Pacific [*Mantua et al.*, 1997], it is very probable that this would be strong source of variability unaccounted for in any CO_2 flux estimates for the BC margin. This imparts a source of uncertainty in our estimates that can only be resolved by long periods of observation.

There are additional sources of uncertainty in our estimates associated with (1) the physical decoupling between our in-water measurements (SST, salinity and pCO_2) and the wind data, (2) differences in the current state-of-the-art gas transfer parameterizations, and (3) the proper combination of wind and pCO_2 data. To consider point (1), the cross-correlation between buoy 46206 and 46204 (positions shown in Fig. 3.1) revealed that the winds were not substantially different between the two locations, making the use of buoy winds instead of ship winds in open water less problematic than in confined waters. Within the confined waters of the straits, using a fixed wind record instead of ship winds may induce more uncertainty because the winds in these locations are probably not as spatially coherent over such large distances. It is likely this uncertainty has its strongest effect in the most confined waters of Johnstone Strait, and it is strongly recommended that future studies aimed at estimating sea-air CO_2 fluxes in these regions rigorously pursue ship-based winds. To consider point (2), the different gas transfer parameterizations can result in large flux differences (as much as 19% as shown by *Jiang et al.* [2008] who considered 6 versions of gas transfer parameterizations for estimating fluxes in the U.S. South Atlantic Bight). The BC margin at times experiences high wind conditions that would result in large differences in the fluxes computed from the various wind-based parameterizations of the gas transfer velocity, because they diverge most

significantly at high wind speeds (*i.e.* compare cubic and quadratic parameterizations). Finally, to address point (3), the combination of different wind and pCO_2 products can have large implications on the fluxes. *Lüger et al.* [2006] observed a 47% difference between fluxes calculated from grid-averaged monthly winds versus collocated winds. *Takahashi et al.* [2009] report no significant correlation between individual ΔpCO_2 measurements and 6-hr mean wind speeds, which supported their decision to use monthly means to approximate sea-air CO_2 flux in their climatology. We did not observe large differences between the fluxes for southwest Vancouver Island calculated using averaged values versus instantaneous values. However, our annual estimates are slightly different, but within the variance (reported as the standard deviation), of that reported by *Chavez and Takahashi* [2007]. *Chavez and Takahashi* [2007] describe the region as a small net annual sink (~-5 ± 80 g C m^{-2} yr^{-1}) and we report the region nearly in balance (-0.01 to 0.54 g C m^{-2} yr^{-1}) using some of the same pCO_2 data but different wind products. The difference between their work and ours is (1) we are considering a much smaller area, and (2) we used buoy winds whereas their analysis used coarse-resolution NCEP winds. We examined the monthly fluxes specifically for the southwest Vancouver Island shelf that went into their estimate for the BC margin, and the trends in their flux estimates are the same as what we present here; strong to moderate efflux in autumn and winter, and strong to moderate CO_2 uptake in spring and summer. It is critical to realize that although their estimate and ours differ slightly, both are weak to near zero. The variance of both these estimates is large, but highlights how sensitive the diagnosis of net annual sea-air CO_2 flux is to time and space variability and that fluxes during the less-sampled portion of the year have a large impact on the net exchanges on this dynamic coastal region.

CONCLUSIONS

We have presented analyses of historical pCO_2 measurements from the CDIAC data set for the southwest Vancouver Island shelf and from a new data set of underway pCO_2 measurements that span a greater spatial area of the BC margin than has been previously sampled. We have used these observations to produce sea-air CO_2 flux estimates that show large time and space variability. Four important features of the BC margin have been identified: (1) The efflux of CO_2 from the ocean is greatest in autumn; (2) Outgassing of CO_2 occurs to a lesser degree in winter; (3) The combined effect of both seasons nearly balances spring and summer CO_2 drawdown for at least the southwest Vancouver Island shelf; (4) There are important differences between subregions: The Strait of Juan de Fuca and Johnstone Strait were persistent sources of CO_2, while the Strait of Georgia and regions in more open water act as sinks at least part of the year. The straits that are persistent CO_2 sources are only a small portion of the total area of the margin considered, but have a significant impact on area-weighted seasonal fluxes. These regions also counteract spring and summer CO_2 drawdown, and are therefore important to include in estimates of sea-air CO_2 flux for the western Canadian coastal margin.

REFERENCES

Borges, A. V., B. Delille, and M. Frankignoulle (2005), Budgeting sinks and sources of CO2 in the coastal ocean: Diversity of ecosystems counts, *Geophysical Research Letters*, *32*, L14601, doi: 14610.11029/12005GL023053.

Cai, W.-J., M. Dai, and Y. Wang (2006), Air-sea exchange of carbon dioxide in ocean margins: A province-based synthesis, *Geophysical Research Letters*, *33*, L12603, doi:12610.11029/12006GL026219.

Chavez, F. P., and T. Takahashi (2007), Coastal Oceans*Rep.*, 157-166 pp, U.S. Climate Change Science Program, Washington, DC.

Chen, C.-T. A., and A. V. Borges (2009), Reconciling opposing views on carbon cycling in the coastal ocean: Continental shelves as sinks and near-shore

ecosystems as sources of atmospheric CO2, *Deep-Sea Research II*, *56*, 579-590.

Dickson, A. G., C. L. Sabine, and J. R. Christian (2007), Guide to Best Practices for Ocean CO_2 Measurements*Rep.*, North Pacific Marine Science Organization.

Evans, W., B. Hales, and P. G. Strutton (2011), The seasonal cycle of surface ocean pCO_2 on the Oregon shelf, *Journal of Geophyiscal Research*, *(accepted)*.

Feely, R. A., T. Takahashi, R. Wanninkhof, M. J. McPhaden, C. E. Cosca, S. C. Sutherland, and M.-E. Carr (2006), Decadal variability of the air-sea CO_2 fluxes in the equatorial Pacific Ocean, *Journal of Geophyiscal Research*, *111*(C08S90), doi: 10.1029/2005JC003129.

Fransson, A., M. Chierici, and Y. Nojiri (2006), Increased net CO_2 outgassing in the upwelling region of the southern Bering Sea in a period of variable marine climate between 1995 and 2001, *Journal of Geophyiscal Research*, *111*(C08008), doi: 10.1029/2004JC002759.

Friederich, G. E., P. M. Walz, M. G. Burczynski, and F. P. Chavez (2002), Inorganic carbon in the central California upwelling system during the 1997-1999 El Niño-La Niña event, *Progress in Oceanography*, *54*, 185-203.

Hales, B., W.-J. Cai, B. G. Mitchell, C. L. Sabine, and O. Schofield (2008), *North American Continental Margins: A Synthesis and Planning Workshop*, 110 pp., U.S. Carbon Cycle Science Program, Washington DC.

Ho, D. T., C. S. Law, M. J. Smith, P. Schlosser, M. Harvey, and P. Hill (2006), Measurements of air-sea gas exchange at high wind speeds in the Southern Ocean: Implications for global parameterizations, *Geophysical Research Letters*, *33*, L16611, doi: 16610.11029/12006GL026817.

Ianson, D., and S. E. Allen (2002), A two-dimensional nitrogen and carbon flux model in a coastal upwelling region, *Global Biogeochemical Cycles*, *16*(1), doi: 10.1029/GB001451.

Ianson, D., S. E. Allen, S. L. Harris, K. J. Orians, D. E. Varela, and C. S. Wong (2003), The inorganic carbon system in the coastal upwelling region west of Vancouver Island, Canada, *Deep-Sea Research I*, *50*, 1023-1042.

Ianson, D., R. A. Feely, C. L. Sabine, and L. W. Juranek (2009), Features of Coastal Upwelling Regions that Determine Net Air-Sea CO_2 Flux, *Journal of Oceanography*, *65*, 677-687.

Jiang, L.-Q., W.-J. Cai, R. Wanninkhof, Y. Wang, and H. Lüger (2008), Air-sea CO2 fluxes on the U.S. South Atlantic Bight: Spatial and seasonal variability, *Journal of Geophysical Research*, *113*, C07019, doi: 07010.01029/02007JC004366.

Lüger, H., R. Wanninkhof, D. W. R. Wallace, and A. Körtzinger (2006), CO_2 fluxes in the subropical and subarctic North Atlantic based on measurements from a volunteer observing ship, *Journal of Geophyiscal Research*, *111*(C06024), doi: 10.1029/2005JC003101.

Mantua, N. J., S. R. Hare, Y. Zhang, J. M. Wallace, and R. C. Francis (1997), A Pacific Interdecadal Climate Oscillation with Impacts on Salmon Production, *Bulletin of the American Meteorological Society*, *78*(6), 1069-1079.

Masson, D. (2006), Seasonal Water Mass Analysis for the Straits of Juan de Fuca and Georgia, *Atmosphere-Ocean*, *44*(1), 1-15.

McNeil, B. I. (2010), Diagnosing coastal ocean CO_2 interannual variability from a 40 year hydrographic time series station off the east coast of Australia, *Global Biogeochemical Cycles*, *24*(GB4034), doi: 10.1029/2010GB003870.

Nemcek, N., D. Ianson, and P. D. Tortell (2008), A high-resolution survey of DMS, CO2, and O2/Ar distributions in productive coastal waters, *Global Biogeochemical Cycles*, *22*, GB2009, doi: 2010.1029/2006GB002879.

Pennington, J. T., G. E. Friederich, C. G. Castro, C. A. Collins, W. Evans, and F. P. Chavez (2010), The Northern and Central California Coastal Upwelling System, in *Carbon and Nutrient Fluxes in Continental Margins*, edited by K.-K. Liu, L. Atkinson, R. A. Quiñones and L. Talaue-McManus, Springer, Berlin.

Takahashi, T., J. Olafsson, J. G. Goddard, D. W. Chipman, and S. C. Sutherland (1993), Seasonal Variation of CO2 and Nutrients in the High-Latitude Surface Oceans: a Comparative Study, *Global Biogeochemical Cycles*, *7*(4), 843-878; doi:810.1029/1093GB02263.

Takahashi, T., et al. (2009), Climatological mean and decadal change in surface ocean pCO2 and net sea-air CO2 flux over the global oceans, *Deep-Sea Research II*, *56*, 554-577.

Wanninkhof, R. (1992), Relationship Between Wind Speed and Gas Exchange Over the Ocean, *Journal of Geophysical Research*, *97*(C5), 7373-7382.

Ware, D. M., and R. E. Thomson (2005), Bottom-Up Ecosystem Trophic Dynamics Determine Fish Production in the Northeast Pacific, *Science*, *308*, 1280-1284.

Wong, C. S., J. R. Christian, S.-K. Emmy Wong, J. Page, L. Xie, and S. Johnannessen (2010), Carbon dioxide in surface seawater of the eastern North Pacific Ocean, *Deep-Sea Research I*, *57*, 687-695.

Zeng, J., N. Yukihiro, P. P. Murphy, C. S. Wong, and Y. Fujinima (2002), A comparison of ΔpCO_2 distributions in the northern North Pacific using results from a commercial vessel in 1995-1999, *Deep-Sea Research II*, *49*, 5303-5315.

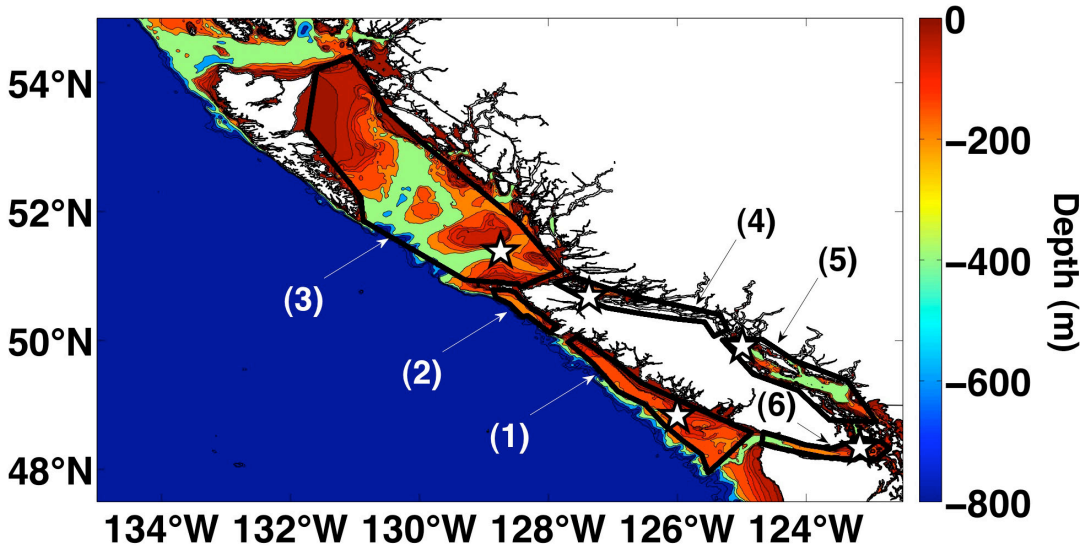

Figure 3.1: Map of the study area in the Pacific Canadian coastal margin. The black enclosures represent the subregions where cruise data are selected for calculating sea-air CO2 fluxes (subregion 1 = southwest Vancouver Island shelf; subregion 2 = northwest Vancouver Island shelf; subregion 3 = Queen Charlotte Sound; subregion 4 = Johnstone Strait; subregion 5 = Strait of Georgia; subregion 6 = Strait of Juan de Fuca). White stars in subregions 1,3 and 5 are Environment Canada buoys 46206, 46204 and 46131, respectively. The white star in subregion 4 is the Port Hardy Airport on Vancouver Island, and the white star in subregion 6 is the NOAA NDBC buoy 46088. Wind records from these locations were used to calculate gas transfer velocities. Bathymetry (colorbar, m) provided by the National Geophysical Data Center (http://www.ngdc.noaa.gov/mgg/global/global.html).

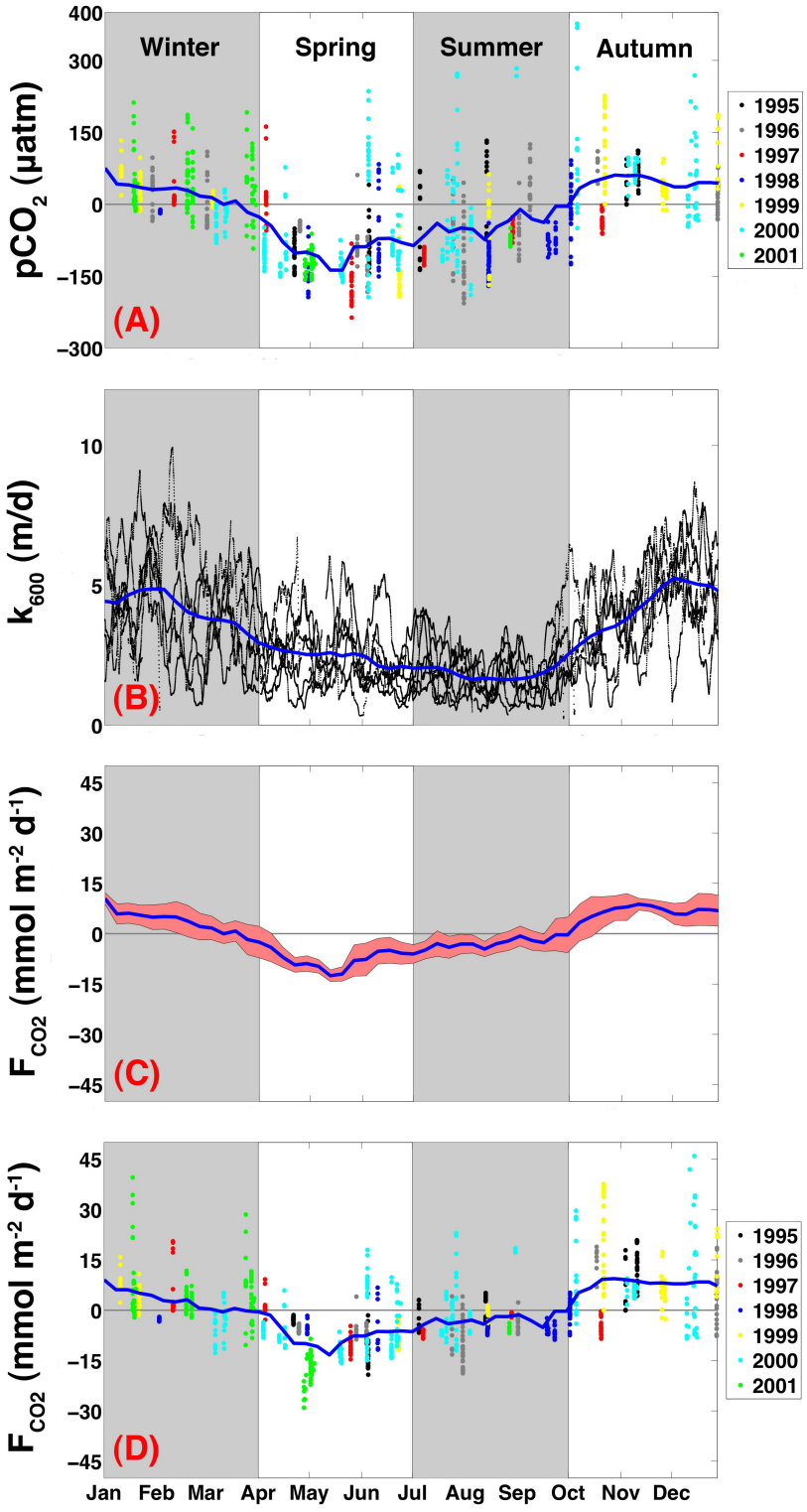
Winter
Spring
Summer
Autumn
pCO2 (µatm)
400
300
150
0
−150
−300
(A)
1995
1996
1997
1998
1999
2000
2001
k600 (m/d)
10
5
0
(B)
FCO2 (mmol m-2 d-1)
45
30
15
0
−15
−30
−45
(C)
(D)
Jan
Feb
Mar
Apr
May
Jun
Jul
Aug
Sep
Oct
Nov
Dec

Figure 3.2:

Figure 3.2: Panel (A) is the seasonal cycle of CDIAC underway ΔpCO_2 (surface seawater pCO_2 minus the atmospheric pCO_2; µatm) collected on the southwest Vancouver Island shelf (Fig. 3.1; subregion 1) from January 1995 to August 2001 (shown by year as colored dots). Panel (B) is the weekly running average gas transfer velocity (m/d) calculated from hourly winds recorded at the Environment Canada buoy 46206 over the period January 1995 to August 2001. The blue lines in panels (A) and (B) are climatologies of ΔpCO_2 and the gas transfer velocity calculated using 30-day running averages made at weekly intervals. Panel (C) is a climatology of sea-air CO_2 flux (mmol m^{-2} d^{-1}) computed using the ΔpCO_2 and the gas transfer velocity climatologies. The red area as a measure of the flux variability calculated as ± the product of the standard deviations of the 30-Julian day running averages of ΔpCO_2 and gas transfer velocity multiplied by the solubility. Panel (D) is a climatology of sea-air CO_2 flux (mmol m^{-2} d^{-1}) calculated from individual flux estimates (shown by year as colored dots) made by time-syncing the ΔpCO_2 data in panel (A) with the weekly running average gas transfer velocity data in panel (B).

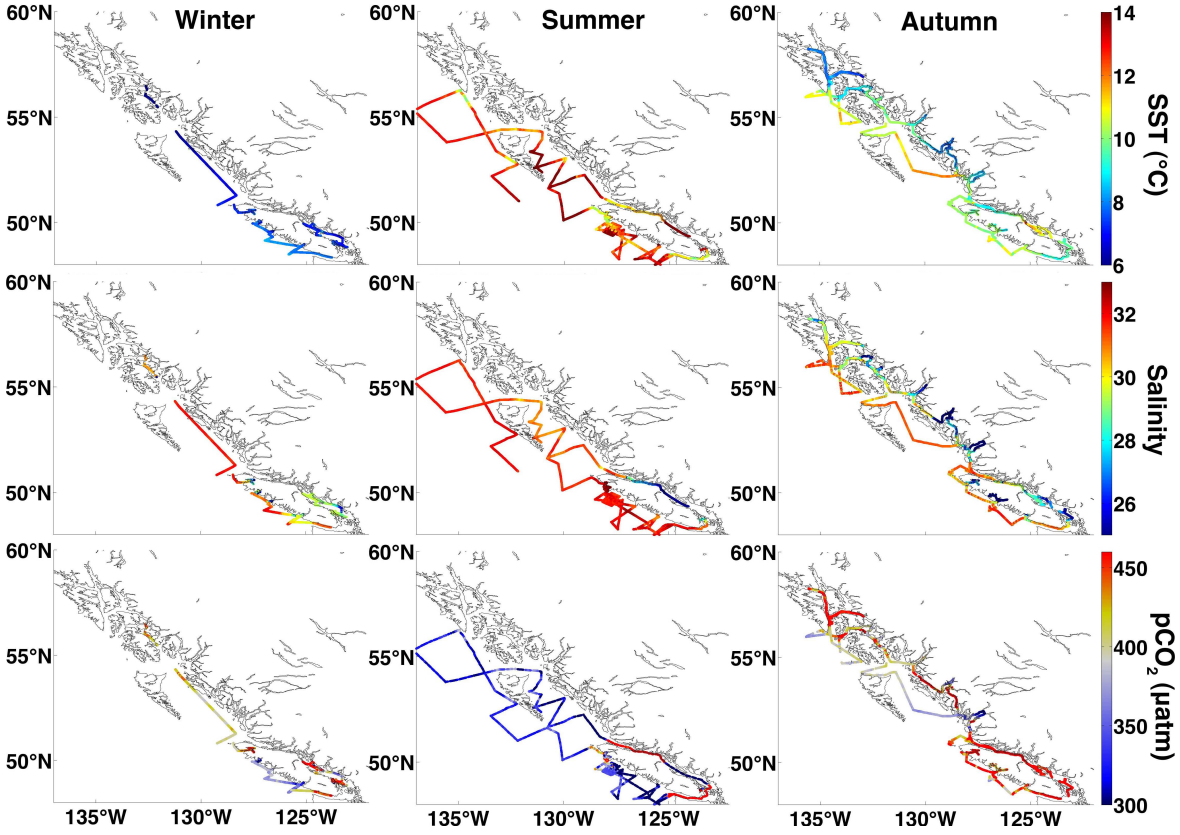

Figure 3.3: SST (top row; °C), salinity (middle row) and pCO_2 (lower row; µatm) for the winter (middle column; February 25 to March 14, 2009), summer (right column; July 20 to August 15, 2010) and autumn (left column; October 8 to November 14, 2008) cruises.

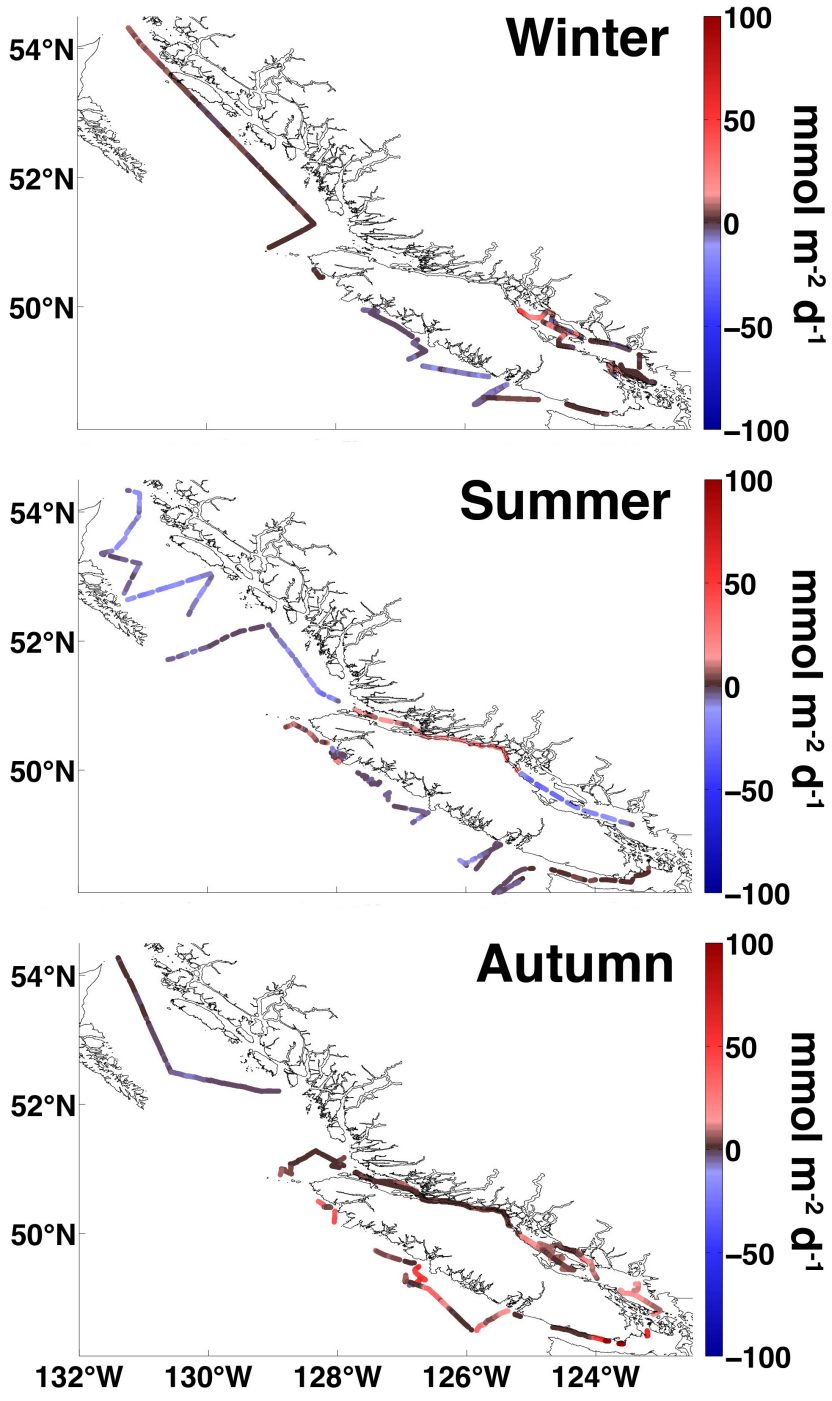

Figure 3.4: Sea-air CO_2 fluxes (mmol m^{-2} d^{-1}) from winter (top), summer (middle) and autumn (lower) calculated from data collected within each subregion shown in Fig. 3.1.

Table 3.1: Seasonal means, standard deviations, minima and maxima of the sea-air CO_2 fluxes (mmol m^{-2} d^{-1}) from the data shown in Fig. 3.4 for each subregion defined in Fig 3.1.

subregion	winter mean	winter std	winter min	winter max	summer mean	summer std	summer min	summer max	autumn mean	autumn std	autumn min	autumn max	km^2
1	**-3.9**	3.1	-11.9	5.0	**-3.2**	2.9	-14.8	1.8	**17.4**	18.4	-5.7	64.6	3979
2	**0.3**	0.7	-0.7	2.7	**2.9**	6.0	-10.4	23.0	**21.3**	15.8	3.0	44.1	1357
3	**2.9**	3.1	-2.0	19.1	**-8.0**	5.3	-26.8	0.0	**-0.4**	2.7	-7.4	7.9	39945
4	no data	no data	no data	no data	**15.6**	5.9	2.5	28.8	**7.1**	13.1	0.0	66.0	3463
5	**5.5**	9.7	-9.7	48.5	**-17.5**	10.4	-31.8	37.0	**10.0**	6.4	0.1	26.7	7036
6	**0.4**	0.5	0.0	4.1	**2.0**	1.1	0.0	4.9	**28.4**	41.1	0.0	141.3	3316

Table 3.2: Seasonal and annual means (mmol CO_2 m^{-2} d^{-1}) from the two approaches used to construct the climatologies of sea-air CO_2 flux for the southwest Vancouver Island shelf from CDIAC data. Also shown are the seasonal fluxes calculated from the new data for region 1 (Table 3.1).

mmol m^{-2} d^{-1}	Climatology Approach	Instanteous Approach	New Data
winter	**3.8**	**3.1**	**-3.9**
spring	**-7.5**	**-7.3**	**X**
summer	**-2.9**	**-3.0**	**-3.2**
autumn	**6.8**	**7.9**	**17.4**
annual	**-0.01**	**0.12**	**X**

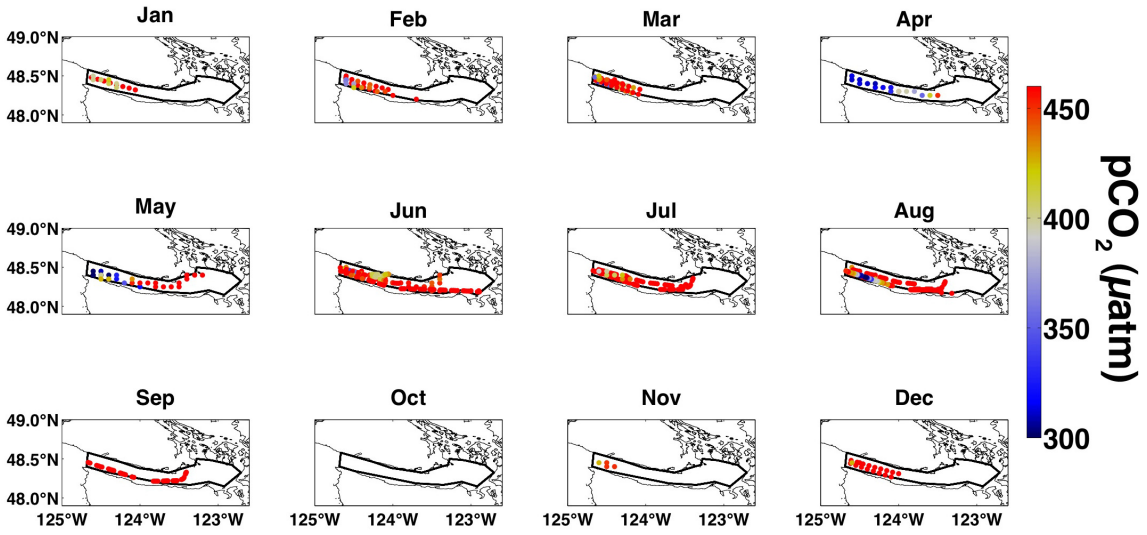

Figure 3.5: Monthly distribution of pCO_2 (µatm) from CDIAC for the Juan de Fuca Strait, subregion 6 (Fig. 3.1), highlighting the dominance of oversaturation conditions within this region.

CHAPTER 4: Air-Water CO_2 Fluxes in the Columbia River Estuary and Plume

Wiley Evans

For submission to *Estuaries and Coasts*

Journal of the Coastal and Estuarine Research Federation

ACKNOWLEDGEMENTS

We thank the crew of the OSU *R/V Wecoma*. We are also exceptionally grateful for Dale Hubbard's guidance and training during the early cruises presented here. We also thank the Center of Coastal Margin Ocean and Prediction for allowing participation in their cruises. This work was supported by NSF Chemical Oceanography award OCE-0752576.

ABSTRACT

Seasonal variability in air-water carbon dioxide (CO_2) flux in the Columbia River Estuary and plume was revealed from five cruises spanning spring, summer and autumn. The estuary transitioned from being an atmospheric CO_2 sink in spring (-10 mmol m^{-2} d^{-1}) to a source during summer (12 to 1 mmol m^{-2} d^{-1}) and autumn (18 to 9 mmol m^{-2} d^{-1}). The late spring to early summer freshet coincided with the transition from sink to source in the estuary. The largest fluxes from the estuary were during the freshet and during autumn because of the prevalence of strongly oversaturated surface water pCO_2 coupled with moderate to high gas transfer velocities (~10 to ~70 m/d). Late summer pCO_2 levels were lower than during the freshet, and lower than what would be expected from summer warming alone, suggesting that primary production was important for counteracting thermal effects during this season. In autumn, reduced surface water temperatures did not cause a reduction in pCO_2, presumably because respiration was significant to offset any cooling effects. Strong winds associated with an autumn storm event caused the largest effluxes observed (223 mmol m^{-2} d^{-1}), but these are transient events that quickly dissipated as the waters equilibrated with the atmosphere. In contrast with the estuary, the plume was a persistent sink during all seasons (-23 to -1 mmol m^{-2} d^{-1}), likely because of high plume-associated primary production and river-ocean end-member mixing. This work highlights the seasonal variability in air-water CO_2 exchange within the Columbia River Estuary and plume, and describes some important points that should be addressed in future research in this system.

INTRODUCTION

Estuaries are substantial net sources of atmospheric CO_2 [*Cai and Wang*, 1998; *Frankignoulle et al.*, 1998; *Gattuso et al.*, 1998; *Jiang et al.*, 2008b] that collectively have an important role in balancing atmospheric CO_2 uptake on continental shelves [*Borges*, 2005; *Borges et al.*, 2005; *Cai*, 2011; *Cai et al.*, 2006; *Laruelle et al.*, 2010]. It has been estimated that estuaries emit 0.27 Pg C yr^{-1} to 0.50 Pg C yr^{-1} [*Borges et al.*, 2005; *Cai et al.*, 2006; *Chen and Borges*, 2009; *Laruelle et al.*, 2010], which is a large fraction of the total ocean atmospheric CO_2 uptake of ~1.8 Pg C yr^{-1} (Pg = 10^{15} g; based on combining most recent uptake estimates for the open ocean and continental shelves from *Takahashi et al.* [2009] and *Laruelle et al.* [2010]). However, the estimate of estuarine CO_2 exchange with the atmosphere is based on scant spatial data. To date regions where estuarine air-water CO_2 flux studies exist are mostly along the European, Asian, Indian and eastern North American coasts, with no air-water CO_2 fluxes reported from estuaries on the western coast of North and South America (see *Laruelle et al.* [2010] Fig. 1). Given the importance of estuaries in global CO_2 budgets, it is imperative to expand the examination of estuarine air-water CO_2 fluxes worldwide. Here we report spring, summer and autumn air-water CO_2 fluxes from the Columbia River Estuary on the northwestern coast of North America.

We adopt the following definition from *Borges* [2005; and references therein] for describing the inner and outer regions of the Columbia River Estuary. The inner estuary is the semi-enclosed region that is connected to the ocean and where seawater is diluted with freshwater from land (referred to here as the estuary). The upstream boundary of the estuary is where tidal influence is limited, and where currents and sedimentary processes become different from those in the river. The defined mouth at 46.25°N and 124.08°W represents the seaward

limit of the estuary. The extension of the low-salinity waters from the estuary mouth into the coastal ocean is referred to here as the plume.

Repeated observations of surface water pCO_2 oversaturation with respect to the atmosphere in estuaries have been used to suggest these waters are net heterotrophic [*Caffrey*, 2004; *Cai*, 2011; *Gattuso et al.*, 1998]; that is net ecosystem metabolism in negative, meaning primary production is outweighed by ecosystem respiration. However, there is some disagreement concerning the source of organic carbon respired in estuaries, particularly within large rivers that have short water residence times. For example, *Abril et al.* [2002] suggest that as much as 50% of riverine particulate organic carbon (POC) is respired within European estuaries, while *Cai and Wang* [1998] report almost all of the degassing of CO_2 within the Satilla River Estuary is caused by lateral transport of dissolved inorganic carbon (DIC) from microbial decomposition in the surrounding wetlands. In either case, estuaries are important pathways by which land-derived organic material (both dissolved and particulate) is transported from the continent to the marine environment, and the heterotrophic status of these systems is maintained by the respiration of dissolved and particulate carbon input from the river, local runoff and groundwater discharge, as well as local respiration [*Borges*, 2005].

The Columbia is the largest river that enters the Pacific Ocean from the North American continent with a mean discharge of ~7500 $m^3\ s^{-1}$ [*Perry et al.*, 1996]. Its drainage basin covers a total area of 6.6×10^5 km^2 over seven U.S. states and two Canadian provinces [*Simenstad et al.*, 1990]. The headwaters of the Columbia are located in the mountains of British Columbia, and its drainage basin consists of eastern and coastal sub-basins [*Simenstad et al.*, 1990]. The

coastal sub-basin is only ~8% of the total drainage basin, yet supplies ~24% of the total riverflow because of mild, wet winters and a large excess of precipitation over evaporation [*Jay and Good*, 1978; *Sherwood et al.*, 1990]. The coastal sub-basin major tributaries have riverflows 5 to 10 times greater during winter compared to the remainder of the year [*Sherwood et al.*, 1990]. In contrast, the arid climate of the eastern sub-basin imparts its largest influence on riverflow during late spring snowmelts [*Sherwood et al.*, 1990], which causes a pronounced freshet. The Columbia is a highly flow-regulated river system that includes fourteen hydroelectric dams on its mainstem, and thirty more on its major tributaries. Most of the dams on the Columbia are located in its eastern basin, and they have sharply curtailed the snowmelt freshet. Pre-regulated (prior to 1969) freshets were on average 5000 m^3 s^{-1} greater than modern freshets [*Sherwood et al.*, 1990], and annual peak discharge now seldom exceeds 17,000 m^{-3} s^{-1}. The flow-regulated reduction in snowmelt freshets is caused by the retention of water in catchments. River water is then released throughout the year such that the seasonality in river discharge is dramatically reduced relative to pre-regulated flows [*Sherwood et al.,* 1990]. This engineering venture has radically altered the Columbia River from its free-flowing state, and presently the longest free-flowing segment on the mainstem is a 240 km stretch between Bonneville Dam and the river mouth [*Prahl et al.*, 1998].

The plume of the Columbia River is a major feature of the coastal ocean off Oregon and Washington [*Hickey et al.*, 2009; *Hickey et al.*, 2010] which supplies the shelf with silicate, manganese, dissolved iron, organic carbon, and moderate concentrations of nitrate [relative to upwelling source waters; [*Aquilar-Islas and Bruland*, 2006; *Bruland et al.*, 2008; *Chase et al.*, 2007; *Hill and Wheeler*, 2002; *Lohan and Bruland*, 2006], and also buoyancy that provide more stable mixed layers which allow more efficient phytoplankton response [*Kudela et*

al., 2010]. Within the plume, supply of nitrate and dissolved iron is also enhanced by vertical mixing of primary marine-source waters [*Bruland et al.*, 2008; *Lohan and Bruland*, 2006]. The plume's advective pathway is influenced by the winds, and is typically directed southwest and offshore during summer when winds are predominantly from the north, while it is directed northward and confined along the Washington shoreline during winter when winds blow from the south [*Landry et al.*, 1989]. More recently it has been shown that the plume can have a bifurcated distribution in summer [*Hickey et al.*, 2009], and that the near-estuary plume water can be trapped outside of the Columbia River mouth in a recirculating bulge [*Kudela et al.*, 2010]. The character of the plume facilitates high local primary productivity when nutrient conditions are less favorable for growth elsewhere along the shelf [*Kudela et al.*, 2010].

Air-water CO_2 fluxes within the Columbia River Estuary and plume have been largely unaddressed, as have fluxes in general from any estuarine systems on the west coasts of North and South America [*Laruelle et al.,* 2010]. Prior to this work, a single study measured pCO_2 in the Columbia River Estuary. *Park et al.* [1969] reported measurements between 200 and 870 parts per million above their measured atmospheric values from a single cruise in December 1968 that sampled the estuary to up-river near Portland, Oregon. Here we describe air-water CO_2 fluxes calculated from data collected during 5 cruises that sampled the Columbia River Estuary and plume during spring, summer and autumn.

METHODS

Sample Collection

We equipped the Oregon State University R/V *Wecoma* with a underway pCO_2 measurement system described in *Evans et al*. [2011a; modified from

Hales et al., 2004]. This system uses a LI-COR LI-840 infrared (IR) CO_2 sensor with a miniature membrane contactor (Liqui-Cel 1x5.5) as an equilibrator. Prefiltration was achieved using a custom tangential flow filter with an 8-μm element, in which 1-10% of the main flow was directed tangentially to the primary flow and across the filter to the membrane contactor. Sample liquid flow through the contactor was ~300 ml min^{-1} and the atmospheric air carrier flow rate was ~30 ml min^{-1}. Data were collected at 1 Hz, and standard sequences using gases of known CO_2 mixing ratio (xCO_2, ppm) were run every two hours and used to correct for IR analyzer inaccuracy. Atmospheric samples were also taken during the standard sequences. Calibrated seawater xCO_2 data were adjusted to pCO_2 using the measured total pressure in the equilibrator. The calibrated atmospheric xCO_2 data were converted to pCO_2 using atmospheric pressure measured in the LI-COR cell. Measurement-temperature pCO_2 was then corrected to pCO_2 at SST using the difference between ship intake and equilibrator temperatures, after accounting for the ~ 50 s flow-based lag between those two temperature sensor locations, and the relationship for the temperature effect on isochemical seawater described by *Takahashi et al.* [1993].

The pCO_2 system was integrated with a Seabird SBE45 for temperature and salinity, and a chlorophyll fluorometer (WETLabs WetStar; excitation/emission wavelengths of 460/695 nm). Seawater flow rate was also monitored downstream of the pCO_2 equilibrator and used for data quality control; data from all measurements were removed during periods of low flow delivery to the equilibrator. Temperature, salinity and chlorophyll measurements were made at 1 Hz coincident with the pCO_2 measurement. The intake depth for the seawater flow-through system was ~3 m. The chlorophyll fluorometer was kept clean during each cruise. The chlorophyll calibration was done using surface Niskin bottle samples collected during a survey aboard the NOAA ship *McArthur*

II in July 2008 that initiated at the Columbia River estuary. These data, although limited in time, cover a substantial portion of the dynamic range of chlorophyll concentrations encountered in this region (0-20 mg m^{-3}). All measurements were time-matched with ship-provided GPS and wind speed data (acquired every 3 seconds).

Air-water CO_2 Flux Estimates

The air-water CO_2 flux (mmol m^{-2} d^{-1}) was calculated using the following equation:

$$F = k_{CO2} K_{CO2} \Delta pCO_2,$$

where k_{CO2} is the gas transfer velocity (m/d) for CO_2 at SST. k_{CO2} is calculated from the k_{600}, the gas transfer velocity at a Schmidt number of 600 (Schmidt number for CO_2 in freshwater at 20°C), versus wind speed relationship presented by *Jiang et al.* [2008a] adjusted to in situ temperature using the relationship for the Schmidt number dependence of gas transfer described by *Wanninkhof* [1992]. We did not correct k_{CO2} for salinity because the difference between k_{CO2} in freshwater versus saltwater (S=35) is on the order of a few percent. K_{CO2} is the solubility of CO_2 (mol m^{-3} atm^{-1}; [*Weiss*, 1974]) and ΔpCO_2 is the seawater pCO_2 minus the atmospheric pCO_2 (atm). The atmospheric pCO_2 was taken here to be the mean value of 392 µatm reported in *Evans et al.* [2011a], which was the average for spring, summer and autumn cruises on the shelf. All input parameters were 3-second values (ship-based wind speed, SST, salinity, and ΔpCO_2).

Gas transfer velocities in the open ocean are largely dependent on wind stress, and so have been parameterized by wind speed [*Wanninkhof*, 1992]. The

recent parameterization of *Ho et al.* [2006] is similar and extends data coverage to higher wind speeds, and was used to calculate sea-air CO_2 fluxes on the Oregon shelf [*Evans et al.*, 2011a] and the British Columbia coastal margin [*Evans et al.*, 2011b]. In estuaries gas transfer is more complicated than in the open ocean, as the turbulence that drives transport is influenced by currents and bottom stress [*Raymond and Cole*, 2001]. *Raymond and Cole* [2001] suggested much higher wind speed dependences than relationships for the open ocean (Fig. 4.1); however, data in their study were collected at low wind speeds (0-5 m/s), which can result in unreasonably high gas transfer velocities at high wind speeds (Fig. 4.1). *Jiang et al.* [2008a] expanded on the work of *Raymond and Cole* [2001] by including more recent gas transfer velocity measurements in estuaries at higher wind speeds (0-11 m/s). The relationship they developed, based on the square of the wind speed, shows slightly higher gas transfer velocities at nearly all wind speeds relative to the *Ho et al.* [2006] relation, yet follows the open ocean parameterization at high wind speeds (Fig. 4.1). Because the range of wind speeds encountered during this study was large, from 0 to 36 m/s, the relationship proposed by *Jiang et al.* [2008a] was chosen to approximate the gas transfer velocity based on wind speed.

Ancillary Data and Area Definition

Ancillary measurements of river discharge and buoy winds were acquired from USGS (http://waterdata.usgs.gov/usa/nwis/uv?site_no=14246900) and NDBC (http://www.ndbc.noaa.gov/station_page.php?station=46029), respectively, and the locations where these measurements were made are shown in Fig. 4.2. The ship tracks along which underway data were collected are also shown in Fig. 4.2. The ship measurements were segregated between the estuary and plume based on location, with measurements made inshore of the river mouth designated as estuary samples and measurements made offshore of

the river mouth within the defined region designated as plume samples (Fig. 4.2). Average plume air-water CO_2 fluxes were calculated only from measurements made with salinities < 28. The shoreward boundary of the estuary generally follows that of *Simenstad et al.* [1990] and is approximately 65 kilometers from the river mouth. The defined plume region used here is where Columbia River water first enters the coastal ocean and coincides with the recirculating bulge described by *Kudela et al.* [2010]. It should be noted, however, that Columbia River water may be observed much further from the river mouth in the alongshore direction [*Hickey and Banas*, 2008; *Hickey et al.*, 2009; *Hickey et al.*, 2010; *Huyer et al.*, 2007].

River and ocean end-member mixing was described by first approximating the river and ocean total alkalinities. River total alkalinity was approximated by the carbonate alkalinity, based on measured carbonate and bicarbonate concentrations made by the USGS at their monitoring site shown in Fig. 4.2 (red star). These data are collected approximately monthly, beginning October 1995, as part of the Monitoring Large Rivers in the National Stream Quality Accounting Network (NASQAN; http://water.usgs.gov/nasqan/). An average of these data was used to define the total alkalinity river end-member. The total alkalinity ocean end-member was calculated from a salinity relationship for California coastal waters described by *Seidel et al.* [2008; and references therein]. River and ocean end-member total dissolved inorganic carbon (DIC) was estimated with CO2calc (http://pubs.usgs.gov/of/2010/1280/) using the alkalinities described above and average pCO_2 values for estuary water with salinity < 1 and for plume water with salinity between 25 and 28. Conservative mixing lines were then calculated from the river and ocean end-member alkalinity and DIC values. pCO_2 was then calculated using CO2calc from each alkalinity/DIC pair along for

the salinity range from 0 to 28, assuming isothermal conditions equivalent to the mean surface water temperature computed from all estuary and plume data.

Results

The Physical Setting

Five cruises surveyed the Columbia River Estuary and plume from August 18-30 2007, November 2-19 2007, April 13-15 2008, May 31-June 6 2008 and September 19-23 2008 (sample positions shown in Fig. 4.2). Note that the August and November 2007 cruises each occurred in two portions. Thirty-five days of sampling took place, totaling > 480,000 individual measurements, that spanned nearly the full range of river discharge and wind speeds that occurred during the remainder of the August 2007 to September 2008 period (Fig. 4.3). These cruises captured seasonal variability within the Columbia River estuary and plume associated with spring phytoplankton bloom conditions (April 2008), the late spring to early summer freshet (May-June 2008), low river discharge conditions in late summer and early autumn (August 2007 and September 2008), and late autumn pre- and post-storm conditions (November 2007). Over the study period, river discharge ranged from ~3000 to ~14,000 m^3/s. Given a volume estimate for the estuary based on a surface area of 267.8 km^2 and an average depth of 14 m in the main channel [*Hamilton*, 1990], this implied a water residence time of approximately 14 and 3 days for low-flow and high-flow conditions, respectively. However, these residence time estimates are maximal, because the approximation of the volume does not account for the shallow waters surrounding the main channel of the estuary. True residence times are likely shorter. The seasons are delineated following *Evans et al.* [2011a] with winter as December to February, spring as March to May, summer as June to August, and autumn as September to November. Note that the freshet occurred

between May and July, therefore crossed over our delineation of the spring and summer seasons. The data are discussed below according to the season in which the measurements were collected.

Property distributions

Spring

River discharge during the spring survey was ~6500 m^3/s, close to the 6350 m^3/s mean for the study period (August 18, 2007 to September 23, 2008), and winds were light and variable (Fig. 4.3). Surface temperatures were cool (~10 °C) in both the estuary and plume. Salinity in the plume was broadly near 20 (Fig. 4.4). Salinity in the estuary was 5 or less, except near the estuary mouth (Fig. 4.4). Surface chlorophyll concentrations in the estuary were the highest observed in this record, with values ranging reaching as high as 15 mg m^{-3}. Values in the plume were less, only reaching 10 mg m^{-3}. Presumably the high phytoplankton biomass (chlorophyll concentration) resulted from high primary productivity occurring at the time, which caused the low pCO_2 observed in both the estuary and plume (Fig. 4.4; 200 µatm up to saturation with respect to the atmosphere). The lowest pCO_2 values observed in the estuary during this study were in spring (Fig. 4.4).

Summer

Our measurements on May 31 to June 6, 2008 captured the peak of the freshet with discharge rates near 14,000 m^3/s (Fig. 4.3), more than double the annual mean. The entire estuary was essentially fresh (surface salinity < 5) during this time. The discharge had a pronounced effect on the plume. Surface water with salinity near or below 15 was broadly distributed in the plume region

(Fig. 4.4), and surface water temperatures in both the estuary and plume were approximately 13°C. Chlorophyll concentrations were low (~3 mg m^{-3}) except near the southern extent of the plume. Highly variable pCO_2 levels were evident in both the estuary and plume (Fig. 4.4). However, largely oversaturated values with respect to the atmosphere were present within the estuary, reaching values as high as 750 µatm, while undersaturated values as low as 150 µatm were prevalent in the plume (Fig. 4.4).

The late summer conditions sharply contrasted with those of early summer (Fig. 4.4), as river discharge at this time of year was nearly 3 times lower than during the freshet and less than the mean value for the study period (~3700 m^3 s^{-1}; Fig. 4.3). Salinity within most of the estuary was less than 5, however values up to 25 were observed near the estuary month. Surface water temperatures had warmed considerably, with values within the estuary above 18°C. Warm surface water was also present in the plume, however values there were more variable, ranging from 13°C to 16°C. Estuarine pCO_2 exceeded atmospheric during this time, but reached maximal values of only 550 µatm, compared to the much higher values present during the freshet in early summer. Based on thermodynamics alone, the 5°C warming between early and later summer should have caused an increase in pCO_2 in the estuary by as much as ~150 µatm relative to early summer conditions [*Takahashi et al.*, 1993]. However, levels were lower in late summer relative to early summer, and this implies that rates of primary production were strong enough to counteract the effect of warming throughout the summer during low-flow conditions. Higher chlorophyll concentrations during late summer relative to early summer provide evidence for higher standing stocks of phytoplankton (Fig. 4.4). The estuary, however, was still functioning as a potential source of atmospheric CO_2.

Autumn

River discharge in early autumn was near the mean value for the study period (Fig. 4.3). Salinity within the estuary was near 5 or less, except near the estuary month where values as high as 20 were observed (Fig. 4.4). Data from autumn indicate that decreasing temperature across the season did not lead to a drop in pCO_2 in the estuary, as would be expected from purely thermal forcing. During early autumn (September 2008), estuary surface temperatures were as warm (~18°C) as they were in late summer. In late autumn (November 2007), temperatures were significantly cooler (12°C). The 6°C difference in temperature should result in a ~100 µatm pCO_2 decrease [*Sarmiento and Gruber*, 2006; *Takahashi et al.*, 1993] between early and late autumn, assuming isochemical conditions. However this was not the case as pCO_2 was near ~500 µatm in early autumn and as high as ~800 µatm by late autumn (Fig. 4.4). This pCO_2 increase implies a strong respiration signal in the estuary during autumn, perhaps related to the breakdown of vertical stratification as estuary waters cool, that counteracts the effect of cooling. The lower chlorophyll concentrations during late autumn relative to early autumn provide evidence that phytoplankton standing stocks were reduced, and perhaps primary productivity had a decreased role in counterbalancing respiration during the latter portion of the season (Fig. 4.4).

A significant storm event occurred during the second portion of the late autumn survey (Fig. 4.3). During this event R/V *Wecoma* stayed on station for a 37-hour period within the estuary, and maximum wind speeds measured on the ship were 36 m/s. pCO_2 during and following the storm in the estuary peaked near 500 µatm, considerably less than the near ~800 µatm values observed during the first portion of the cruise (Fig. 4.4). The storm-driven change in the estuary is clearly shown by two distinct pCO_2 versus salinity relationships within the late autumn data (Fig. 4.4). Values during and following the storm were

broadly ~200 µatm less than the values preceding the storm across the salinity range from 0 to 20 (Fig. 4.4).

Air-water CO_2 fluxes

The air-water CO_2 fluxes calculated from the data described above indicate that the plume generally acts as a sink, but the source/sink status of the estuary is dependent on the season. ΔpCO_2 during our spring cruise was between -200 and -100 µatm over most of the estuary and plume (Fig. 4.5). Wind speeds during this time caused gas transfer velocities near 10 m/d that drove atmospheric CO_2 influx near -50 mmol m^{-2} d^{-1} in both the estuary and plume (Fig. 4.5). Atmospheric CO_2 uptake to this degree occurring simultaneously in both regions was not observed during any other season.

Summer CO_2 efflux was greatest in the estuary early in the season during the freshet, because of large positive ΔpCO_2 and moderate gas transfer velocities (Fig. 4.5). Some CO_2 outgassing was also apparent in the plume during early summer (Fig. 4.5), but the flux on average was directed into the ocean (Fig. 4.6). During late summer, CO_2 influx was dominant in the plume, while efflux was dominant in the estuary despite a few instances of undersaturated waters there. Influx of atmospheric CO_2 occurred in early autumn in the plume, and contrasted with CO_2 efflux from the estuary. Outgassing fluxes from the estuary were larger in early autumn relative to late summer (Fig. 4.5). This pattern of the estuary/source and plume/sink was also apparent in late autumn, however there were larger fluxes in late autumn as a result of both the presumed strong respiration signal, discussed above, that caused large positive ΔpCO_2 and the storm during the latter portion of the survey. ΔpCO_2 in the estuary was greatest prior to the storm, but the fluxes didn't breach 100 mmol m^{-2} d^{-1} because the

winds were generally light. During the storm, the strong winds resulted in a peak gas transfer velocity of 76 m/d that caused the largest observed air-water CO_2 flux in this study of 223 mmol m^{-2} d^{-1}.

Mean air-water CO_2 fluxes for the Columbia River Estuary and plume from each cruise portion show that the estuary functions on average as an atmospheric CO_2 source most of the time, with the exception of during spring. Fluxes to the atmosphere were greatest in the estuary during the freshet in early summer and during late autumn. Interestingly, the mean flux was higher during the first portion of the late autumn survey (November 2-4, 2007) relative to the second portion during the storm event (November 11-19, 2007). This was because the ΔpCO_2 dropped significantly during and following the storm at the end of the second portion of the cruise, and this resulted in low positive, and even negative fluxes that offset the largest flux during the storm (Fig. 4.5). The plume was always an atmospheric CO_2 sink (Fig. 4.6). The sink term for the plume was largest in spring (-23.4 mmol m^{-2} d^{-1}), and smallest during the late autumn before the storm (-1.3 mmol m^{-2} d^{-1}).

Discussion

Here air-water CO_2 fluxes are reported for the Columbia River Estuary and plume during the spring, summer and autumn. The estuary acts as an atmospheric CO_2 source most of the time, while the plume is consistently an atmospheric CO_2 sink. These observations agree with the widely held view that estuaries are net sources of atmospheric CO_2 [*Borges and Frankignoulle*, 1999; *Borges et al.*, 2005; *Cai*, 2011; *Chen and Borges*, 2009; *Frankignoulle et al.*, 1998], while river plumes are net sinks [*Borges*, 2005; *Körtzinger*, 2010; *Lohrenz and Cai*, 2006]. The source character of estuaries probably results from a

combination of bacterial remineralization of organic matter outweighing the effect of primary productivity on pCO_2 levels [*Gattuso et al.*, 1998] and inherited signals of high pCO_2 from the watershed. This leads to a high pCO_2 signal in estuaries that should be transported to plumes, but strong undersaturation is often observed there due to a combination of chemical and biological effects [*Körtzinger*, 2010; *Lohrenz and Cai*, 2006]. Körtzinger [2010] described how the nonlinear nature of the aquatic CO_2 system leads to reduced pCO_2 in river plumes due to conservative mixing of alkalinity and DIC between the river and ocean. To show this character for the Columbia River Estuary and plume, pCO_2 levels were calculated from river and ocean end-members of DIC and alkalinity, assuming isothermal conditions (Fig. 4.7). This calculation shows that, even in the absence of biological processes, conservative mixing alone can result in pCO_2 undersaturation with respect to the atmosphere. The degree of pCO_2 undersaturation, however, is most dependent on the river alkalinity and DIC end-members. Ocean alkalinity and DIC values are generally near 2200 µmol/kg and vary on the order of ± 200 µmol/kg, while river alkalinity and DIC values can range widely between river/estuary systems. For example, the Mississippi River has been shown to have alkalinity and DIC concentrations ~3000 µmol/kg, actually exceeding oceanic values [*Cai*, 2003; *Lohrenz and Cai*, 2006], while in contrast the Amazon River has values about 5-fold lower [*Körtzinger*, 2010]. The same mixing calculations were done for both of these large rivers [*Körtzinger*, 2010; *Lohrenz and Cai*, 2006], and show that the lower the river end-member values, the more pronounced the pCO_2 reduction will be. This chemical effect acts in concert with biological processes. Elevated nutrients and buoyancy in the plume cause high rates of primary production that drive low pCO_2 conditions. These chemical and biological drivers can combine to create strong atmospheric CO_2 sink regions in areas impacted by river plumes [*Körtzinger*, 2010; *Lohrenz and Cai*, 2006]. We have shown here that the Columbia River plume acts as an atmospheric CO_2 sink across season. The calculation shown in Fig. 4.7

describes the conservative mixing that can aid in driving this condition. The chlorophyll measurements presented here are only indicative of phytoplankton standing stocks, and are not adequate for describing the rates of primary production. However, the River Influences on Shelf Ecosystems (RISE) program demonstrated significantly higher phytoplankton growth rates within the near-field plume compared to Oregon and Washington coastal waters [*Hickey et al.*, 2010; *Kudela et al.*, 2008]. It is assumed that the persistent low pCO_2 levels observed in the Columbia River plume result from the combination of the chemical mixing described above and high primary productivity.

In contrast to the plume, the estuary is an atmospheric CO_2 sink in spring and a source in other seasons. This difference in function is attributed to a spring bloom in the estuary, and spring pCO_2 undersaturation and atmospheric CO_2 influx have been observed in other estuarine systems on the eastern U.S. coast [*Hunt et al.*, 2011; *Raymond et al.*, 2000] and in Europe [*Borges and Frankignoulle*, 1999]. In these systems, the uptake of atmospheric CO_2 was ascribed to spring increases in primary productivity which outweighing respiration, such that net community metabolism was positive. The net community metabolism within select U.S. estuaries has been examined, and, for the most part, Pacific Northwest estuaries all had negative community metabolism during all seasons [*Caffrey*, 2004]. This study did not examine the Columbia River Estuary, but evidence of spring blooms in this system does exist [*Lara-Lara et al.*, 1990; *Roegner et al.*, 2011; *Small et al.*, 1990; *Sullivan et al.*, 2001]. The highest chlorophyll values observed in this study were during spring, which is a sign that the influx of atmospheric CO_2 during this time was caused by high standing stocks of phytoplankton and presumably elevated photosynthetic productivity. High spring primary productivity may be driven by the dominance of freshwater diatoms during this time of year [*Small et al.*, 1990], and the cells of

this group of phytoplankton have been observed to lyse and sink of the water column at salinities above 5 [*Lara-Lara et al.*, 1990]. The data presented shows distinct peaks of chlorophyll at the low and high salinity range during the spring (Fig. 4.4) that may represent the presence of freshwater diatoms in the low salinity waters of the estuary, and coastal diatoms in the saltier plume waters. Two studies have shown that differences in river discharge affect the magnitude of the spring bloom in the estuary [*Roegner et al.*, 2011; *Sullivan et al.*, 2001]. Chlorophyll concentrations during the spring bloom were higher during years of lower spring river discharge relative to higher discharge years. This suggests that even though there is evidence for potentially positive net community metabolism and atmospheric CO_2 uptake in spring in the Columbia River Estuary, this may be strongly dependent on the annual discharge conditions. Years with lower river discharge should experience greater spring CO_2 uptake, whereas higher discharge years should experience reduced uptake. Our spring measurements fell on the shoulder of peak discharge during the freshet, when fluxes transitioned in sign. This follows the above argument, in that not only do interannual differences in spring discharge impact the spring estuary sink, but the seasonal increase in flow associated with the freshet reduces the sink and transitions the system into an atmospheric CO_2 source during the other seasons. The turbidity increase associated with the freshet [*Sullivan et al.*, 2001] likely causes a reduction in light levels and subsequently reduced phytoplankton growth rates that limits the draw down of pCO_2. The high flow rates also likely flush the freshwater diatoms out of the estuary into higher salinity waters where they can no longer survive. Through these possible impacts, the freshet transitions the function of the estuary from sink to source.

Tidal and diel variability are not accounted for in the air-water CO_2 flux estimates presented here. The influence of tides has not been resolved, but on

two occasions, we were able to observe some tidal effects. During August 2007, our survey near the estuary mouth captured the intrusion of plume water with salinity near 25 and pCO_2 near 350 µatm during high tide that, at the time, sharply contrasted with higher pCO_2 in lower salinity waters. It is difficult to define how far this water entered the estuary, but because water of these characteristics was not observed further up estuary, our mean estuarine fluxes are weighted more toward the lower salinity waters. A detailed examination of the impact of tides on the air-water CO_2 fluxes in the Columbia River Estuary would be worthwhile because tidal variability has been observed to be important in other estuarine systems [*Jiang et al.*, 2008a]. In the Columbia River Estuary, this effect is likely more pronounced during low river flow conditions in late summer when the estuary is an atmospheric CO_2 source. The intrusion of lower pCO_2 waters from the plume region during high tides should reduce the magnitude of the fluxes, as has been observed within three estuaries on the Georgia coast [*Jiang et al.*, 2008a]. However, the effect of tides shouldn't change the estuarine seasonal sink/source pattern described here because likely low-pCO_2 water with surface salinity near 25 does not intrude far up estuary. A thorough examination of their impact is warranted to enable a more complete understanding of the variability of sea-air CO_2 fluxes in the estuary. Diel variability, on the other hand, may be important throughout the estuary, as has been seen in the Neuse River Estuary [*Crosswell et al.*, 2011] where 200 µatm fluctuations in pCO_2 have been observed. However, our cruise data do not show fluctuations similar to this in the Columbia River Estuary, and there was no obvious diel pattern during the autumn storm event when the ship stayed on station for 37 hours. This is still a source of variability that should be addressed and may be important within the estuary during summer months when the largest diel pattern in primary productivity is expected.

The storm event in late autumn was a significant source of variability that drove a ~200 µatm change in pCO_2 in the estuary. If alkalinity is assumed to be constant in the estuary, the DIC change associated with the drop in pCO_2 during the storm was only 11 µmol/kg. Assuming a homogenous water column with a 14 m depth, the maximal air-water exchange rates observed during the storm event would exchange that amount of DIC in a 17-hour period. This indicates that pCO_2 in the estuary is not strongly buffered, and can respond rapidly to air-water exchange, as opposed to typical oceanic conditions. This is a significant point when considering how to produce estimates of net annual air-water fluxes from this and other similar systems. Clearly, storm events are critical in setting the net CO_2 exchange; however, the rapid response indicates a steep exponential drop from pre-storm to post-storm pCO_2 levels. The fact that we were in the field during the event and measuring pCO_2 in tight synchronicity with the wind means our flux estimates are robust. This is often not the norm, however, and pCO_2 conditions during high wind events are often interpolated between observations bracketing those events. A simple linear interpolation between pre-storm and post-storm pCO_2 levels combined with a high-resolution wind record with the extreme associated gas transfer velocities would lead to overestimation of the true air-water exchange.

Inherent in the above discussion calculation is the fact that the Revelle factor calculated for these fresh low alkalinity and DIC waters was 36, indicating that a 36% change in pCO_2 will result from a 1% change in DIC. This has significant additional implications for variability within the Columbia River Estuary, and similar high Revelle factor systems, because processes that cause small changes in DIC (*e.g.* daily variability in primary productivity, DIC exchange on tidal cycles, riverine DIC addition, dilution of surface water DIC by rainwater) will impart large changes in pCO_2, which will affect air-water fluxes.

Inadequate seasonal coverage in this study prevents an estimate of the annual air-water CO_2 flux for the Columbia River Estuary and plume, and this inhibits a direct comparison with global compilations of estuarine fluxes (*e.g. Borges et al.,* 2005). However, *Borges et al.* [2005] determine the estuarine CO_2 fluxes for the temperate latitudes are more than twice those of low latitude systems. The results from this study indicate that caution should be made when considering that all temperate latitude estuarine systems are large flux regions, especially river-dominated estuaries. For at least some portion of the year the Columbia River Estuary is a CO_2 sink, and because of its high Revelle factor character, persistent high-flux conditions are not likely to occur. That is, following a large wind event, some amount of time is likely necessary to rebuild high-ΔpCO_2 conditions from up-stream sources and local respiration. Maximum effluxes occur in pulses, followed by periods of reduced fluxes with possible reversals in sign. This implies that the Columbia River Estuary, and other similar regions, requires sample resolution that can resolve high-frequency variability in order to make accurate estimates of the air-water fluxes on seasonal or longer time scales.

Conclusions

The data described above show spring, summer and autumn surface water pCO_2 distributions and air-water CO_2 fluxes within the Columbia River Estuary and plume. The plume was an atmospheric CO_2 sink during each season, whereas the estuary was a sink during the spring and a source in summer and autumn. A phytoplankton bloom, evidenced by high chlorophyll concentrations and probably consisting of freshwater diatom *spp*, is believed to have caused the sink character of the estuary during spring. The late spring to early summer freshet marked the transition in the estuary from an atmospheric CO_2 sink to a source during other seasons. The largest fluxes to the atmosphere

from the estuary were during the freshet and in autumn, when large positive ΔpCO_2 occurred with moderate to high gas transfer velocities. An autumn storm drove the largest outgassing fluxes observed in this study, but this was ephemeral and followed by lower ΔpCO_2 relative to pre-storm autumn conditions. The large pre- and post-storm difference in estuary pCO_2, with assumed constant alkalinity, showed that small changes in DIC in this system cause large changes in pCO_2. More data are needed to calculate an annual air-water CO_2 flux from this region, but it is likely that outgassing conditions (*i.e.* positive ΔpCO_2) continue during winter in the estuary until the initiation of the spring bloom. Diel variability, including the tides, should be further examined because these unresolved components of the system impart uncertainty in the fluxes. These data the seasonality of air-water CO_2 fluxes in the Columbia River Estuary and plume, and highlight important points that require further work.

REFERENCES

Aquilar-Islas, A. M., and K. W. Bruland (2006), Dissolved manganese and silicic acid in the Columbia River plume: A major source to the California current and coastal waters off Washington and Oregon, *Marine Chemistry*, *101*, 233-247.

Borges, A., and M. Frankignoulle (1999), Daily and seasonal variations of the partial pressure of CO_2 in surface seawater along Belgian and southern Dutch coastal areas, *Journal of Marine Systems*, *19*, 251-266.

Borges, A. V. (2005), Do We Have Enough Pieces of the Jigsaw to Integrate CO_2 Fluxes in the Coastal Ocean?, *Estuaries*, *28*(1), 3-27.

Borges, A. V., B. Delille, and M. Frankignoulle (2005), Budgeting sinks and sources of CO2 in the coastal ocean: Diversity of ecosystems counts, *Geophysical Research Letters*, *32*, L14601, doi: 14610.11029/12005GL023053.

Bruland, K. W., M. C. Lohan, A. M. Aquilar-Islas, G. Smith, J., B. Sohst, and A. M. Baptista (2008), Factors influencing the chemistry of the near-field Columbia River plume: Nitrate, silicic acid, dissolved Fe, and dissolved Mn, *Journal of Geophyiscal Research*, *113*(C00B02), doi: 10.1029/2007JC004702.

Caffrey, J. M. (2004), Factors Controlling Net Ecosystem Metabolism in U.S. Estuaries, *Estuaries*, *27*(1), 90-101.

Cai, W.-J. (2011), Estuarine and Coastal Ocean Carbon Paradox: CO_2 Sinks or Sites of Terrestrial Carbon Incineration?, *Annual Review of Marine Science*, *3*, 123-145.

Cai, W.-J., and Y. Wang (1998), The chemistry, fluxes, and sources of carbon dioxide in the estuarine waters of the Satilla and Altamaha Rivers, Georgia, *Limnology and Oceanography*, *43*(4), 657-668.

Cai, W.-J., M. Dai, and Y. Wang (2006), Air-sea exchange of carbon dioxide in ocean margins: A province-based synthesis, *Geophysical Research Letters*, *33*, L12603, doi:12610.11029/12006GL026219.

Chen, C.-T. A., and A. V. Borges (2009), Reconciling opposing views on carbon cycling in the coastal ocean: Continental shelves as sinks and near-shore ecosystems as sources of atmospheric CO2, *Deep-Sea Research II*, *56*, 579-590.

Evans, W., B. Hales, and P. G. Strutton (2011a), The seasonal cycle of surface ocean pCO_2 on the Oregon shelf, *Journal of Geophyiscal Research*, *(accepted)*.

Evans, W., B. Hales, P. G. Strutton, and D. C. Ianson (2011b), Sea-Air Carbon Dioxide Fluxes on the Western Canadian Coastal Margin, *Journal of Geophyiscal Research*, (*in preparation)*.

Frankignoulle, M., G. Abril, A. Borges, I. Bourge, C. Canon, B. Delille, E. Libert, and J.-M. Théate (1998), Carbon Dioxide Emission from European Estuaries, *Science*, *282*, 434-436.

Gattuso, J.-P., M. Frankignoulle, and R. Wollast (1998), Carbon and Carbonate Metabolism in Coastal Aquatic Ecosystems, *The Annual Review of Ecology, Evolution and Systematics*, *29*, 405-434.

Hales, B., D. Chipman, and T. Takahashi (2004), High-frequency measurements of partial pressure and total concentration of carbon dioxide in seawater using microporous hydrophobic membrane contactors, *Limnology and Oceanography: Methods*, *2*, 356-364.

Hickey, B., and N. S. Banas (2008), Why is the Northern End of the California Current System so Productive?, *Oceanography*, *21*(4), 91-107.

Hickey, B., R. McCabe, S. Geier, E. Dever, and N. Kachel (2009), Three interacting freshwater plumes in the northern California Current System, *Journal of Geophysical Research*, *114*, C00B03, doi: 10.1029/2008JC004907.

Hickey, B., et al. (2010), River Influences on Shelf Ecosystems: Introduction and Synthesis, *Journal of Geophysical Research*, *115*, C00B17, doi:10.1029/2009JC005452.

Hill, J. K., and P. A. Wheeler (2002), Organic carbon and nitrogen in the northern California current system: comparison of offshore, river plume, and coastally upwelled waters, *Progress in Oceanography*, *53*, 369-387.

Ho, D. T., C. S. Law, M. J. Smith, P. Schlosser, M. Harvey, and P. Hill (2006), Measurements of air-sea gas exchange at high wind speeds in the Southern Ocean: Implications for global parameterizations, *Geophysical Research Letters*, *33*, L16611, doi: 16610.11029/12006GL026817.

Hunt, C. W., J. E. Salisbury, D. Vandemark, and W. R. McGillis (2011), Contrasting Carbon Dioxide Inputs and Exchange in Three Adjacent New England Estuaries, *Estuaries and Coasts*, *34*, 68-77.

Huyer, A., P. A. Wheeler, P. T. Strub, R. L. Smith, R. Letelier, and P. M. Kosro (2007), The Newport line off Oregon - Studies in the North East Pacific, *Progress in Oceanography*, *75*, 126-160.

Jiang, L.-Q., W.-J. Cai, R. Wanninkhof, Y. Wang, and H. Lüger (2008), Air-sea CO2 fluxes on the U.S. South Atlantic Bight: Spatial and seasonal variability, *Journal of Geophysical Research*, *113*, C07019, doi: 07010.01029/02007JC004366.

Körtzinger, A. (2010), The Outer Amazon Plume: An Atmospheric CO_2 Sink, in *Carbon and Nutrient Fluxes in Continental Marginis*, edited by K.-K. Liu, L. Atkinson, R. A. Quiñones and L. Talaue-McManus, Springer, Berlin.

Kudela, R. M., et al. (2010), Multiple trophic levels fueled by recirculation in the Columbia River plume, *Geophysical Research Letters*, *37*(L18607), doi: 10.1029/2010GL044342.

Landry, M. R., J. R. Postel, W. K. Peterson, and J. Newman (1989), Broad-scale distributional patterns of hydroghraphic variabiles on the Washington/Oregon shelf, in *Coastal Oceanography of Washington and Oregon*, edited by M. R. Landry and B. M. Hickey, Elsevier Science Publishers B.V., Amsterdam, The Netherlands.

Laruelle, G. G., H. H. Dürr, C. P. Slomp, and A. V. Borges (2010), Evalution of sinks and sources of CO_2 in the global coastal ocean using a spatially-explicit typology of estuaries and continental shelves, *Geophysical Research Letters*, *37*(L15607), doi: 10.1029/2010GL043691.

Lohan, M. C., and K. W. Bruland (2006), Importance of vertical mixing for additional sources of nitrate and iron to surface waters of the Columbia River plume: Implications for biology, *Marine Chemistry*, *98*(260-273).

Park, P. K., L. I. Gordon, S. W. Hager, and M. C. Cissell (1969), Carbon Dioxide Partial Pressure in the Columbia River, *Science*, *166*(3907), 867-868.

Perry, G. D., P. B. Duffy, and N. L. Miller (1996), An extended data set of river discharges for validation of general circulation models, *Journal of Geophyiscal Research*, *101*(D16), 21,339-321,349.

Raymond, P. A., and J. J. Cole (2001), Gas Exchange in Rivers and Estuaries: Choosing a Gas Transfer Velocity, *Estuaries*, *24*(2), 312-317.

Raymond, P. A., J. E. Bauer, and J. J. Cole (2000), Atmospheric CO_2 evasion, dissolved inorganic carbon production and net heterotrophy in the York River estuary, *Limnology and Oceanography*, *45*(8), 1707-1717.

Roegner, G. C., C. Seaton, and A. M. Baptista (2011), Climatic and Tidal Forcing of Hydrography and Chlorophyll Concentrations in the Columbia River Estuary, *Estuaries and Coasts*, *34*(2), 281-296.

Salisbury, J., M. Green, C. Hunt, and J. Campbell (2008), Coastal Acidification by Rivers: A Threat to Shellfish?, *EOS, Transactions, American Geophysical Union*, *89*(50), 513-514.

Sarmiento, J. L., and N. Gruber (2006), *Ocean Biogeochemical Dynamics*, Princeton University Press, Princeton.

Simenstad, C. A., L. F. Small, C. D. McIntire, D. A. Jay, and C. Sherwood (1990), Columbia River Estuary studies: An introduction to the estuary, a brief history, and prior studies, *Progress in Oceanography*, *25*, 1-13.

Small, L. F., C. D. McIntire, K. B. Macdonald, J. R. Lara-Lara, B. E. Frey, M. C. Amspoker, and T. Winfield (1990), Primary productivity, plant and detrital biomass, and particle transport in the Columbia River Estuary, *Progress in Oceanography*, *25*, 175-210.

Suchet, P. A., J.-L. Probst, and W. Ludwig (2003), Worldwide distribution of continental rock lithology: Implications for the atmospheric/soil CO_2 uptake by

continental weathering and alkalinity river transport to the oceans, *Global Biogeochemical Cycles*, *17*(2), doi: 10.1029/2002GB001891.

Takahashi, T., J. Olafsson, J. G. Goddard, D. W. Chipman, and S. C. Sutherland (1993), Seasonal Variation of CO2 and Nutrients in the High-Latitude Surface Oceans: a Comparative Study, *Global Biogeochemical Cycles*, *7*(4), 843-878; doi:810.1029/1093GB02263.

Vandemark, D., J. E. Salisbury, C. W. Hunt, S. M. Shellito, J. D. Irish, W. R. McGillis, C. L. Sabine, and S. M. Maenner (2011), Temporal and spatial dynamics of CO_2 air-sea flux in the Gulf of Maine, *Journal of Geophyiscal Research*, *116*(C01012), doi: 10.1029/2010JC006408.

Venegas, R. M., P. T. Strub, E. Beier, R. Letelier, A. C. Thomas, T. Cowles, C. James, L. Soto-Mardones, and C. Cabrera (2008), Satellite-derived variability in chlorophyll, wind stress, sea surface height, and temperature in the northern California Current System, *Journal of Geophyiscal Research*, *113*(C03015), doi: 10.1029/2007JC004481.

Wanninkhof, R. (1992), Relationship Between Wind Speed and Gas Exchange Over the Ocean, *Journal of Geophysical Research*, *97*(C5), 7373-7382.

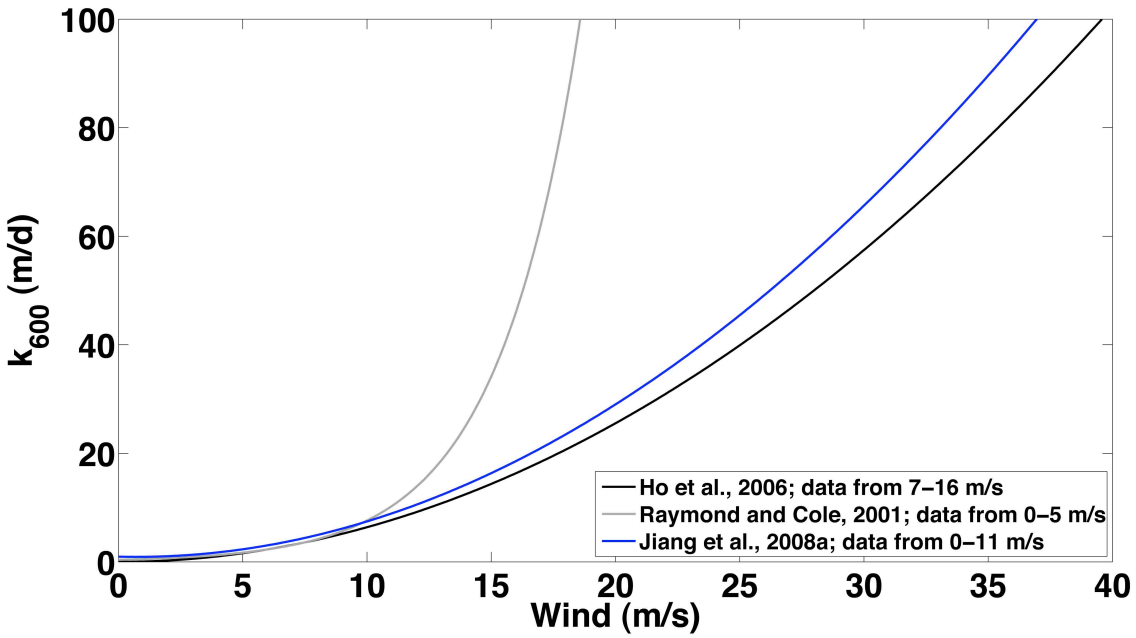

Figure 4.1: Three different relations for k_{600} (m/d), the gas transfer velocity of CO_2 at a Schmidt number of 600, as a function of wind speed (m/s). The *Ho et al.* [2006] relation (black line) is for the open ocean during moderate to high wind conditions, and has been used in recent coastal ocean sea-air CO_2 flux studies [*Evans et al.*, 2011a; *Evans et al.*, 2011b; *Jiang et al.*, 2008b; *Vandemark et al.*, 2011]. *Raymond and Cole* [2001] is an exponential regression equation (light gray line) from data collected within estuaries. Note that this relationship was developed from data collected at low wind speeds (0-5 m/s). The more recent compilation of *Jiang et al.* [2008a] includes data from *Raymond and Cole* [2001] and newly collected estuarine data over a broader wind speed range (0-11). The relation they have developed (dark gray line) more closely follows the *Ho et al.* [2006] open ocean case for high wind speeds, and was used in this study for calculating air-water CO_2 fluxes.

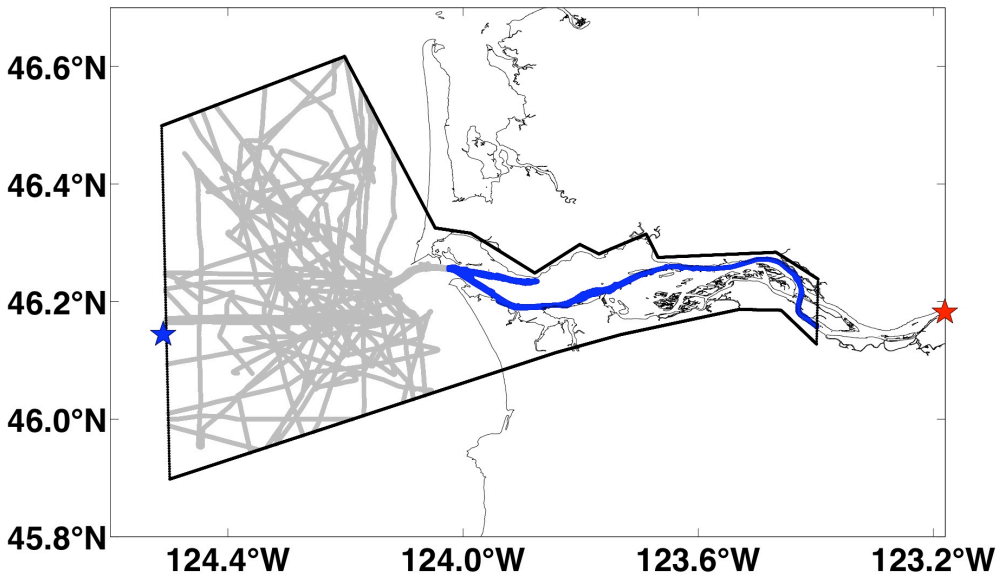

Figure 4.2: Locations of pCO_2 measurements within the Columbia River Estuary (blue dots) and plume region (gray dots) defined by the polygon. The red star is the position of river discharge measurements provided by USGS (http://waterdata.usgs.gov/usa/nwis/uv?site_no=14246900). The blue star is the buoy position where wind vector information was provided by NDBC (http://www.ndbc.noaa.gov/station_page.php?station=46029).

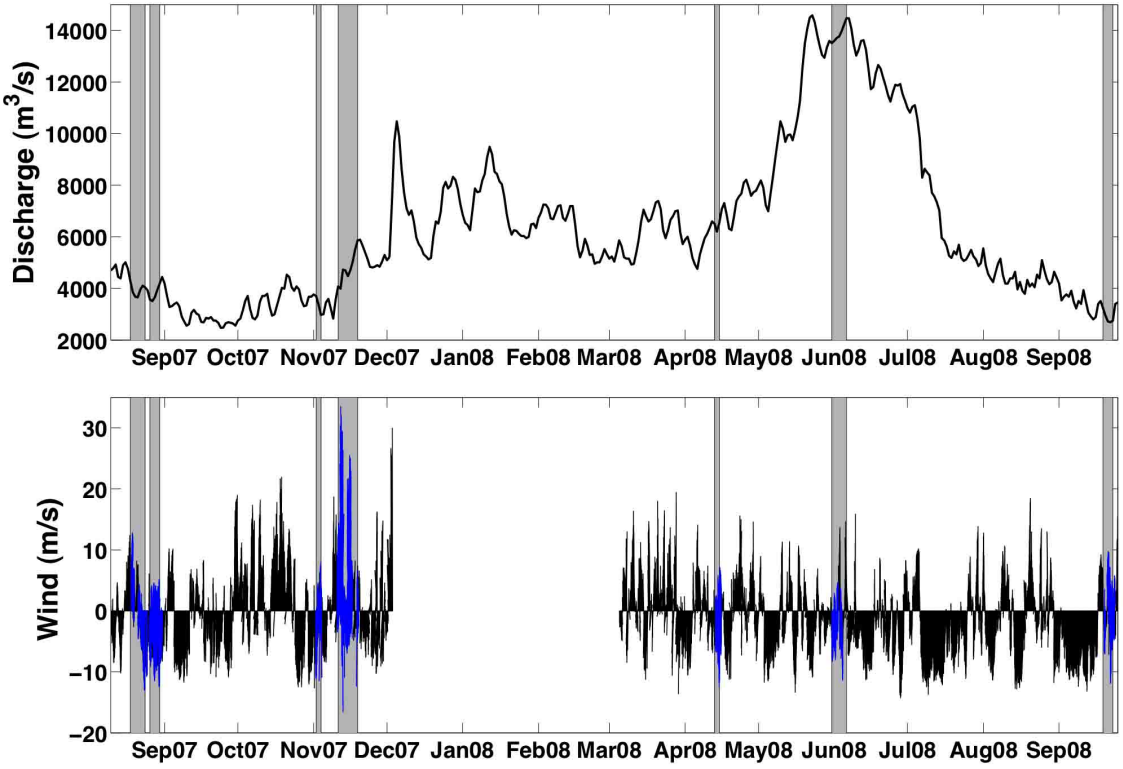

Figure 4.3: Columbia River discharge (upper panel: m^3/s) recorded at the USGS Beaver Army Terminal (red star in Fig. 2) and buoy (black; buoy position shown as blue star in Fig. 2) and ship (blue) winds (m/s) over the study period. Gray vertical bars represent cruise dates when the Columbia River Estuary and plume were sampled. The gap in the wind record was the result of the buoy breaking loose from its mooring during a storm event in December 2007.

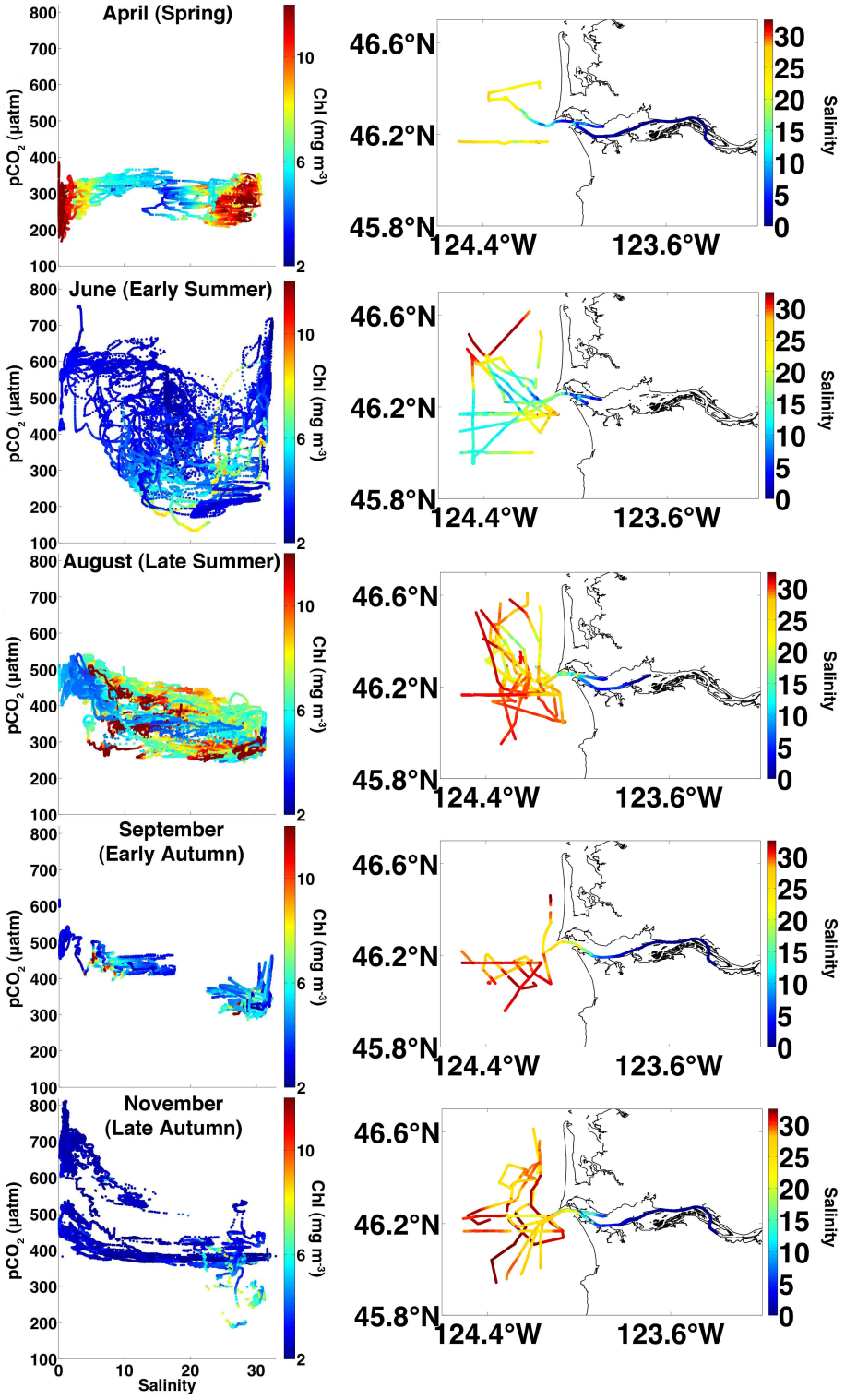
April (Spring)
June (Early Summer)
August (Late Summer)
September (Early Autumn)
November (Late Autumn)
pCO2 (µatm)
Chl (mg m-3)
Salinity
46.6°N
46.2°N
45.8°N
124.4°W
123.6°W

Figure 4.4

Figure 4.4: pCO_2 versus salinity from each cruise presented in order of season (from top to bottom). The data are colored by their corresponding chlorophyll concentrations (mg m^{-3}). Also shown with the pCO_2 versus salinity relationships are the corresponding salinity distributions from each cruise within the Columbia River Estuary and plume regions.

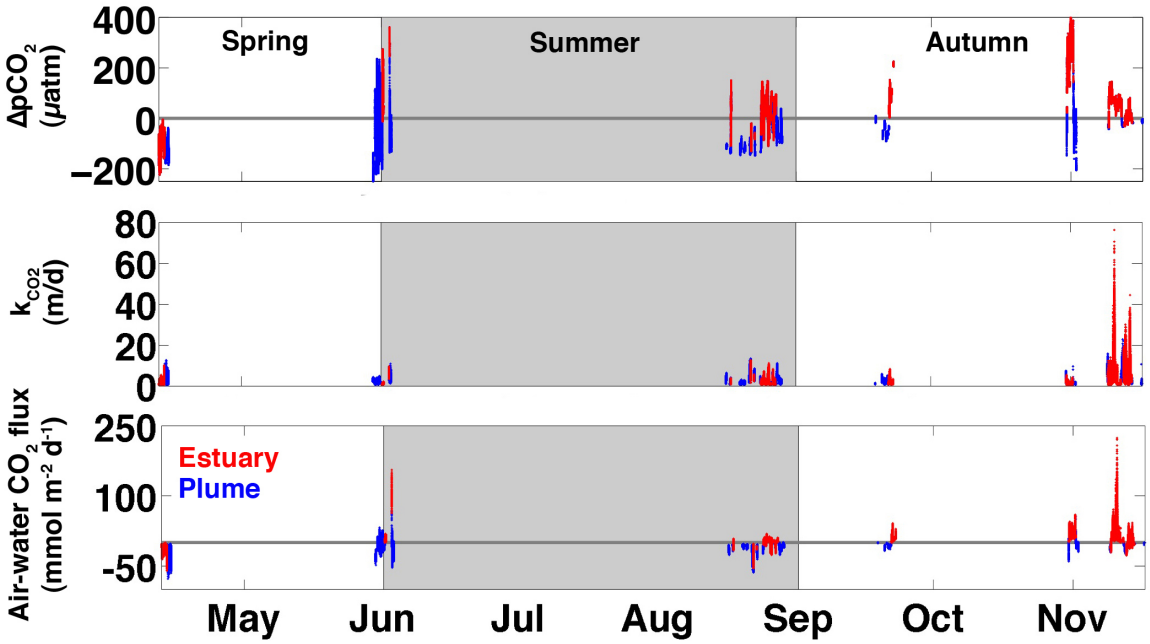

Figure 4.5: Time series of estuary (red) and plume (blue) ΔpCO_2 (µatm; upper), k_{CO2} (m/d; middle), and air-water CO_2 flux (mmol m^{-2} d^{-1}; lower) for spring, summer (shaded) and autumn.

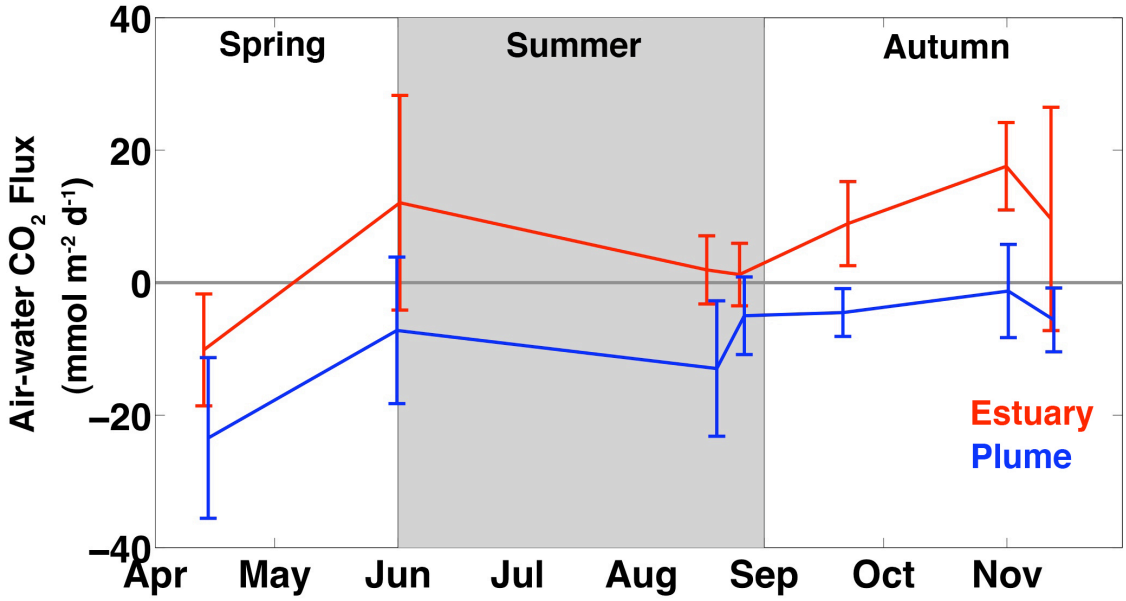

Figure 4.6: Average air-water CO_2 fluxes (mmol m^{-2} d^{-1}) for the estuary (red) and the plume (blue) from each cruise portion (shaded time periods in Fig. 3). Error bars are one standard deviation from the mean, and used to represent the observed variability.

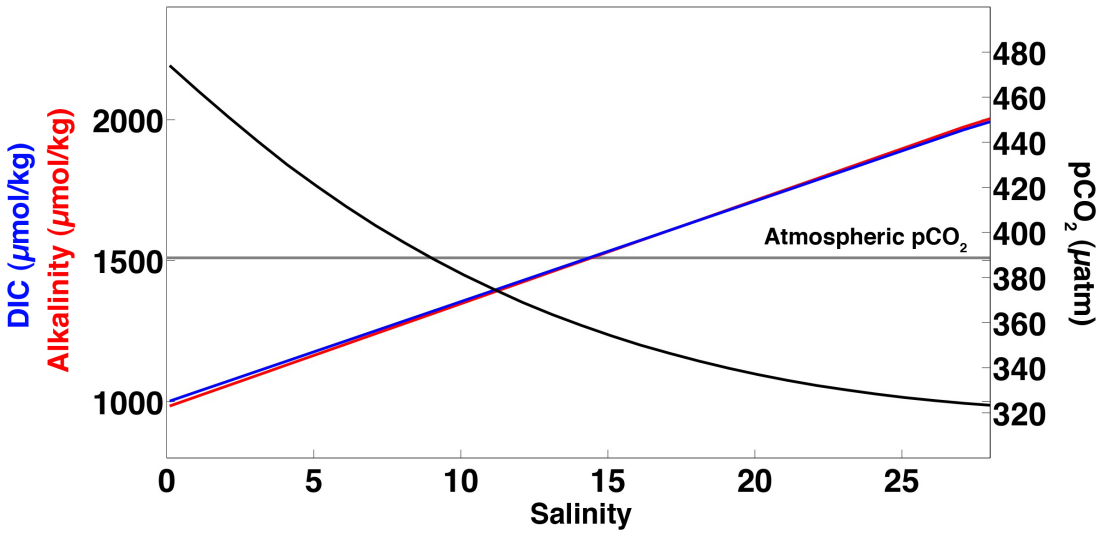

Figure 4.7: pCO_2 (µatm) calculated from conservative mixing of alkalinity (µmol/kg) and DIC (µmol/kg) end-members typical of the Columbia River Estuary and plume. The gray horizontal line is the average atmospheric pCO_2 level for the study period.

CHAPTER 5: Prolonged CO_2 Outgassing on the Oregon Shelf During July 2008

Wiley Evans

For submission to *Journal of Geophysical Research*

American Geophysical Union

ACKNOWLEDGMENTS

We thank Bill Peterson for allowing our participation in the July 2008 cruise, and for sharing nutrient data with us from that cruise. We thank the officers and crew of the NOAA Ship *McArthur II*. We thank Murray Levine, Craig Risien and Walt Waldorf for the NH-10 mooring data and platform, which is funded by the National Science Foundation through the cooperative agreement OCE-0424602 known as CMOP (Coastal Margin Observation & Prediction) and by NOAA through NANOOS (Northwest Association of Networked Ocean Observing Systems), the Pacific Northwest Regional Association of the U.S. Integrated Ocean Observing System (IOOS). This work was supported by NSF Chemical Oceanography award OCE-0752576.

ABSTRACT

During summer, upwelled water with elevated CO_2 partial pressure (pCO_2) and nutrients outcrops over the inner shelf along the Oregon (OR) coast and drives high rates of primary production, resulting in net atmospheric CO_2 drawdown over the shelf. Upwelled source-waters typically have pCO_2 approaching 1000 μatm that is then reduced to ~200 μatm over the shelf. For almost the whole month of July 2008, strong and persistent upwelling outcropped cold (~8°C), salty (~33.5), high-pCO_2 (>1000 μatm) water at our mid-shelf buoy site ~20 km from shore, and pCO_2 near 800 μatm was broadly distributed over the shelf. Chlorophyll levels were low (< 2 mg m^{-3}) on the shelf during the period of intense upwelling, with satellite data showing no evidence of a downstream bloom. A doubling of chlorophyll concentrations was observed at our mooring site coincident with a decrease in the strength of upwelling-favorable winds. A larger increase in chlorophyll followed a relaxation in the winds and the appearance of water masses with temperature and salinity properties distinct from the recently upwelled water. Rapid offshore transport of upwelled water followed by subduction, before phytoplankton populations could respond, is the most likely explanation for the low chlorophyll and elevated surface-water pCO_2 during the July upwelling event. This mechanism likely dominates under conditions of strong and persistent upwelling-favorable winds that coincide with close proximity of low-density offshore waters.

INTRODUCTION

The magnitude of the open ocean sink for atmospheric CO_2 is becoming well constrained [*Takahashi et al.,* 1997; *Takahashi et al.,* 2002; *Takahashi et al.,* 2009], but this is not the case for the coastal ocean [*Borges et al.,* 2005; *Hales et al.,* 2008; *Laruelle et al.,* 2010]. In a global sense, coastal margins are regarded as a net sink for atmospheric CO_2 [*Borges,* 2005; *Borges et al.,* 2005; *Cai et al.,* 2006; *Laruelle et al.,* 2010], but uncertainty arises because of the extremely dynamic nature of these systems relative to the open ocean [*Liu et al.,* 2010]. The range of surface water pCO_2 observed in coastal oceans far exceeds that seen in the open ocean, and values change significantly on sub-daily to super-annual frequencies [*Evans et al.,* 2011a; *Friederich et al.,* 2002; *Hales et al.,* 2005a; *Jiang et al.,* 2008]. Physical forcings include tides, freshwater input, wind variability, and climate modes such as the El Niño Southern Oscillation. This extreme variability is particularly relevant for upwelling-dominated coastal regions in the mid-high latitudes that experience highly variable upwelling conditions [*Borges and Frankignoulle,* 2002; *Cai et al.,* 2006; *Evans et al.,* 2011a; *Evans et al.,* 2011b; *Hales et al.,* 2005a]. The overarching issue regarding the uncertainty in coastal ocean CO_2 exchange with the atmosphere is inadequate data coverage to resolve the extreme variability over appropriate spatial and temporal scales.

The OR coast is a seasonally upwelling-dominated coastal margin that experiences highly variable upwelling conditions [*Huyer et al.,* 2007; *Huyer et al.,* 2005; *Pierce et al.,* 2006]. This region is part of the larger Cascadian margin that extends from northern California to Vancouver Island. Beginning in approximately April and ending around October, CO_2- and nutrient-rich waters from depth upwell to the surface nearshore. The nitrate concentrations and pCO_2 within the upwelled source water have been observed to be ~35 μM and ~1000 μatm,

respectively [*Evans et al.*, 2011a; *Hales et al.*, 2005a; *Hales et al.*, 2005b; *Hill and Wheeler*, 2002; *van Geen et al.*, 2000]. These waters are advected off- and alongshore, as fast-growing phytoplankton assemblages bloom [*Dugdale et al.,* 2006; *Wetz and Wheeler,* 2003], nutrients are driven to near zero [*Hales et al.,* 2005b] and pCO_2 levels are drawn down to below atmospheric values [*Hales et al.,* 2005a].

Recently observations made near Newport, OR showed pCO_2 levels above 1000 µatm, with values in excess of 800 µatm broadly distributed over the shelf [*Evans et al.,* 2011a]. These high-pCO_2 waters first appeared in June 2008, during two pulses of strong upwelling-favorable winds that drove the surface exposure of cold (~8°C), saline (~34) water. Following the brief June events, the shelf experienced a prolonged period of upwelling-favorable winds and high-pCO_2 conditions for most of July. These persistent high-pCO_2 conditions had a large effect on the estimate of the net annual sea-air CO_2 flux for this region [*Evans et al.,* 2011a]. Our goal here is to understand, using concurrent ship, mooring and satellite observations, why the phytoplankton community did not flourish during these conditions in July 2008 and draw down the elevated pCO_2.

METHODS

To examine the response of the phytoplankton community to the July 2008 upwelling event, we have combined ship and mooring data with satellite observations. The ship data were collected with a system of sensors that make measurements of temperature, salinity, pCO_2, dissolved oxygen and chlorophyll fluorescence from the seawater flow-through system (referred to hereafter as the OSU underway pCO_2 system). These data were collected from a single cruise from July 12 to 21, 2008 aboard the NOAA Ship McArthur II (Fig. 5.1). This

cruise began in the Columbia River estuary (46.2°N, 123.9°W) and traveled south sampling on-offshore transects along the OR shelf and into northern California waters, before turning north and resampling some transects, most notably the Newport Hydrographic line (NH line; 44.6°N), before ending in Seattle, Washington. Mooring observations were collected from the OSU NH10 buoy (Fig. 5.1), which is located ~20 km from shore (about halfway between the shore and the shelf break at 200 m) directly west of Newport at the 80 m isobath. The following sections describe the OSU underway pCO_2 system, the mooring instruments, the satellite data, and ancillary measurements used in this study. All times reported in this manuscript are in UTC.

The OSU underway pCO_2 system

Our pCO_2 measurement system used a LI-COR LI-840 infrared (IR) CO_2 analyzer to detect CO_2 in a gas stream equilibrated with seawater from the shipboard flow-through system. Seawater was delivered to a miniature membrane contactor (Liqui-Cel 1x5.5) at ~300 ml min^{-1}, and prefiltration was achieved using a custom tangential flow filter, in which 1-10% of the main flow was directed radially through an 8-μm screen to the membrane contactor. Airflow through the equilibrator was fixed at 30 ml min^{-1} and data were collected at 1 Hz. Standard sequences using gases of known CO_2 mixing ratio (xCO_2, ppm) were used to correct for IR analyzer inaccuracy. The standards were run with atmospheric samples every two hours. Calibrated seawater xCO_2 data were adjusted to pCO_2 using the measured total equilibrator pressure, and calibrated atmospheric xCO_2 data were converted to pCO_2 using atmospheric pressure measured in the LI-COR cell. Measurement-temperature seawater pCO_2 was then corrected to pCO_2 at sea surface temperature (SST) using the difference between ship intake and equilibrator temperatures following [*Takahashi et al.,* 1993] and [*Dickson et al.,* 2007]. This correction was done after accounting for

the flow-based lag time (~ 1 min) between temperature sensor locations. The pCO_2 system was integrated with a Seabird SBE45 for temperature and salinity, and a chlorophyll fluorometer (WETLabs WetStar; excitation/emission wavelengths of 460/695 nm). The seawater flow rate was monitored downstream of the pCO_2 equilibrator and used for data quality control; data from all measurements were removed during periods of low flow delivery to the equilibrator (<100 ml min^{-1}). All ancillary measurements are made at 1 Hz coincident with the pCO_2 measurement, and the fluorometer was kept clean during each cruise. Chlorophyll calibration was done using surface Niskin bottle samples collected during the cruise, and the intake depth for the seawater flow-through system was 3 m.

Moored Measurements

Moored pCO_2 measurements were made using a Submersible Autonomous Moored Instrument CO_2 sensor [SAMI-CO_2; *DeGrandpre et al.*, 1995] produced by Sunburst Sensors. The SAMI-CO_2 was factory calibrated prior to deployment and positioned immediately under the surface float on the OSU NH10 buoy. In addition to the pCO_2 sensor, we also deployed a Seabird SBE16plus that measured and logged temperature and salinity and recorded the signals from a SBE43 sensor for dissolved oxygen and a WETLabs C-star transmissometer (660 nm) for optical beam transmission. Data from additional thermistors and salinometers positioned at select depths along the mooring line were provided by the Oregon Coastal Ocean Observing System (OrCOOS; http://agate.coas.oregonstate.edu/index.html). We also deployed a WETLabs combination chlorophyll fluorometer and turbidity sensor (FLNTUSB which uses excitation/emission wavelengths of 470/695 nm for chlorophyll and backscatter at 700 nm for turbidity). The SAMI-CO_2, SBE16plus and the additional optics sensors were all positioned at approximately 1 m depth in the bridle of the buoy,

and measurements were recorded hourly. Copper tape, faceplates and shutters were used to help prevent biofouling on the FLNTUSB. We only present the chlorophyll fluorescence data here, which were calibrated with a two-point calibration curve using the Niskin bottle sample collected at the OSU NH10 buoy position during the July 2008 cruise. Hourly measurements of dissolved oxygen, chlorophyll fluorescence, and pCO_2 were smoothed using a 32-hour running mean.

Dissolved oxygen values are presented here as ΔO_2, which represent the surface water concentration (μmol kg^{-1}) minus the oxygen saturation concentration (μmol kg^{-1}) at the in situ temperature and salinity. The oxygen saturation concentrations were calculated using the equations described by *García and Gordon* [1992]. To remove the effect of warming of upwelled water during the July 2008 event, we normalized our mooring pCO_2 data to a reference temperature of 7.7°C. This was the minimum 32-hour running mean temperature observed in the record on July 13, 2008. The normalization of mooring pCO_2 data at SST ($pCO_{2(SST)}$) to a temperature of 7.7°C ($pCO_{2(7.7°C)}$) is done using the equation from *Takahashi et al.* [1993; 2002] . $pCO_{2(SST)}$ and $pCO_{2(7.7°C)}$ are identical during the exposure of coldest upwelled water, and normalized values are lower than values at SST during other times because the effect of warming has been removed such that we are largely considering changes resulting from changing water chemistry alone.

Satellite Observations

Level 2 SST (11 μ wavelength) and chlorophyll data from the Aqua satellite's MODerate resolution Imaging Spectroradiometer (MODIS) were extracted from the NASA Ocean Color website (http://oceancolor.gsfc.nasa.gov/)

for the time period July 1 through August 5, 2008. Level 2 data are swaths with 1 km resolution. Usually there are two swaths per day, and cloud contamination inhibits satellite infrared SST and ocean color measurements. Each Level 2 file was examined to find the clearest cloud-free images spanning the July 2008 upwelling event. Hovmuller plots were also created using data extracted for on-offshore and alongshore boxes (Fig. 5.1). The pixels in the green box for each 1 km latitude band were averaged to create a time versus longitude section, and the pixels in the gray box for each 1 km longitude band were averaged to create a latitude versus time section. The latitude bands for the on-offshore box were from 44.2°N to 45°N, and included a maximum of 89 pixels. The longitude band for the alongshore box were from 124°W to 124.65°W, and includes a maximum of 51 pixels.

Ancillary Data

Wind data were obtained from the NDBC buoy 46050, approximately 33 km offshore (Fig. 5.1), to illustrate the wind pattern throughout the July 2008 upwelling event. The Pacific Fisheries Environmental Laboratory (PFEL) 6-hourly coastal upwelling index (UI; http://www.pfeg.noaa.gov/products/PFEL/modeled/indices/upwelling/upwelling.html) was also used to aid in describing the upper ocean response to the July 2008 upwelling-favorable wind forcing. The UI used here was for 45°N, 125°W.

RESULTS

Starting July 5, 2008 winds on the OR shelf began transitioning from downwelling- to upwelling-favorable, becoming equatorward on July 6 and peaking in velocity (~13 m s^{-1}) on July 7 (Fig. 5.2A). The PFEL coastal upwelling index followed the change in winds, and indicated that the upwelling event began

on July 6 (Fig. 5.2B). Temperature at 20 m and 25 m on the OSU NH10 buoy closely followed the change in winds, peaking near ~10°C on July 6, before dropping to < 8°C with the onset of upwelling (Fig. 5.2C). SST at the NH10 buoy peaked at ~15.5°C on July 6 prior to a precipitous (~7°C decrease) drop in temperature over the next several days (Fig. 5.2C). Satellite SST show cool surface water (~11°C) nearshore on July 7 (Fig. 5.3). The 12.5°C isotherm was chosen, by inspection of SST imagery, to mark the position of the SST front. On July 7 the front was inshore of the buoy site, 10 km off Newport (Fig. 5.3). Satellite chlorophyll concentrations were near or > 3 mg m^{-3} and broadly distributed over the shelf north of 43°N (Fig. 5.3) on both sides of the SST front. Our mooring data confirm ~3 mg m^{-3} chlorophyll concentrations at the buoy site on July 7 (Fig. 5.2E). Both mooring ΔO_2 and $pCO_{2(SST)}$ were near equilibrium with the atmosphere at the start of upwelling on July 6, before an extended period of very low ΔO_2 and high pCO_2 that lasted about three weeks (Fig. 5.2F and G).

Strong (>10 m s^{-1}) southward winds blew from July 7 to 15 (Fig. 5.2A), and the PFEL coastal upwelling index indicated the strongest upwelling of 2008 over this period (Fig. 5.2B). According to this index, upwelling peaked on July 10 at ~180 m^3/s/100m of coastline. The coldest SSTs were observed at the buoy site on July 13 (Fig. 5.2C). Equatorward winds decreased in strength on July 15, and remained moderately strong (between 5 and 10 m s^{-1}) until July 20. Temperatures throughout the water column where ~8°C from July 11 through 20, but the salinity data show stratification was still present. ΔO_2 and pCO_2 showed steep changes starting with the initiation of upwelling on July 6, both reaching plateaus on July 10 with ΔO_2 near -120 µmol kg^{-1} and $pCO_{2(SST)}$ at 850 µatm. $pCO_{2(7.7°C)}$ was 820 µatm, indicating that warming had little effect on the high pCO_2 concentrations at this time. Chlorophyll measured at the buoy site reached minimum values on July 9 (~1.3 mg m^{-3}) that persisted until July 12 (Fig. 5.2E).

Satellite SST data from July 12 show the transition to strong upwelling conditions, with the SST front now 55 km from shore and SST near 8°C covering much of the shelf off Newport (Fig. 5.3). The satellite chlorophyll Hovmuller section revealed the offshore advection of the ~3 mg m^{-3} chlorophyll waters, which were replaced with water that contained significantly lower chlorophyll concentrations from July 7 to 15 (Fig. 5.5). Near the peak of intense upwelling, the entire shelf off Newport and north had chlorophyll concentrations ≤ 1 mg m^{-3} (Fig. 5.3). Chlorophyll concentrations during this time were highest offshore, seaward of the SST front (Fig. 5.3).

Ship data verify the mooring and satellite observations, indicating cold (~8°C), low-chlorophyll (< 2 mg m^{-3}) water was broadly distributed over the shelf near and north of Newport (Fig. 5.4). The highest pCO_2 values (~1100 µatm) were observed in inner shelf waters off Newport on July 13. Surface water with pCO_2 > 1000 µatm was first observed at the mooring site on July 15, and values increased to 1100 µatm on July 16 (Fig. 5.2G). Chlorophyll concentrations began to increase at the buoy site starting on July 12, and values reached 4 mg m^{-3} on July 15. The slight increase in chlorophyll was the first indication of any response from the phytoplankton on the shelf off Newport to the July upwelling event, but this small chlorophyll increase was not evident in the satellite data. The Hovmuller sections show chlorophyll concentrations generally < 2 mg m^{-3} on the shelf near Newport throughout the period of strong upwelling from July 9 to July 15 (Figs. 5.5 and 5.6), and the clear image from July 12 shows that there was no large bloom south of Newport (Fig. 5.3).

Beginning July 15, the equatorward winds weakened (Fig. 5.2A) and there were sustained moderate levels of chlorophyll near 4 mg m^{-3} (Fig. 5.2E) that

coincided with a steady increase in ΔO_2 (Fig. 5.2F) and a decrease in pCO_2 over the following 10 days (Fig. 5.2G). SSTs also slowly began to warm on July 15, increasing from ~8.2°C to ~10.9°C by July 24 (Fig. 5.2C). Satellite SST data indicate that warmer (> 10°C) surface waters were present on the shelf near and north of Newport on July 23, and that the offshore SST front was closer to the coast (45 km offshore; Fig. 5.3). Chlorophyll concentrations inshore of the front and south of Newport increased from the previous clear image on July 7, particularly south of Newport over Heceta Bank (Fig. 5.1). Chlorophyll off Newport was highest inshore of the NH10 buoy position (Fig. 5.3). The satellite chlorophyll Hovmuller sections indicate increased chlorophyll along most of the Oregon coast beginning July 22 (Figs. 5.5 and 5.6), seven days into the period of reduced upwelling-favorable winds. Although the second half of our cruise did not have the same coverage of the shelf as the first, ship-based observations verified that chlorophyll concentrations were generally higher (near 4 mg m^{-3}) and pCO_2 values were lower than earlier in the cruise (Fig. 5.4). Upwelling ceased and winds turned poleward on July 25 (Fig. 5.2A and B), ending the 19-day July upwelling event.

The transition from persistent upwelling to variable wind conditions coincided with some large short-term variability in surface water properties at the NH10 buoy site. From July 23 to August 3, there were large excursions in all parameters that were likely related to reversals in the winds and advection of water masses with distinct SST and salinity characteristics (Fig. 5.2). Winds became poleward on July 26, and a warm, low-salinity surface layer moved past the NH10 buoy which initially drove an increase in ΔO_2 and a decrease in pCO_2. Following this first reversal, a brief moderate equatorward wind event coincided with a sharp drop in ΔO_2 to -40 μmol kg^{-1} and $pCO_{2(SST)}$ increased to 1200 μatm on July 27 and 28. $pCO_{2(7.7°C)}$ was 170 μatm lower than pCO_2 at SST during this

event, indicating that some of the observed increase was due to warming, but that most of the signal was from an increase in DIC caused by the brief transition in the winds (Fig. 5.2G).

Following this first oscillation between poleward and equatorward winds on July 28, the surface waters present at the mooring were warmer (approaching 12°C) and a large phytoplankton bloom became evident in response to the July 2008 upwelling event, which spanned much of the OR shelf (Figs. 5.2E, 5.3, 5.5 and 5.6). Satellite chlorophyll data show a massive bloom had developed over the OR shelf by July 28, and the SST front was no longer evident in some places (Fig. 5.3). Between July 28 and August 1, water present at the mooring had salinity equivalent to that observed previously in upwelled water (~33.5; Fig. 5.2D), indicating that the water mass present at the mooring site at that time was aged upwelled water that had been at the surface long enough for SSTs to warm by ~4°C (Fig. 5.2C). Phytoplankton biomass in this water had increased by 5-fold from the levels observed at the peak of the upwelling event (Fig. 5.2E). On August 2, a water mass with lower salinity (~32), that likely was from the Columbia River plume [*Huyer et al.*, 2007], was present at the mooring site. This water mass also contained high phytoplankton biomass, and chemical signatures of high rates of primary productivity. The large bloom resulted in high positive ΔO_2, and pCO_2 below saturation with respect to the atmosphere (Fig. 5.2F and G), ending a 23-day period of CO_2 outgassing on the OR shelf.

DISCUSSION

The data presented are from a prolonged and strong upwelling event that occurred on the OR coast in July 2008. This event was characterized by the strongest upwelling-favorable winds of 2008, and caused the extended exposure

of high-pCO_2 water to the atmosphere. The combination of persistent strong winds and elevated pCO_2 had a large impact on the annual sea-air CO_2 flux estimate for the region [*Evans et al.,* 2011a]. The goal of this work was to understand why the phytoplankton community did not flourish and draw down the elevated pCO_2, driving the shelf towards a net sink for CO_2 as described by *Hales et al.* [2005a]. These waters are upwelled with abundant iron [*Chase et al.,* 2005] and performed nutrients [*Hales et al.*, 2005a], and phytoplankton assemblages in this system typically consist of fast-growing coastal diatoms [*Wetz and Wheeler,* 2003] capable of drawing high initial NO_3^- to low levels within a few days [*Dugdale et al.,* 2006]. This was the explanation given by *Hales et al.* [2005a] for the low observed pCO_2, but this response was not observed in July 2008. The expected response time for a fast-growing diatom bloom to nutrient addition to the euphotic zone would be on the order of ~5 days, and this was seen during a deck incubation study conducted in the region to examine organic matter partitioning in upwelling-induced phytoplankton blooms *[Wetz and Wheeler,* 2003]. However, other work has shown that strong upwelling conditions can delay the development of a bloom until wind relaxation occurs [*Kudela et al.,* 2006; *Wilkerson et al.,* 2006], and modeling exercises have demonstrated the adverse effects of strong upwelling on shelf primary productivity [*Botsford et al.*, 2003; 2006]. The strong upwelling conditions likely played a similar role here, but before considering this it is necessary to dismiss some other possibilities.

Iron limitation can not be invoked here because OR shelf waters are high in iron, and iron stress has never been demonstrated [*Chase et al.,* 2007; *Chase et al.,* 2005]. Dissolved organic carbon (DOC) has been suggested to act as a chelator similar to EDTA that enhances the availability of trace metals [*Reynolds,* 2006], and low concentrations in upwelled waters have been shown to delay bloom development [*Toyota,* 1994], but generally on the order of days. High

ammonium concentrations can inhibit nitrate uptake in upwelling regions [*Kokkinakis and Wheeler,* 1987], however the values observed during our cruise were at most 0.8 μM (W. Peterson, unpublished data) and not high enough to cause a long delay in growth (P. Wheeler, personal communication). Seed stock can not be an issue because incubation studies using water collected below the mixed layer (~28 to 70 m) and from the benthic boundary layer have developed blooms on the order of days [*Wetz and Wheeler,* 2003; *Wetz et al.,* 2004]. Similarly, light limitation likely is not a factor because growth was observed to occur at 40 to 50% of the surface irradiance in winter [*Wetz et al.,* 2004]. Based on the July 2008 mooring record of salinity (Fig. 5.2D), the mixed layer was consistently shallower than 30 m. Therefore it is likely that these summertime light levels were equal to or greater than the levels observed by *Wetz et al.* [2004].

The process that most likely explains the delay of a large bloom is rapid cross-shelf transport followed by subduction at the SST front. Cross-shelf transport controls the exposure time of freshly upwelled water at the surface, in that the slower the transport, the longer upwelled water will be exposed to the atmosphere over the shelf. Estimates of the exposure time of freshly upwelled water at the mooring site can be made from both the physical and chemical data. The average PFEL Upwelling Index over the July 7 to 15 period of strong upwelling was 107 m^3/s/100m of coastline. Assuming a surface mixed layer of 20 m and that upwelled water first outcrops at the beach in Newport OR (~20 km from the mooring site), this equates to an exposure time of 4 days. Exposure time can also be estimated from the oxygen data, which has the added benefit of not requiring an assumption about the source region of upwelled water. Since dissolved O_2 is not a buffered gas, unlike CO_2, its response to gas exchange is rapid. The period of persistent strongly undersaturated ΔO_2 between July 10 and

15 in the face of swift gas exchange implies very short exposure times. Given a gas transfer velocity for O_2 of 6 m d^{-1} and a 20 m mixed layer, the response time for O_2 to reach equilibration with the atmosphere should be 3 days. This was not observed. Therefore based on these physical and chemical estimates, the exposure time of upwelled water at the mooring site during the period of strong upwelling was at most four days, but likely shorter, given the assumption of a maximal cross-shelf distance between the mooring and the hypothetical locus of upwelling. During upwelling conditions, surface water is generally moving offshore and alongshore [*Barth et al.*, 2005] such that the possibility exists for a phytoplankton bloom downstream of Newport OR. However, no downstream phytoplankton bloom was observed from the ship (Fig. 5.4) or satellite (Figs. 5.3, 5.5 and 5.6), which further supports the idea of short exposure time. Recently upwelled water was not at the surface over the shelf long enough for a phytoplankton response to occur such that pCO_2 could be drawn down to below atmospheric levels and prevent the large effluxes that were observed [*Evans et al.*, 2011a].

Subduction of recently upwelled water must be occurring in order for no phytoplankton bloom to develop on the time scale expected (~5 days) following the initiation of the July 2008 upwelling event. Only within the region of Heceta Bank did satellite data show any indication of blooming phytoplankton (Fig. 5.3) during the period of strong upwelling (Fig. 5.2). Subduction of cold shelf surface water below warmer offshore waters at the convergent SST front may be responsible for the removal of recently upwelled water from the surface, and strong vertical transport processes have been observed to inject coastal chlorophyll and biogenic particulate carbon below the euphotic zone in offshore waters [*Barth et al.*, 2002; *Flament et al.*, 1985; *Kadko et al.*, 1991]. However, these studies do not agree on the exact physical mechanism for injecting coastal

water into the open ocean. *Flament et al.* [1985] suggested the mechanism was related to the convergence of heavier coastal water with lighter offshore water, which causes a secondary circulation [*Mooers et al.*, 1976] that can result in vertical transports on the order of 9 m/d [*Flament et al.*, 1985]. *Kadko et al.* [1991] did not suggest a mechanism for the deep chlorophyll feature they observed offshore, however they proposed vertical velocities of 27 m/d based on the ^{222}Rn deficit in subducted water. *Barth et al.* [2002] suggested that these features are caused by the conservation of potential vorticity along the meandering path of the California Current jet [*Barth et al.*, 2005]. As a coastal water mass is moved offshore, the water column height increases, and the water mass is forced downward along sloping isopycnals. Obviously there is some disagreement amongst the physical oceanographic community as to the mechanisms that cause subduction features in the coastal ocean, however there is no disagreement that deep features of coastal origin do exist offshore. Subduction processes were likely responsible for removing freshly upwelled surface water during the July 2008 upwelling event, preventing the development of a phytoplankton bloom and allowing the persistence of high-pCO_2 conditions over the shelf. This of course has consequences for the DIC and nutrient status of ocean interior waters, and the subsequent biological response, when they outcrop once again at the ocean surface.

An interesting feature at the front during strong upwelling is the higher satellite chlorophyll on the seaward side of the SST front relative to the landward side on July 12 (Fig. 5.3). Increased chlorophyll has been observed on the warm side of convergent fronts in the equatorial Pacific [*Archer et al.,* 1997; *Yoder et al.,* 1994]. The processes believed responsible for this are the concentration and subduction of buoyant phytoplankton, which then separate from the subducting cool water mass and rise into the overriding warm surface water mass [*Yoder et*

al., 1994]. This is unlikely here because the horizontal scale of the high chlorophyll observed on the warm side of the front is more than double that observed by *Yoder et al.* [1994]. A more plausible mechanism is vertical diapycnal mixing between high-nutrient, high-pCO_2 recently subducted water and nutrient-poor water offshore of the front [*Mooers et al.*, 1976]. Also, the aggregation of buoyant phytoplankton implies some growth in the recently upwelled water that should have been evident in our ship data and from satellite. However, this was not the case (Figs. 5.3, 5.4, 5.5 and 5.6). The higher chlorophyll offshore of the front is local growth of offshore phytoplankton supported by nutrients supplied by the subducted coastal water.

Another line of evidence supporting the strong upwelling, rapid cross-shelf transport and subduction argument is the decrease in the strength of upwelling-favorable winds that coincided with the changes in chlorophyll, ΔO_2 and pCO_2 at NH10. During the period of decreased upwelling-favorable winds from July 16 to 25, the average PFEL Upwelling index was 54 m^3/s/100m of coastline. Again assuming a 20 m mixed layer and that upwelled water outcrops at the beach, this implies a longer exposure time of 9 days that permitted a phytoplankton response from the upwelling event. The slight increase in chlorophyll, steady increase in ΔO_2 and the decrease in pCO_2 were all evidence of the phytoplankton community having a longer exposure time to respond to the upwelling-supplied nutrients.

The July 2008 upwelling event was remarkable in that it caused high-pCO_2 water to persist at the surface for an extended period of time because of the lack of a strong phytoplankton response. The lack of phytoplankton response was the result of strong upwelling, rapid cross-shelf transport and then

subduction at the SST front. There is some evidence of increased upwelling intensity and persistence over the 20th Century [*Bakun*, 1990; *McGregor et al.*, 2007], and upwelling intensity has been predicted to increase under climate change scenarios [*Snyder et al.,* 2003]. In addition, the surface warming of open ocean waters predicted by climate change scenarios [*Levitus et al.*, 2000] will result in a stronger convergent front at the shelfbreak. Thus, as upwelling intensity increases and the surface waters of the offshore North Pacific warm, this process will become more prevalent.

This mechanism has significant implications for the carbon cycling in these coastal waters in a changing climate. First, *Evans et al.* [2011a] showed that these events have a significant impact on the net annual sea-air CO_2 exchange for the region. System changes leading to dominance of these conditions would shift the region from a significant net annual sink to a net annual source. Second, *Hales et al.* [2006] suggested that the absence of relaxation events could be linked to on-shelf retention of particulate organic carbon produced by shelf phytoplankton. This labile material [*Wetz et al.,* 2006] would be respired in already low-O_2 upwelled waters and lead to on-shelf hypoxia, perhaps explaining the apparent trend of increasing hypoxia reported by *Chan et al.* [2008]. Finally, low aragonite and calcite saturation states characterize high-pCO_2 upwelled water [*Feely et al.*, 2008]. During this event in July 2008, there was a collapse in oyster seed production at the Whiskey Creek Hatchery in Netarts Bay, OR (C. Langdon; personal communication). This collapse was likely caused by the introduction of corrosive upwelled waters to the hatchery during the July event [*Kerr*, 2010]. If these events become more prevalent in the future, the consequences for coastal marine life due to increased exposure to corrosive waters are clearly serious.

CONCLUSIONS

The data presented are from a prolonged and intense upwelling event in July 2008 that had a large impact on the annual sea-air CO_2 flux for the OR shelf. Cross-shelf transport was rapid relative to phytoplankton response times, and was followed by subduction of upwelled water below low-density offshore waters at the SST front prior to bloom formation. Once upwelling weakened, cross-shelf transport slowed, and a phytoplankton response was observed. These observations show that the surface exposure time of upwelled water is critical for a phytoplankton response and CO_2 drawdown, with consequences for the overall sink/source nature of the shelf, the chemical composition of the offshore subducted waters and the exposure of coastal animals to hypoxic and corrosive waters.

REFERENCES

Archer, D., et al. (1997), A meeting place of great ocean currents: shipboard observations of a convergent front at 2°N in the Pacific, *Deep-Sea Research II*, *44*, 1827-1850.

Bakun, A. (1990), Global Climate Change and Intensification of Coastal Ocean Upwelling, *Science*, *247*, 198-201.

Barth, J. A., S. D. Pierce, and T. Cowles (2005), Mesoscale structure and its seasonal evolution in the northern California Current System, *Deep-Sea Research II*, *52*, 5-28.

Barth, J. A., T. J. Cowles, P. M. Kosro, R. K. Shearman, A. Huyer, and R. L. Smith (2002), Injection of carbon from the shelf to offshore beneath the euphotic zone in the California Current, *Journal of Geophyiscal Research*, *107*, doi: 10.1029/2001JC000956.

Borges, A., and M. Frankignoulle (2002), Aspects of dissolved inorganic carbon dynamics in the upwelling system off the Galician coast, *Journal of Marine Systems*, *32*, 181-198.

Borges, A. V. (2005), Do We Have Enough Pieces of the Jigsaw to Integrate CO_2 Fluxes in the Coastal Ocean?, *Estuaries*, *28*(1), 3-27.

Borges, A. V., B. Delille, and M. Frankignoulle (2005), Budgeting sinks and sources of CO_2 in the coastal ocean: Diversity of ecosystems counts, *Geophysical Research Letters*, *32*, L14601, doi: 14610.11029/12005GL023053.

Botsford, L. W., C. A. Lawrence, E. P. Dever, A. Hastings, and J. Largier (2003), Wind strength and biological productivity in upwelling systems: an idealized study, *Fisheries Oceanography*, *12*(4/5), 245-259.

Botsford, L. W., C. A. Lawrence, E. P. Dever, A. Hastings, and J. Largier (2006), Effects of variable winds on biological productivity on continental shelves in coastal upwelling systems, *Deep-Sea Research II*, *53*, 3116-3140.

Cai, W.-J., M. Dai, and Y. Wang (2006), Air-sea exchange of carbon dioxide in ocean margins: A province-based synthesis, *Geophysical Research Letters*, *33*, L12603, doi:12610.11029/12006GL026219.

Chase, Z., P. G. Strutton, and B. Hales (2007), Iron links river runoff and shelf width to phytoplankton biomass along the U.S. West Coast, *Geophysical Research Letters*, *34*, L04607, doi: 04610.01029/02006GL028069.

Chase, Z., B. Hales, T. Cowles, R. Schwartz, and A. van Geen (2005), Distribution and variability of iron input to Oregon coastal waters during the upwelling season, *Journal of Geophysical Research*, *110*, C10S12, doi:10.1029/2004JC002590.

DeGrandpre, M. D., T. R. Hammar, S. P. Smith, and F. L. Sayles (1995), In situ measurements of seawater pCO2, *Limnology and Oceanography*, *40*(5), 969-975.

Dickson, A. G., C. L. Sabine, and J. R. Christian (2007), Guide to Best Practices for Ocean CO_2 Measurements*Rep.*, North Pacific Marine Science Organization.

Dugdale, R. C., F. P. Wilkerson, V. E. Hogue, and A. Marchi (2006), Nutrient controls on new production in the Bodega Bay, California, coastal upwelling plume, *Deep-Sea Research II*, *53*(25-26), 3049-3062.

Evans, W., B. Hales, and P. G. Strutton (2011a), The seasonal cycle of surface ocean pCO_2 on the Oregon shelf, *Journal of Geophyiscal Research*, *116*(C05012), doi: 10.1029/2010JC006625.

Evans, W., B. Hales, P. G. Strutton, and D. C. Ianson (2011b), Sea-Air Carbon Dioxide Fluxes on the Western Canadian Coastal Margin, *Journal of Geophyiscal Research*, (*in preparation)*.

Feely, R. A., C. L. Sabine, M. Hernandez-Ayon, D. Ianson, and B. Hales (2008), Evidence for Upwelling of Corrosive "Acidified" Water onto the Continental Shelf, *Science*, *320*(5882), 1490-1492.

Flament, P., L. Armi, and L. Washburn (1985), The Evolving Structure of an Upwelling Filament, *Journal of Geophyiscal Research*, *90*(C6), 11765-11778.

Friederich, G. E., P. M. Walz, M. G. Burczynski, and F. P. Chavez (2002), Inorganic carbon in the central California upwelling system during the 1997-1999 El Niño-La Niña event, *Progress in Oceanography*, *54*, 185-203.

García, H. E., and L. I. Gordon (1992), Oxygen solubility in seawater: Better fitting equations, *Limnology and Oceanography*, *37*(6), 1301-1312.

Hales, B., T. Takahashi, and L. Bandstra (2005a), Atmospheric CO_2 uptake by a coastal upwelling system, *Global Biogeochemical Cycles*, *19*, GB1009, doi: 1010.1029/2004GB002295.

Hales, B., J. N. Moum, P. Covert, and A. Perlin (2005b), Irreversible nitrate fluxes due to turbulent mixing in a coastal upwelling system, *Journal of Geophysical Research*, *110*, C10S11, doi: 10.1029/2004JC002685.

Hales, B., L. Karp-Boss, A. Perlin, and P. A. Wheeler (2006), Oxygen production and carbon sequestration in an upwelling coastal margin, *Global Biogeochemical Cycles*, *20*, GB3001, doi: 3010.1029/2005GB002517.

Hales, B., W.-J. Cai, B. G. Mitchell, C. L. Sabine, and O. Schofield (2008), *North American Continental Margins: A Synthesis and Planning Workshop*, 110 pp., U.S. Carbon Cycle Science Program, Washington DC.

Hill, J. K., and P. A. Wheeler (2002), Organic carbon and nitrogen in the northern California current system: comparison of offshore, river plume, and coastally upwelled waters, *Progress in Oceanography*, *53*, 369-387.

Huyer, A., P. A. Wheeler, P. T. Strub, R. L. Smith, R. Letelier, and P. M. Kosro (2007), The Newport line off Oregon - Studies in the North East Pacific, *Progress in Oceanography*, *75*, 126-160.

Huyer, A., J. H. Fleischbein, J. Keister, P. M. Kosro, N. Perlin, R. L. Smith, and P. A. Wheeler (2005), Two coastal upwelling domains in the northern California Current system, *Journal of Marine Research*, *63*, 901-929.

Jiang, L.-Q., W.-J. Cai, R. Wanninkhof, Y. Wang, and H. Lüger (2008), Air-sea CO2 fluxes on the U.S. South Atlantic Bight: Spatial and seasonal variability, *Journal of Geophysical Research*, *113*, C07019, doi: 07010.01029/02007JC004366.

Kadko, D. C., L. Washburn, and B. Jones (1991), Evidence of Subduction Within Cold Filaments of the Northern California Coastal Transition Zone, *Journal of Geophyiscal Research*, *96*(C8), 14909-14926.

Kerr, R. A. (2010), Ocean Acidification Unprecedented, Unsettling, *Science*, *328*, 1500-1501.

Kokkinakis, S. A., and P. A. Wheeler (1987), Nitrogen Uptake and Phytoplankton Growth in Coastal Upwelling Regions, *Limnology and Oceanography*, *32*(5), 1112-1123.

Kudela, R. M., N. Garfield, and K. W. Bruland (2006), Bio-optical signatures and biogeochemistry from intense upwelling and relaxation in coastal California, *Deep-Sea Research II*, *53*, 2999-3022.

Laruelle, G. G., H. H. Dürr, C. P. Slomp, and A. V. Borges (2010), Evalution of sinks and sources of CO_2 in the global coastal ocean using a spatially-explicit typology of estuaries and continental shelves, *Geophysical Research Letters*, *37*(L15607), doi: 10.1029/2010GL043691.

Levitus, S., J. I. Antonov, T. P. Boyer, and C. Stephens (2000), Warming of the World Ocean, *Science*, *287*, 2225-2229.

Liu, K.-K., L. Atkinson, R. A. Quiñones, and L. Talaue-McManus (2010), Biogeochemistry of Continental Margins in a Global Context, in *Carbon and Nutrient Fluxes in Continental Margins*, edited by K.-K. Liu, L. Atkinson, R. A. Quiñones and L. Talaue-McManus, pp. 3-24, Springer, Stockholm.

McGregor, H. V., M. Dima, and H. W. M. Fischer, S. (2007), Rapid 20th-Century Increase in Coastal Upwelling off Northwest Africa, *Science*, *315*(5812), 637-639.

Mooers, C. N. K., C. A. Collins, and R. L. Smith (1976), The Dynamic Structure of the Frontal Zone in the Coastal Upwelling Region off Oregon, *Journal of Physical Oceanography*, *6*(1), 3-21.

Pierce, S., J. A. Barth, R. E. Thomas, and G. W. Fleischer (2006), Anomalously warm July 2005 in the northern California Current: Historical context and the significance of cumulative wind stress, *Geophysical Research Letters*, *33*(L22S04), doi: 10.1029/2006GL027149.

Reynolds, C. (2006), *Ecology of Phytoplankton*, Cambridge University Press, New York.

Snyder, M. A., L. C. Sloan, N. S. Diffenbaugh, and J. L. Bell (2003), Future climate change and upwelling in the California Current, *Geophysical Research Letters*, *30*(15), doi: 10.1029/2003GL017647.

Takahashi, T., J. Olafsson, J. G. Goddard, D. W. Chipman, and S. C. Sutherland (1993), Seasonal Variation of CO2 and Nutrients in the High-Latitude Surface Oceans: a Comparative Study, *Global Biogeochemical Cycles*, *7*(4), 843-878; doi:810.1029/1093GB02263.

Takahashi, T., R. A. Feely, R. F. Weiss, R. Wanninkhof, D. W. Chipman, S. C. Sutherland, and T. T. Takahashi (1997), Global Air-Sea Flux of CO_2: An Estimate Based on Measurements of Sea-Air pCO_2 Difference *Proceedings of the National Academy of Sciences of the United States of America*, *94*(16), 8292-8299.

Takahashi, T., et al. (2002), Global sea-air CO2 flux based on climatological surface ocean pCO2, and seasonal biological and temperature effects, *Deep-Sea Research II*, *49*, 1601-1622.

Takahashi, T., et al. (2009), Climatological mean and decadal change in surface ocean pCO2 and net sea-air CO2 flux over the global oceans, *Deep-Sea Research II*, *56*, 554-577.

Toyota, T. (1994), Growth Inhibition of Phytoplankton Populations Cultured in Disphotic Zone Water by INsufficient Amounts of Dissolved Organic Carbon, *Journal of Oceanography*, *50*, 499-514.

van Geen, A., R. K. Takesue, J. Goddard, T. Takahashi, J. A. Barth, and R. L. Smith (2000), Carbon and nutrient dynamics during coastal upwelling off Cape Blanco, Oregon, *Deep-Sea Research II*, *47*, 975-1002.

Wetz, M. S., and P. A. Wheeler (2003), Production and partitioning of organic matter during simulated phytoplankton blooms, *Limnology and Oceanography*, *48*(5), 1808-1817.

Wetz, M. S., P. A. Wheeler, and R. M. Letelier (2004), Light-induced growth of phytoplankton collected during the winter from the benthic boundary later off Oregon, USA, *Marine Ecology Progress Series*, *280*, 95-104.

Wilkerson, F. P., A. M. Lassiter, R. C. Dugdale, A. Marchi, and V. E. Hogue (2006), The phytoplankton bloom response to wind events and upwelled nutrients during the CoOP WEST study, *Deep-Sea Research II*, *53*(25-26), 3023-3048.

Yoder, J. A., S. G. Ackleson, R. T. Barber, P. Flament, and W. M. Balch (1994), A line in the sea, *Nature*, *371*, 689-692.

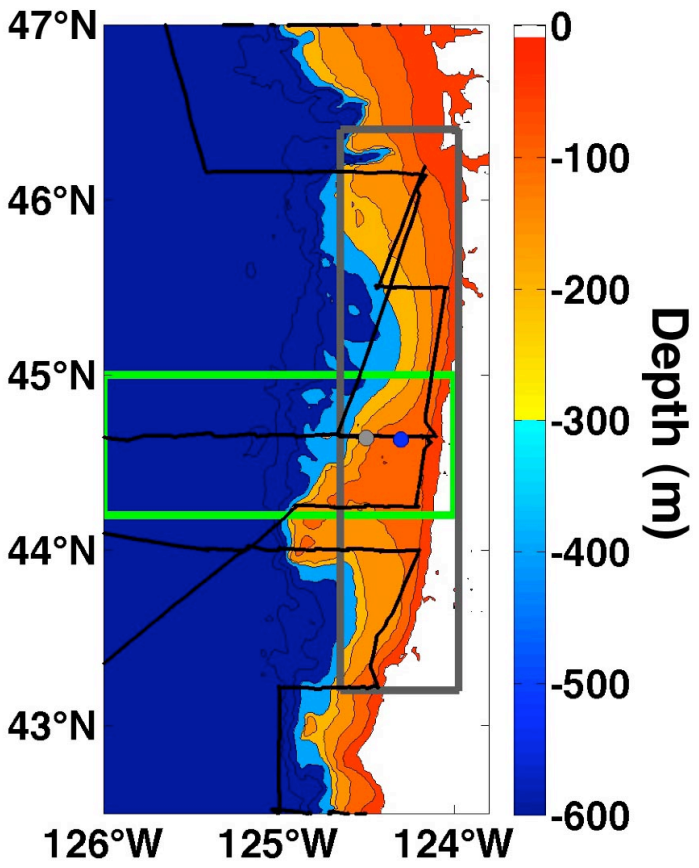

Figure 5.1: Map of Oregon coastal margin bathymetry (colorbar, m) provided by the National Geophysical Data Center (http://www.ngdc.noaa.gov/mgg/global/global.html). Warm colors highlight the shelf (<200m). The black line is the track from the cruise aboard the NOAA Ship McArthur II. The blue dot is the OSU NH10 buoy position (44.633°N, 124.304°W) and the gray dot is the position of NDBC buoy 46050 (44.641°N, 124.5°W), both of which are due west of Newport, OR. The broad shelf region south of Newport, OR is Heceta Bank. MODIS Level 2 satellite data were extracted for boxes in the offshore (green) and alongshore (gray) direction for the construction of Hovmuller diagrams.

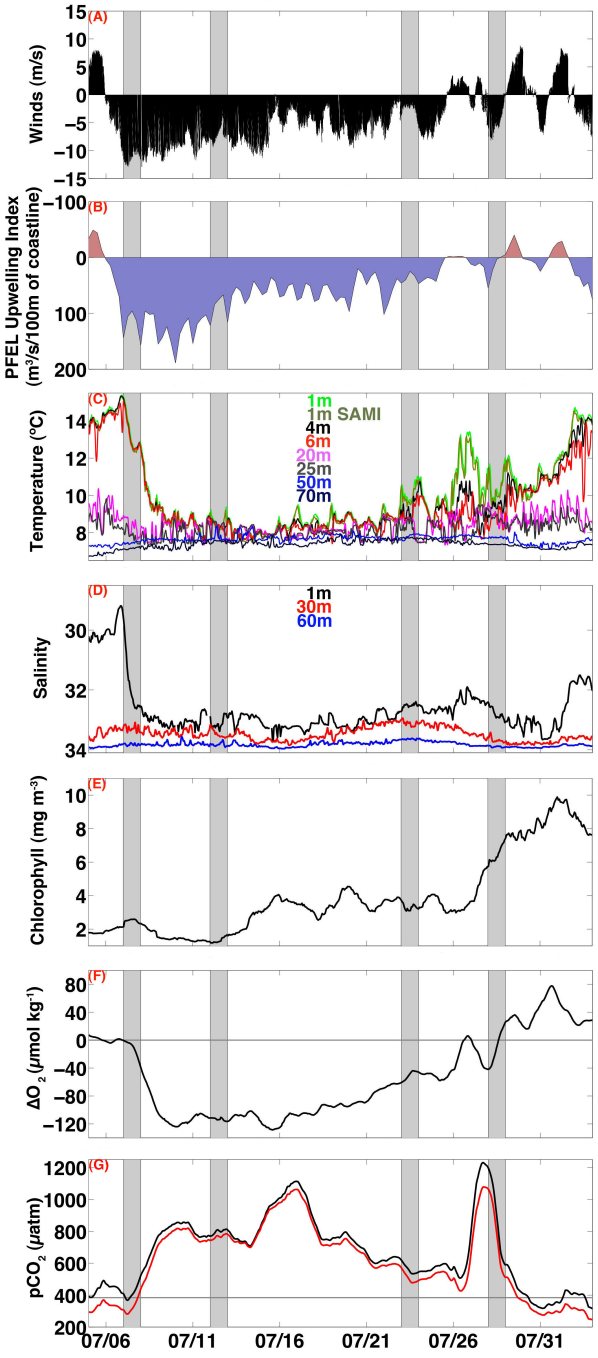
(A)
Winds (m/s)
15
10
5
0
−5
−10
−15
(B)
PFEL Upwelling Index
(m³/s/100m of coastline)
−100
0
100
200
(C)
Temperature (°C)
14
12
10
8
1m
1m SAMI
4m
6m
20m
25m
50m
70m
(D)
Salinity
30
32
34
1m
30m
60m
(E)
Chlorophyll (mg m⁻³)
10
8
6
4
2
(F)
ΔO₂ (μmol kg⁻¹)
80
40
0
−40
−80
−120
(G)
pCO₂ (μatm)
1200
1000
800
600
400
200
07/06
07/11
07/16
07/21
07/26
07/31

Figure 5.2

Figure 5.2: 10-min wind vectors from the NOAA buoy 46050 (panel A; m/s), PFEL 6-hourly coastal upwelling index (panel B; m^3/s/100m of coastline), temperature (panel C; ºC) and salinity (panel D) at various depths in the water column (indicated by color). Panels E-G are data collected from ~1m depth on the NH10 buoy: chlorophyll (panel E; mg m^{-3}), ΔO_2 (panel F; µmol kg^{-1}) and pCO_2 (µatm) at SST (black) and referenced to the minimum SST which occurred on July 11 (7.7°C; red line). Records are from July 5 through August 3, 2008, and the vertical gray bars represent days where clear skies permitted the retrievals of MODIS data shown in Figure 3.

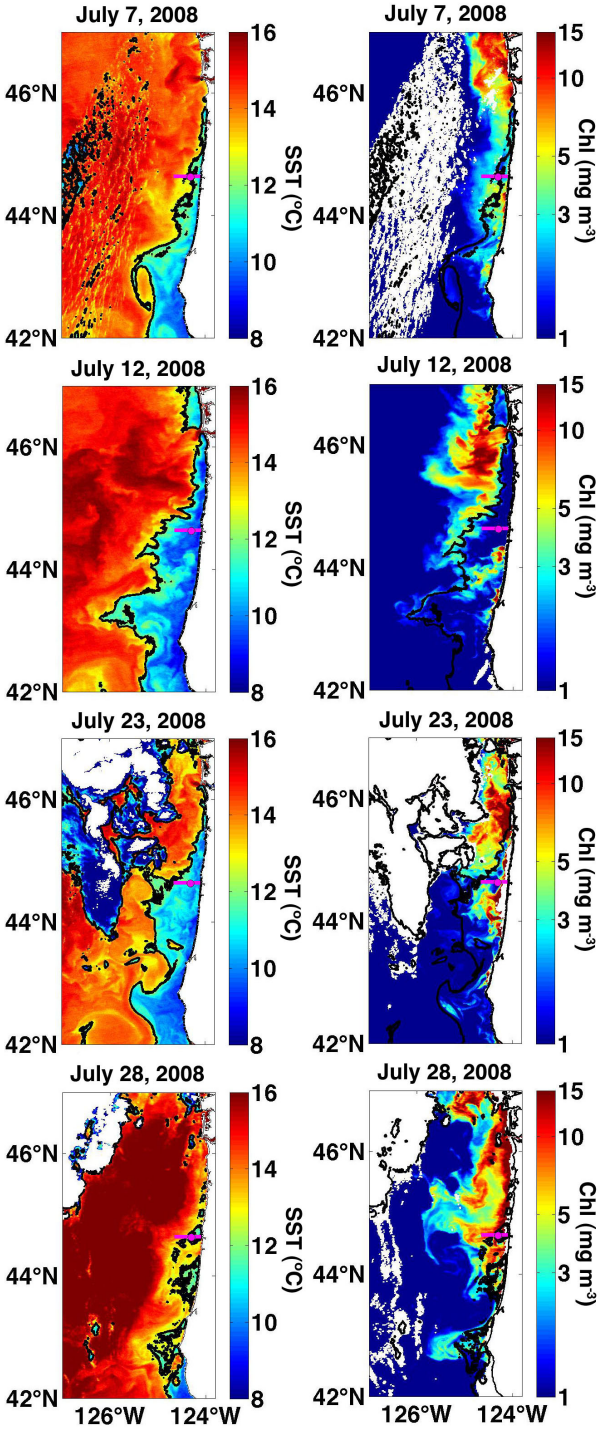
July 7, 2008
July 12, 2008
July 23, 2008
July 28, 2008
46°N
44°N
42°N
126°W
124°W
SST (°C)
Chl (mg m-3)
16
14
12
10
8
15
10
5
3
1

Figure 5.3

Figure 5.3: MODIS Aqua Level 2 SST (ºC) and chlorophyll (mg m^{-3}) from individual passes on select clear days over the period of extended upwelling in July 2008. The black contours mark the 12.5ºC temperature contour, taken here to be the position of the seaward convergent SST front. The pink east-west horizontal bar is the Newport Hydrographic line (NH line) extending from the shore to near the shelf break, and is shown here to represent the shelf width off Newport. The dot near the center of this line is the OSU NH10 buoy position. Chlorophyll data are plotted in log scale. The offshore cool SSTs, most evident on July 23, are cloud-contaminated data.

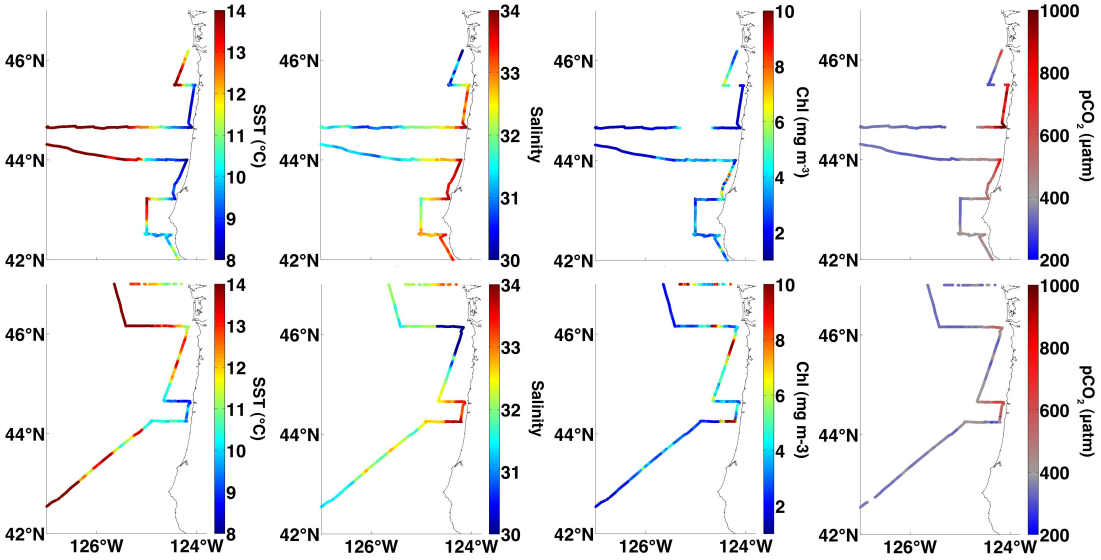

Figure 5.4: Upper panel is SST (°C), salinity, chlorophyll (mg m^{-3}) and pCO_2 (µatm) from the southbound portion of the cruise (July 12 to July 17, 2008). Lower panel is same as the top but for the northbound portion (July 17 to 21, 2008).

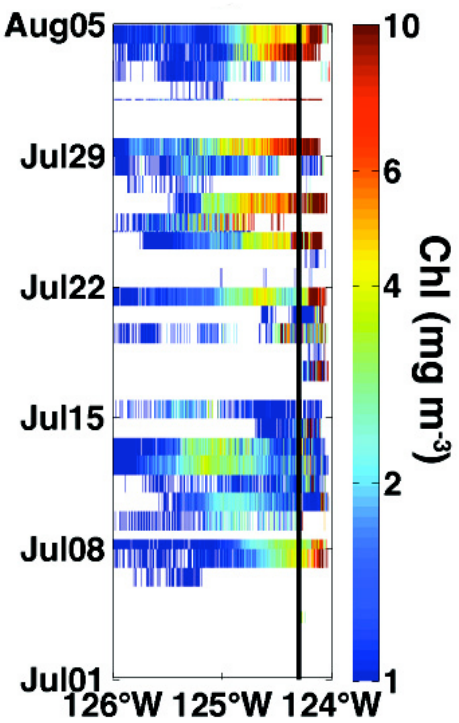

Figure 5.5: Time versus longitude Hovmuller section of MODIS chlorophyll (mg m^{-3}) data made in the on-offshore box shown in Figure 1. Chlorophyll data are in log scale and the black vertical line is the longitude of the OSU NH10 buoy.

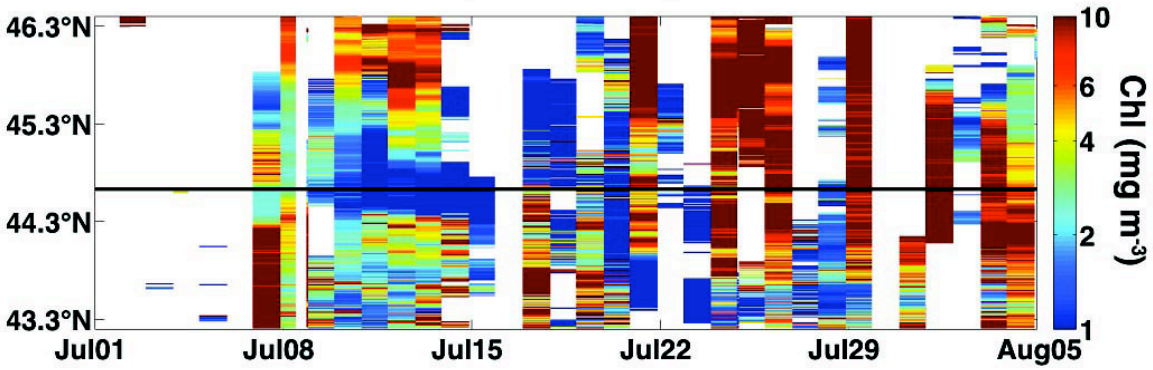

Figure 5.6: Latitude versus time Hovmuller section of MODIS chlorophyll (mg m^{-3}) data obtained within the alongshore box shown in Figure 1. Chlorophyll data are plotted in log scale. The black horizontal line is the latitude of the OSU NH10 buoy.

CHAPTER 6: Conclusions

In this dissertation, results are presented from sea-air CO_2 flux studies across three specific regions of the northeast Pacific coastal margin that describe variability from interannual to daily time scales. Resolving time variability at appropriate spatial scales is critical for assessing fluxes in coastal margin settings because of inherently extreme variability. The results from these studies have provided key information on CO_2 exchange within each region, and have also captured conditions that resulted in large fluxes, which have been mostly unobserved in the absence of aggressive sampling. In the following discussion, I highlight some of these extreme conditions and describe their importance for determining regional flux estimates for the Oregon shelf, the western Canadian coastal margin, and the Columbia River Estuary and plume.

The results from the Oregon shelf have shown strong seasonal and interannual variability in surface ocean pCO_2 and sea-air CO_2 flux. During this study, the highest surface water pCO_2 yet reported on the Oregon shelf was observed, and prolonged exposure of this water to the atmosphere had a large impact on the net annual sea-air CO_2 flux. Wind conditions drove the prolonged CO_2 outgassing during the study period, and it was shown that wind thresholds are important for the occurrence of these conditions. The largest fluxes occurred when 10-day running averaged southward wind magnitude exceeded 4 m s^{-1} for a 10-day period or more. These wind conditions have happened before, most notably during the most extreme hypoxic events of 2002 [*Grantham et al.*, 2004] and 2006 [*Chan et al.*, 2008; *Grantham et al.*, 2004]. The persistence of high-pCO_2 water at the surface with no clear rapid biological response was perplexing. If the characteristic time for a phytoplankton response to upwelling is fast in comparison to the exposure time of freshly upwelled water, low pCO_2 conditions

and CO_2 influx will dominate; if the upwelled water has a shorter exposure time than that for which the phytoplankton can respond, high pCO_2 conditions and CO_2 efflux will occur. Without the constant monitoring of pCO_2 conditions at the NH10 buoy site during this study, these events could have gone completely unobserved, or periodic ship sampling could have misrepresented the duration of high-pCO_2 water exposed to the atmosphere. Contrasting the results from this study with previous work conducted in 2001 [*Hales et al.*, 2005], clearly illustrates how temporally and spatially well-resolved pCO_2 observations are essential to diagnose the dynamic nature of sea-air CO_2 fluxes on the Oregon shelf.

The new observations collected on the western Canadian coastal ocean during winter, summer and autumn covered a greater areal portion of the region than had been previously sampled. Historical measurements with the best temporal coverage in this region were made on the southwest Vancouver Island shelf because of the tracks of vessels-of-opportunity en route to the Pacific. During this study, climatologies were developed from the historical data to diagnose the seasonal variability in sea-air CO_2 fluxes for this specific portion of the margin. These fluxes were then compared to flux estimates made from the new data set for specific regions of the margin, including the straits around Vancouver Island. It was shown that CO_2 outgassing is greater during autumn than during winter, over more of the margin than the southwest Vancouver Island shelf, and that the efflux during the autumn and winter seasons nearly balance CO_2 drawdown that occurs the remainder of the year. A key aspect of this work for the discussion of extreme conditions was the inclusion of data collected in the straits, particularly Johnstone Strait and the Strait of Juan de Fuca. These two areas were never observed to experience pCO_2 undersaturation with respect to the atmosphere, and high winds during autumn caused some large fluxes to be observed. This illustrates two important points regarding the assessment of

coastal margin sea-air CO_2 fluxes. (1) As was shown from the Oregon work, spatially and temporally well-resolved data are critical for diagnosing CO_2 exchange. Resolving the influence of the straits was important for this study, and although our temporal resolution in these areas was poor, their importance for regional fluxes was clear. However, there were differences between estimates made from spatially well-resolved data and temporally well-resolved data, and observations capturing both frames of reference are clearly required for the most precise estimates of net CO_2 exchange. (2) The ability to capture high-wind events is important for accurately accessing coastal sea-air CO_2 fluxes. The occurrence of surface water pCO_2 that is out of equilibrium with the atmosphere creates the potential for sea-air gas exchange, but without coincident high-wind conditions, the effects would be muted. If not for observations during high wind events, surface water pCO_2 levels could be erroneously interpolated between low-wind conditions. High-wind events play a key role in coastal environments where large deviations from pCO_2 equilibration with the atmosphere are typical.

The observations from the Columbia River Estuary and plume showed the impact of one such high-wind event within this region. This work reported the seasonal variability in air-water CO_2 fluxes in this system during spring, summer and autumn, and showed that the plume is always an atmospheric CO_2 sink while the estuary sink/source character is seasonally modified. Relevant to the discussion here, a strong storm was observed during the autumn sampling period that caused a large increase in air-water CO_2 fluxes in the estuary, despite a relatively large drop in air-water supersaturation. Excluding this event from the analysis results in significantly lower estuarine efflux, while assuming that the pre-storm levels of CO_2 supersutaturation would have led to a massive overestimate of this outgassing. This is because pCO_2 was more oversaturated prior to the storm compared to during and after the event, but the strong winds

during the storm drove the largest instantaneous fluxes. This clearly highlights the importance of extreme events in setting the net fluxes for regions such as this, and future work should more closely consider the effect of storms within the Columbia River estuary. An annual estimate of air-water CO_2 flux was not calculated for the estuary because the data had inadequate temporal coverage, but storm events clearly have important consequences for the annual air-water CO_2 flux.

The final component of this thesis was an examination of the weak phytoplankton response to the prolonged exposure of high-pCO_2, high-nutrient upwelled water on the Oregon shelf during a strong and persistent upwelling event during July of 2008. Strong upwelling, rapid cross shore transport, and subduction on timescales that were short relative to phytoplankton responses were most likely responsible for maintaining low chlorophyll in the presence of high nutrients and pCO_2. A large bloom developed only after upwelling ceased, and pCO_2 above atmospheric levels persisted at the surface for a 23-day period at the NH10 buoy site. This period of upwelling had a large impact on the annual sea-air flux estimate for the Oregon shelf, but may also be related to recent observations of extreme hypoxia [*Chan et al.*, 2008] and intensification of ocean acidification events in the upwelling system [*Feely et al.*, 2008]. Given predictions of increased upwelling intensity and duration at the mid-latitudes [*Bakun*, 1990], these conditions will have increasingly important consequences not only for regional flux estimates but also for coastal marine life [*Fabry et al.*, 2008].

The final points regarding the extreme conditions observed during these studies clearly illustrate the necessity for constant monitoring of the coastal ocean over broad spatial scales at high temporal resolution. Properly resolving

the time and space scales of variability is critical because not doing so can result in missing or improperly extrapolating important high-intensity events, which can have large regional impacts. In the coastal ocean so-called extremes may be the norm, and these events are important for setting the net carbon transfer between key reservoirs bounding the margins. Spatial and temporal variability need each be sampled exhaustively, and this presents a critical challenge for future studies as it will likely be impossible to simply make direct measurements in all places, at all times, in perpetuity. The existing approach of opportunistic and dedicated sampling must be augmented by synthetic techniques relying on a combination of in-water observations, remote-sensing, and modeling approaches, as attempted by *Hales et al.* [2011].

BIBLIOGRAPHY

Aquilar-Islas, A. M., and K. W. Bruland (2006), Dissolved manganese and silicic acid in the Columbia River plume: A major source to the California current and coastal waters off Washington and Oregon, *Marine Chemistry*, *101*, 233-247.

Archer, D., et al. (1997), A meeting place of great ocean currents: shipboard observations of a convergent front at 2°N in the Pacific, Deep-Sea Research II, 44, 1827-1850.

Barth, J. A., T. J. Cowles, P. M. Kosro, R. K. Shearman, A. Huyer, and R. L. Smith (2002), Injection of carbon from the shelf to offshore beneath the euphotic zone in the California Current, Journal of Geophyiscal Research, 107, doi: 10.1029/2001JC000956.

Barth, J. A., and P. A. Wheeler (2005), Introduction to special section: Coastal Advances in Shelf Transport, *Journal of Geophysical Research*, *110*, C10S01, doi: 10.1029/2005JC003124.

Barth, J. A., S. D. Pierce, and T. Cowles (2005), Mesoscale structure and its seasonal evolution in the northern California Current System, *Deep-Sea Research II*, *52*, 5-28.

Behrenfeld, M. J., and P. G. Falkowski (1997), Photosynthetic rates derived from satellite-based chlorophyll concentration, *Limnology and Oceanography*, *42*(1), 1-20.

Borges, A., and M. Frankignoulle (1999), Daily and seasonal variations of the partial pressure of CO_2 in surface seawater along Belgian and southern Dutch coastal areas, *Journal of Marine Systems*, *19*, 251-266.

Borges, A. V. (2005), Do We Have Enough Pieces of the Jigsaw to Integrate CO_2 Fluxes in the Coastal Ocean?, *Estuaries*, *28*(1), 3-27.

Borges, A. V., B. Delille, and M. Frankignoulle (2005), Budgeting sinks and sources of CO2 in the coastal ocean: Diversity of ecosystems counts, *Geophysical Research Letters*, *32*, L14601, doi: 14610.11029/12005GL023053.

Bruland, K. W., M. C. Lohan, A. M. Aquilar-Islas, G. Smith, J., B. Sohst, and A. M. Baptista (2008), Factors influencing the chemistry of the near-field Columbia River plume: Nitrate, silicic acid, dissolved Fe, and dissolved Mn, *Journal of Geophyiscal Research*, *113*(C00B02), doi: 10.1029/2007JC004702.

Bakun, A. (1990), Global Climate Change and Intensification of Coastal Ocean Upwelling, *Science*, *247*, 198-201.

Caffrey, J. M. (2004), Factors Controlling Net Ecosystem Metabolism in U.S. Estuaries, *Estuaries*, *27*(1), 90-101.

Cai, W.-J. (2011), Estuarine and Coastal Ocean Carbon Paradox: CO_2 Sinks or Sites of Terrestrial Carbon Incineration?, *Annual Review of Marine Science*, *3*, 123-145.

Cai, W.-J., and Y. Wang (1998), The chemistry, fluxes, and sources of carbon dioxide in the estuarine waters of the Satilla and Altamaha Rivers, Georgia, *Limnology and Oceanography*, *43*(4), 657-668.

Cai, W.-J., M. Dai, and Y. Wang (2006), Air-sea exchange of carbon dioxide in ocean margins: A province-based synthesis, *Geophysical Research Letters*, *33*, L12603, doi:12610.11029/12006GL026219.

Chan, F., J. A. Barth, J. Lubchenco, A. Kirincich, H. Weeks, W. T. Peterson, and B. A. Menge (2008), Emergence of Anoxia in the California Current Large Marine Ecosystem, *Science*, *319*(5865), doi:10.1126/science.1149016.

Chase, Z., P. G. Strutton, and B. Hales (2007), Iron links river runoff and shelf width to phytoplankton biomass along the U.S. West Coast, *Geophysical Research Letters*, *34*, L04607, doi: 04610.01029/02006GL028069.

Chase, Z., B. Hales, T. Cowles, R. Schwartz, and A. van Geen (2005), Distribution and variability of iron input to Oregon coastal waters during the upwelling season, Journal of Geophysical Research, 110, C10S12, doi:10.1029/2004JC002590.

Chavez, F. P., J. Ryan, L.-C. E. Salvador, and Ñ. C. Miguel (2003), From Anchovies to Sardines and Back: Multidecadal Change in the Pacific Ocean, *Science*, *299*(217), doi:10.1126/science.1075880.

Chavez, F. P., and T. Takahashi (2007), Coastal Oceans*Rep.*, 157-166 pp, U.S. Climate Change Science Program, Washington, DC.

Chen, C.-T. A., and A. V. Borges (2009), Reconciling opposing views on carbon cycling in the coastal ocean: Continental shelves as sinks and near-shore ecosystems as sources of atmospheric CO2, *Deep-Sea Research II*, *56*, 579-590.

Colbert, D., and J. McManus (2003), Nutrient Biogeochemistry in an Upwelling-Influenced Estuary of the Pacific Northwest (Tillamook Bay, Oregon, USA), *Estuaries*, *26*(5), 1205-1219.

DeGrandpre, M. D., T. R. Hammar, S. P. Smith, and F. L. Sayles (1995), In situ measurements of seawater pCO2, *Limnology and Oceanography*, *40*(5), 969-975.

Dickson, A. G., C. L. Sabine, and J. R. Christian (2007), Guide to Best Practices for Ocean CO_2 Measurements*Rep.*, North Pacific Marine Science Organization.

Dugdale, R. C., F. P. Wilkerson, and A. Morel (1990), Realization of new production in coastal upwelling areas: A means to compare relative performance, *Limnology and Oceanography*, *35*(4), 822-829.

Dugdale, R. C., F. P. Wilkerson, V. E. Hogue, and A. Marchi (2006), Nutrient controls on new production in the Bodega Bay, California, coastal upwelling plume, *Deep-Sea Research II*, *53*(25-26), 3049-3062.

Evans, W., B. Hales, and P. G. Strutton (2011), The seasonal cycle of surface ocean pCO_2 on the Oregon shelf, *Journal of Geophyiscal Research*, *(accepted)*.

Evans, W., B. Hales, P. G. Strutton, and D. C. Ianson (2011b), Sea-Air Carbon Dioxide Fluxes in the Western Canadian Coastal Ocean, *Journal of Geophyiscal Research*, (*in preparation)*.

Fabry, V. J., B. A. Seibel, R. A. Feely, and J. C. Orr (2008), Impacts of ocean acidification on marine fauna and ecosystem processes, *ICES Journal of Marine Science*, *65*, 414-432.

Feely, R. A., C. L. Sabine, M. Hernandez-Ayon, D. Ianson, and B. Hales (2008), Evidence for Upwelling of Corrosive "Acidified" Water onto the Continental Shelf, *Science*, *320*(5882), 1490-1492.

Feely, R. A., T. Takahashi, R. Wanninkhof, M. J. McPhaden, C. E. Cosca, S. C. Sutherland, and M.-E. Carr (2006), Decadal variability of the air-sea CO_2 fluxes in the equatorial Pacific Ocean, *Journal of Geophyiscal Research*, *111*(C08S90), doi: 10.1029/2005JC003129.

Frankignoulle, M., G. Abril, A. Borges, I. Bourge, C. Canon, B. Delille, E. Libert, and J.-M. Théate (1998), Carbon Dioxide Emission from European Estuaries, *Science*, *282*, 434-436.

Fransson, A., M. Chierici, and Y. Nojiri (2006), Increased net CO2 outgassing in the upwelling region of the southern Bering Sea in a period of variable marine

climate between 1995 and 2001, *Journal of Geophyiscal Research*, *111*(C08008), doi: 10.1029/2004JC002759.

Friederich, G. E., P. M. Walz, M. G. Burczynski, and F. P. Chavez (2002), Inorganic carbon in the central California upwelling system during the 1997-1999 El Nino-La Nina event, *Progress In Oceanography*, *54*(1-4), 185-203.

García, H. E., and L. I. Gordon (1992), Oxygen solubility in seawater: Better fitting equations, Limnology and Oceanography, 37(6), 1301-1312.

Gattuso, J.-P., M. Frankignoulle, and R. Wollast (1998), Carbon and Carbonate Metabolism in Coastal Aquatic Ecosystems, *The Annual Review of Ecology, Evolution and Systematics*, *29*, 405-434.

Grantham, B. A., F. Chan, K. Nielsen, D. S. Fox, J. A. Barth, A. Huyer, J. Lubchenco, and B. A. Menge (2004), Upwelling-driven nearshore hypoxia signals ecosystem and oceanographic changes in the northeast Pacific, *Nature*, *429*, 749-754.

Hales, B., D. Chipman, and T. Takahashi (2004), High-frequency measurements of partial pressure and total concentration of carbon dioxide in seawater using microporous hydrophobic membrane contactors, *Limnology and Oceanography: Methods*, *2*, 356-364.

Hales, B., T. Takahashi, and L. Bandstra (2005a), Atmospheric CO2 uptake by a coastal upwelling system, *Global Biogeochemical Cycles*, *19*, GB1009, doi: 1010.1029/2004GB002295.

Hales, B., J. N. Moum, P. Covert, and A. Perlin (2005b), Irreversible nitrate fluxes due to turbulent mixing in a coastal upwelling system, *Journal of Geophysical Research*, *110*, C10S11, doi:10.1029/2004JC002685.

Hales, B., L. Karp-Boss, A. Perlin, and P. A. Wheeler (2006), Oxygen production and carbon sequestration in an upwelling coastal margin, *Global Biogeochemical Cycles*, *20*, GB3001, doi: 3010.1029/2005GB002517.

Hales, B., W.-J. Cai, B. G. Mitchell, C. L. Sabine, and O. Schofield (2008), *North American Continental Margins: A Synthesis and Planning Workshop*, 110 pp., U.S. Carbon Cycle Science Program, Washington DC.

Hales, B., P. G. Strutton, M. Saraceno, R. Letelier, T. Takahashi, R. A. Feely, C. L. Sabine, and F. P. Chavez (2011), Satellite-based prediction of pCO_2 in coastal waters, *Progress in Oceanography*, *(submitted)*.

Hickey, B. (1989), Patterns and processes of circulation over the Washington continental shelf and slope, in *Coastal Oceanography of Washington and Oregon*, edited, Elsevier Science Publishers B.V., New York

Hickey, B., and N. S. Banas (2008), Why is the Northern End of the California Current System so Productive?, *Oceanography*, *21*(4), 91-107.

Hickey, B., R. McCabe, S. Geier, E. Dever, and N. Kachel (2009), Three interacting freshwater plumes in the northern California Current System, *Journal of Geophysical Research*, *114*, C00B03, doi: 10.1029/2008JC004907.

Hickey, B., et al. (2010), River Influences on Shelf Ecosystems: Introduction and Synthesis, *Journal of Geophysical Research*, *115*, C00B17, doi:10.1029/2009JC005452.

Hill, J. K., and P. A. Wheeler (2002), Organic carbon and nitrogen in the northern California current system: comparison of offshore, river plume, and coastally upwelled waters, *Progress in Oceanography*, *53*, 369-387.

Ho, D. T., C. S. Law, M. J. Smith, P. Schlosser, M. Harvey, and P. Hill (2006), Measurements of air-sea gas exchange at high wind speeds in the Southern Ocean: Implications for global parameterizations, *Geophysical Research Letters*, *33*, L16611, doi: 16610.11029/12006GL026817.

Hunt, C. W., J. E. Salisbury, D. Vandemark, and W. R. McGillis (2011), Contrasting Carbon Dioxide Inputs and Exchange in Three Adjacent New England Estuaries, *Estuaries and Coasts*, *34*, 68-77.

Huyer, A. (1977), Seasonal variation in temperature, salinity, and density over the continental shelf off Oregon, *Limnology and Oceanography*, *22*(3), 442-453.

Huyer, A., and R. L. Smith (1978), Physical characteristics of Pacific northwestern coastal waters. , in *The Marine Plant Biomass of the Pacific Northwest Coast*, edited by R. Knauss, pp. 37-55, Oregon State University Press.

Huyer, A., J. H. Fleischbein, J. Keister, P. M. Kosro, N. Perlin, R. L. Smith, and P. A. Wheeler (2005), Two coastal upwelling domains in the northern California Current system, Journal of Marine Research, 63, 901-929.

Huyer, A., P. A. Wheeler, P. T. Strub, R. L. Smith, R. Letelier, and P. M. Kosro (2007), The Newport line off Oregon - Studies in the North East Pacific, *Progress in Oceanography*, *75*, 126-160.

Ianson, D., and S. E. Allen (2002), A two-dimensional nitrogen and carbon flux model in a coastal upwelling region, *Global Biogeochemical Cycles*, *16*(1), doi: 10.1029/GB001451.

Ianson, D., S. E. Allen, S. L. Harris, K. J. Orians, D. E. Varela, and C. S. Wong (2003), The inorganic carbon system in the coastal upwelling region west of Vancouver Island, Canada, *Deep-Sea Research I*, *50*, 1023-1042.

Ianson, D., R. A. Feely, C. L. Sabine, and L. W. Juranek (2009), Features of Coastal Upwelling Regions that Determine Net Air-Sea CO_2 Flux, *Journal of Oceanography*, *65*, 677-687.

Jiang, L.-Q., W.-J. Cai, R. Wanninkhof, Y. Wang, and H. Lüger (2008), Air-sea CO2 fluxes on the U.S. South Atlantic Bight: Spatial and seasonal variability, *Journal of Geophysical Research*, *113*, C07019, doi: 07010.01029/02007JC004366.

Jiang, L.-Q., W.-J. Cai, R. Wanninkhof, Y. Wang, and H. Lüger (2008), Air-sea CO2 fluxes on the U.S. South Atlantic Bight: Spatial and seasonal variability, *Journal of Geophysical Research*, *113*, C07019, doi: 07010.01029/02007JC004366.

Kokkinakis, S. A., and P. A. Wheeler (1987), Nitrogen Uptake and Phytoplankton Growth in Coastal Upwelling Regions, Limnology and Oceanography, 32(5), 1112-1123.

Körtzinger, A. (2010), The Outer Amazon Plume: An Atmospheric CO_2 Sink, in *Carbon and Nutrient Fluxes in Continental Marginis*, edited by K.-K. Liu, L. Atkinson, R. A. Quiñones and L. Talaue-McManus, Springer, Berlin.

Kudela, R. M., N. Garfield, and K. W. Bruland (2006), Bio-optical signatures and biogeochemistry from intense upwelling and relaxation in coastal California, Deep-Sea Research II, 53, 2999-3022.

Kudela, R. M., et al. (2010), Multiple trophic levels fueled by recirculation in the Columbia River plume, *Geophysical Research Letters*, *37*(L18607), doi: 10.1029/2010GL044342.

Kosro, P. M. (2005), On the spatial structure of coastal circulation off Newport, Oregon, during spring and summer 2001 in a region of varying shelf width, *Journal of Geophysical Research*, *110*, C10S06, doi: 10.1029/2004JC002769.

Landry, M. R., J. R. Postel, W. K. Peterson, and J. Newman (1989), Broad-scale distributional patterns of hydroghraphic variabiles on the Washington/Oregon shelf, in *Coastal Oceanography of Washington and Oregon*, edited by M. R.

Landry and B. M. Hickey, Elsevier Science Publishers B.V., Amsterdam, The Netherlands.

Laruelle, G. G., H. H. Dürr, C. P. Slomp, and A. V. Borges (2010), Evalution of sinks and sources of CO_2 in the global coastal ocean using a spatially-explicit typology of estuaries and continental shelves, *Geophysical Research Letters*, *37*(L15607), doi: 10.1029/2010GL043691.

Liu, K.-K., L. Atkinson, R. A. Quiñones, and L. Talaue-McManus (2010), Biogeochemistry of Continental Margins in a Global Context, in *Carbon and Nutrient Fluxes in Continental Margins*, edited by K.-K. Liu, L. Atkinson, R. A. Quiñones and L. Talaue-McManus, pp. 3-24, Springer, Stockholm.

Lohan, M. C., and K. W. Bruland (2006), Importance of vertical mixing for additional sources of nitrate and iron to surface waters of the Columbia River plume: Implications for biology, *Marine Chemistry*, *98*(260-273).

Lüger, H., R. Wanninkhof, D. W. R. Wallace, and A. Körtzinger (2006), CO_2 fluxes in the subropical and subarctic North Atlantic based on measurements from a volunteer observing ship, *Journal of Geophyiscal Research*, *111*(C06024), doi: 10.1029/2005JC003101.

Mantua, N. J., S. R. Hare, Y. Zhang, J. M. Wallace, and R. C. Francis (1997), A Pacific Interdecadal Climate Oscillation with Impacts on Salmon Production, *Bulletin of the American Meteorological Society*, *78*(6), 1069-1079.

Martz, T. R., M. D. DeGrandpre, P. G. Strutton, W. R. McGillis, and W. M. Drennan (2009), Sea surface pCO_2 and carbon export during the Labrador Sea spring-summer bloom: An in situ mass balance approach, *Journal of Geophysical Research*, *114*(C09008), doi:10.1029/2008JC005060.

Masson, D. (2006), Seasonal Water Mass Analysis for the Straits of Juan de Fuca and Georgia, *Atmosphere-Ocean*, *44*(1), 1-15.

McGregor, H. V., M. Dima, and H. W. M. Fischer, S. (2007), Rapid 20th-Century Increase in Coastal Upwelling off Northwest Africa, Science, 315(5812), 637-639.

McNeil, B. I. (2010), Diagnosing coastal ocean CO_2 interannual variability from a 40 year hydrographic time series station off the east coast of Australia, *Global Biogeochemical Cycles*, *24*(GB4034), doi: 10.1029/2010GB003870.

Muller-Karger, F., R. Varela, R. Thunell, R. Luerssen, C. Hu, and J. J. Walsh (2005), The importance of continental margins in the global carbon cycle, *Geophysical Research Letters*, *32*, L01602, doi: 01610.01029/02004GL021346.

Nemcek, N., D. Ianson, and P. D. Tortell (2008), A high-resolution survey of DMS, CO2, and O2/Ar distributions in productive coastal waters, *Global Biogeochemical Cycles*, *22*, GB2009, doi: 2010.1029/2006GB002879.

Park, P. K., L. I. Gordon, S. W. Hager, and M. C. Cissell (1969), Carbon Dioxide Partial Pressure in the Columbia River, *Science*, *166*(3907), 867-868.

Pennington, J. T., G. E. Friederich, C. G. Castro, C. A. Collins, W. Evans, and F. P. Chavez (2010), The Northern and Central California Coastal Upwelling System, in *Carbon and Nutrient Fluxes in Continental Margins*, edited by K.-K. Liu, L. Atkinson, R. A. Quiñones and L. Talaue-McManus, Springer, Berlin.

Perry, G. D., P. B. Duffy, and N. L. Miller (1996), An extended data set of river discharges for validation of general circulation models, *Journal of Geophyiscal Research*, *101*(D16), 21,339-321,349.

Pierce, S., J. A. Barth, R. E. Thomas, and G. W. Fleischer (2006), Anomalously warm July 2005 in the northern California Current: Historical context and the significance of cumulative wind stress, Geophysical Research Letters, 33(L22S04), doi: 10.1029/2006GL027149.

Salisbury, J., M. Green, C. Hunt, and J. Campbell (2008), Coastal Acidification by Rivers: A Threat to Shellfish?, *EOS, Transactions, American Geophysical Union*, *89*(50), 513-514.

Sarmiento, J. L., and N. Gruber (2006), *Ocean Biogeochemical Dynamics*, Princeton University Press, Princeton.

Schwing, F. B., T. Murphree, L. deWitt, and P. M. Green (2002), The evolution of oceanic and atmospheric anomalies in the Pacific during the El Niño and La Niña events of 1995-2001, *Progress in Oceanography*, *54*, 459-491.

Simenstad, C. A., L. F. Small, C. D. McIntire, D. A. Jay, and C. Sherwood (1990), Columbia River Estuary studies: An introduction to the estuary, a brief history, and prior studies, *Progress in Oceanography*, *25*, 1-13.

Small, L. F., C. D. McIntire, K. B. Macdonald, J. R. Lara-Lara, B. E. Frey, M. C. Amspoker, and T. Winfield (1990), Primary productivity, plant and detrital biomass, and particle transport in the Columbia River Estuary, *Progress in Oceanography*, *25*, 175-210.

Snyder, M. A., L. C. Sloan, N. S. Diffenbaugh, and J. L. Bell (2003), Future climate change and upwelling in the California Current, Geophysical Research Letters, 30(15), doi: 10.1029/2003GL017647.

Strub, P. T., J. S. Allen, A. Huyer, and R. L. Smith (1987), Seasonal Cycles of Currents, Temperatures, Winds, and Sea Level over the Northeast Pacific Continental Shelf: 35ºN to 48ºN, *Journal of Geophyiscal Research*, *92*(C2), 1507-1526.

Suchet, P. A., J.-L. Probst, and W. Ludwig (2003), Worldwide distribution of continental rock lithology: Implications for the atmospheric/soil CO_2 uptake by continental weathering and alkalinity river transport to the oceans, *Global Biogeochemical Cycles*, *17*(2), doi: 10.1029/2002GB001891.

Takahashi, T., J. Olafsson, J. G. Goddard, D. W. Chipman, and S. C. Sutherland (1993), Seasonal Variation of CO2 and Nutrients in the High-Latitude Surface Oceans: a Comparative Study, *Global Biogeochemical Cycles*, *7*(4), 843-878; doi:810.1029/1093GB02263.

Takahashi, T., R. A. Feely, R. F. Weiss, R. Wanninkhof, D. W. Chipman, S. C. Sutherland, and T. T. Takahashi (1997), Global Air-Sea Flux of CO_2: An Estimate Based on Measurements of Sea-Air pCO_2 Difference *Proceedings of the National Academy of Sciences of the United States of America*, *94*(16), 8292-8299.

Takahashi, T., et al. (2002), Global sea-air CO2 flux based on climatological surface ocean pCO2, and seasonal biological and temperature effects, Deep-Sea Research II, 49, 1601-1622.

Takahashi, T., et al. (2009), Climatological mean and decadal change in surface ocean pCO2 and net sea-air CO2 flux over the global oceans, *Deep-Sea Research II*, *56*, 554-577.

Toyota, T. (1994), Growth Inhibition of Phytoplankton Populations Cultured in Disphotic Zone Water by INsufficient Amounts of Dissolved Organic Carbon, Journal of Oceanography, 50, 499-514.

van Geen, A., R. K. Takesue, J. Goddard, T. Takahashi, J. A. Barth, and R. L. Smith (2000), Carbon and nutrient dynamics during coastal upwelling off Cape Blanco, Oregon, *Deep-Sea Research II*, *47*, 975-1002.

Vandemark, D., J. E. Salisbury, C. W. Hunt, S. M. Shellito, J. D. Irish, W. R. McGillis, C. L. Sabine, and S. M. Maenner (2011), Temporal and spatial dynamics of CO_2 air-sea flux in the Gulf of Maine, *Journal of Geophyiscal Research*, *116*(C01012), doi: 10.1029/2010JC006408.

Venegas, R. M., P. T. Strub, E. Beier, R. Letelier, A. C. Thomas, T. Cowles, C. James, L. Soto-Mardones, and C. Cabrera (2008), Satellite-derived variability in chlorophyll, wind stress, sea surface height, and temperature in the northern

California Current System, *Journal of Geophyiscal Research*, *113*(C03015), doi: 10.1029/2007JC004481.

Wanninkhof, R. (1992), Relationship Between Wind Speed and Gas Exchange Over the Ocean, *Journal of Geophysical Research*, *97*(C5), 7373-7382.

Ware, D. M., and R. E. Thomson (2005), Bottom-Up Ecosystem Trophic Dynamics Determine Fish Production in the Northeast Pacific, *Science*, *308*, 1280-1284.

Wetz, M. S., and P. A. Wheeler (2003), Production and partitioning of organic matter during simulated phytoplankton blooms, *Limnology and Oceanography*, *48*(5), 1808-1817.

Wetz, M. S., P. A. Wheeler, and R. M. Letelier (2004), Light-induced growth of phytoplankton collected during the winter from the benthic boundary later off Oregon, USA, Marine Ecology Progress Series, 280, 95-104.

Wetz, M. S., B. Hales, Z. Chase, P. A. Wheeler, and M. M. Whitney (2006), Riverine input of macronutrients, iron, and organic matter to the coastal ocean off Oregon, U.S.A., during the winter, *Limnology and Oceanography*, *51*(5), 2221-2231.

Wilkerson, F. P., R. C. Dugdale, R. M. Kudela, and F. P. Chavez (2000), Biomass and productivity in Monterey Bay, California: contribution of the large phytoplankton, *Deep-Sea Research II*, *47*, 1003-1022.

Wong, C. S., J. R. Christian, S.-K. Emmy Wong, J. Page, L. Xie, and S. Johnannessen (2010), Carbon dioxide in surface seawater of the eastern North Pacific Ocean, *Deep-Sea Research I*, *57*, 687-695.

Zeng, J., N. Yukihiro, P. P. Murphy, C. S. Wong, and Y. Fujinima (2002), A comparison of ΔpCO_2 distributions in the northern North Pacific using results from a commercial vessel in 1995-1999, *Deep-Sea Research II*, *49*, 5303-5315.

Yoder, J. A., S. G. Ackleson, R. T. Barber, P. Flament, and W. M. Balch (1994), A line in the sea, Nature, 371, 689-692.